Faculté des Sciences appliquées
Département d'Electricité, Electronique et Informatique
(Institut Montefiore)

Distributed and Centralized System Protection Schemes Against Voltage and Thermal Emergencies

Dissertation présentée en vue
de l'obtention du grade de
Docteur en Sciences de l'Ingénieur

par

Bogdan OTOMEGA

Ingénieur en énergétique (orientation électroénergétique)

Année académique 2007-2008

To my wife Dana,
for her love,
friendship and
understanding

Acknowledgments

In the first place, I would like to express my deepest gratitude and appreciation to my supervisor Prof. Thierry Van Cutsem. His support, guidance, encouragements and patience during these years helped me to complete this research. Working with him was a unique experience which hopefully will continue after the defence of this thesis.

Special thanks to the members of the Jury who accepted to assess this report and devoted their time to this.

I wish to thank Profs. Mircea Eremia and Constantin Bulac for trusting my capabilities and offering me the opportunity to finalize my engineering studies at University of Liège.

Sincere thanks go to colleagues and friends from the Electrical Engineering and Computer Science Department of the University of Liège for providing a stimulating work environment. Special thoughts to Florin Căpitănescu for his moral support and interesting comments and suggestions. I would like to thank also Prof. Mevludin Glavic and Adamantios Marinakis for sharing their knowledge and ideas with me. I hope to keep on collaborating with them.

I gratefully acknowledge the RTE company for making realistic data available to me.

Many thanks to the “Rue Darchis” friends for trying from time to time to fill the hole in my soul. Sorry for not having enough space to mention you all.

Finally, my thoughts are going to my family, especially to my beloved wife Dana whom I have to thank for her support and comprehension.

Abstract

The main objective of this thesis was to develop appropriate system protection schemes against two important causes of failure in power systems, namely, long-term voltage instability and cascade tripping of overloaded transmission lines, mainly due to overloading.

To this purpose a distributed undervoltage load shedding scheme against voltage instability, and a centralized protection meant to alleviate line overload are proposed.

The former, through the chosen system protection scheme characteristics, has the ability to adjust its actions to the disturbance location and severity. This behavior is achieved without resorting to a dedicated communication network. The distributed controllers do not exchange information, but are rather informed of their respective actions through voltage measurements. Neither do the controllers require a model of the system. This and the absence of communication makes the protection scheme simple and reliable.

The other protection scheme, inspired of model predictive control, is aimed at bringing the currents in the overloaded lines below their limits in the time interval left by protections, while accounting for constraints on control changes. Its closed-loop nature allows to compensate for model uncertainties and measurement noise.

In order to tune the proposed system protection schemes parameters and validate their performance it was preferred to detect plausible cascading event scenarios. To this purpose, an algorithm meant to identify such complex sequences has been developed. It encompasses hidden failures and the resulting system response.

The tests performed on small systems as well as on a real-life one confirm not only that proposed protection schemes appropriately deal with the problems for which they were designed, but also that they cooperate satisfactorily for combined voltage and thermal problems that are beyond their individual capabilities.

Contents

Chapter 1

Introduction

1.1 Trends in power system operation

Modern interconnected power systems have grown in size and complexity in order to satisfy the increasing load demand. Initially the interconnections were means for supporting neighboring power systems in case of emergencies and sharing the responsibility for the frequency regulation in normal operation, thus reducing the burden and expenses of each participant. As the generation in one power system tended to be less expensive than in another system, or the load centers were closer to the neighboring power system generation, interchange transactions were established, providing for these long-term contracts. As a result, the tie-lines have become internal lines to the entire interconnected grid and are an indispensable part of the entire load supply process [HLP01]. Altogether, interconnections make economical use of the generated power and generally improve the overall reliability of the interconnected systems.

Each power system, part of an interconnection, is designed to withstand pre-defined disturbances. To this purpose, all power system components are equipped with dedicated protection schemes, some system protection schemes designed to maintain stability are implemented, and system operators are trained to take measures in order to restore the system to normal conditions following a disturbance. However, the impact of a disturbance is accompanied with sources of vulnerability such as human errors, protection/control system failures, changing power flows due to electricity market, missing or uncertain information in decision making or lack of communication between neighboring systems.

In these conditions, if the designed protection/control systems fail to maintain stability in one of the interconnected power systems, the whole interconnection becomes vulnerable. In such a case, the disturbance could spread in cascade over large distances and affect other power systems than the one where the initial disturbance took place.

Major wide-spread events are rare, but their impact is important. Very often these outages result in a condition where some areas of a system separate from the rest of the system causing

power imbalances in the so created islands. If an imbalance is not quickly contained this can lead to further loss of generation and transmission resources, and in the end to total blackout.

In order to illustrate the impact of such events, in terms of affected areas/customers and costs, some of the recent large-scale incidents and blackouts from North America and Europe are presented below. Furthermore, we point out the main events contributing to the initiation and/or development of the cascading outage by writing them with italics.

1.1.1 United States and Canada August 14, 2003 blackout [USC04]

On August 14, 2003, large portions of the Midwest and Northeast United States (U.S.) and Ontario, Canada, experienced an electric power blackout. The outage affected an area with an estimated 50 million people and over 60,000 MW of electric load in eight states from U.S. and the Canadian province of Ontario. The blackout began a few minutes after 16:00 Eastern Daylight Time (EDT), and power was not restored for 4 days in some parts of U.S.. Parts of Ontario suffered rolling blackouts for more than a week before full power was restored. Estimates of total costs in the U.S. range between $4 billion and $10 billion (U.S. dollars). In Canada, gross domestic product was down 0.7% in August, there was a net loss of 18.9 million work hours, and manufacturing shipments in Ontario were down $2.3 billion (Canadian dollars).

More than 800 events occurred during the blackout cascade. The events included the opening and closing of transmission lines and transformers, the tripping and starting of generators. Most of these events occurred in the few minutes after the cascade initiation between 16:06 and 16:12 EDT.

Blackout causes and contributory factors were identified as:

- *Inadequate vegetation management* - several lines were tripped down because they were contacting overgrown trees within the lines right-of-way areas.
- *Inadequate coordination of relays and other protective devices or systems* - one line was tripped by its protective relays detecting low apparent impedance (as a result of abnormal system operation, i.e., depressed voltage and high line current); the relay reacted as if the high flow was due to a short circuit. The trip of this line was the turning point at which system problems, experienced up to that moment, triggered the uncontrollable cascading blackout.
- *Failure to ensure operation within secure limits* - operational monitoring equipment was not adequate to alert system operators regarding important deviations in operating conditions and the need for corrective actions. Moreover, state estimation and contingency analysis tools were not used to assess system conditions.
- *Failure to identify emergency conditions and communicate that status to neighboring systems* - non-real-data were used into the state estimator, preventing the system operator

from detecting the security criteria violation and determining the necessary preventive actions. Furthermore, neighboring system operators lacked joint procedures and guidelines on when and how to relieve a security limit violation when it appears in an area and the best remedy is in another area.

- *Inadequate operator training* - system operators were not adequately trained to maintain reliable operation under emergency conditions.
- *Inadequate regional-scale visibility over the power system* - system operators lacked additional or back-up monitoring tools to understand or visualize the status of their transmission system after the failure of their primary monitoring/alarming systems.

1.1.2 United Kingdom, London, August 28, 2003 blackout [UK03]

A combination of events led to an electricity power supply failure in South London that occurred on August 28, 2003. About 700 MW of supplies were lost, amounting to around 20% of total London supplies at that time and affecting around 410,000 customers, with supplies being lost to parts of London Underground and NetworkRail. System restoration began immediately after the incident and power supplies were fully restored in about 30 minutes.

The fault which started the blackout, occurred due to a *transformer incorrect protection relay* installed when an old equipment was replaced (smaller rating). This incorrect installation was not discovered despite the appropriate training, authorization, experience and skills of engineers involved in the quality control of the automatic protection equipment.

The sole transformer loss did not directly contribute to the cause of the incident. The consequential increase in flows due to maintenance activities in nearby substations and the disconnection of another transformer in the same substation due to a Buchholz alarm, initiated the operation of the protection relay. *Power flows in the area being within operational limits, system operators did not expect that their actions to remove the equipment will cause the loss of supply.*

1.1.3 Sweden, September 23, 2003 blackout [SWE03]

On September 23, 2003, the southern part of Sweden and the eastern part of Denmark were blacked-out. The loss of supply was approximately 3000 MW in Sweden and 1850 MW in Denmark. The cause was a close coincidence of severe faults leading to an abnormal system situation far beyond the contingencies regarded in normal system design and operating security standards. In about 7 hours all supplies in Sweden and Denmark were reported to be re-energized.

Two main events caused the blackout. The first event was the *full shut-down of a nuclear power plant* on which manual control was performed in order to reduce the generation due to

internal valve problems in the feedwater circuits. The second event occurred only 5 minutes after, another two nuclear units being lost due to a *double busbar fault*. The reason for the fault was a damage to one isolator device located between the two busbars to which the nuclear units were connected. The loading current of the isolator had increased from around 1000 A to some 1500 A following the first event. This, however, was far below its rating for maximum load which is 3100 A. The isolator was inspected in March 2003 with respect to thermal overloads but nothing irregular was detected.

After the loss of the last two nuclear units the grid became heavily overloaded, and the demand in the area was recovering gradually, through the action of the numerous feeder transformer tap-changers, from the initial voltage drop caused by the first generation loss. These actions further lowered voltages on the 400 kV grid, down to critical levels, and the situation developed into a voltage collapse. Within seconds following the voltage collapse, circuit breakers in the entire southern grid were tripped by distance protections and zero-voltage automatic controls.

The fact that the faults occurred few minutes apart and the grid lost vital parts, led to classify the entire disturbance as an "N-3", which is far beyond the severity degree that the Nordic Power System was designed and operated to cope with.

1.1.4 Italy, September 28, 2003 blackout [ITA04]

The Italian incident was a nation wide blackout resulting from a sequence of technical problems and critical management conditions which led to the separation of the Italian grid from the European network UCTE (Union for Co-ordination of Transmission of Electricity). Furthermore, the UCTE system was strongly affected and the dynamic response of different physical quantities caused an unusual and endangered system condition during the transient phase which followed the disconnection of the Italian grid. Indeed, most of the grid operation centers had to deal with overfrequency and overvoltage problems, deviation of power exchange from the scheduled value, tripping of grid elements, generation and pump units.

The sequence of events was triggered by a trip of the Swiss "Lukmanier" line caused by *tree flashover*. Several attempts to automatically and manually re-close the line were unsuccessful, due to an automatic device, aimed at preventing re-closure in the presence of a large angular deviation between terminal voltages. According to its design settings, the protection blocked the action to put the line back into service.

Despite the efforts of the Italian transmission system operator to relieve the overloads in the interconnection lines, another line, the "San Bernardino" line, tripped after a *tree flashover*. This flashover was probably caused by the sag in the line, due to overheating of the conductors. In about 12 seconds after the loss of the latter, the remaining interconnections of Italy with UCTE were *disconnected by automatic protections due to overloading*.

The result was an unsatisfactory low voltage level in northern Italy and consequently, the trip of several generation plants. After separation the fast frequency drop was temporarily stopped at approximately 49 Hz, by frequency primary control, automatic shedding of pumped stor-

age power plants and load shedding. Subsequently, additional generating units (among which many cogeneration plants) were tripped for various reasons: *turbine tripping, underfrequency and undervoltage relay operation, loss of synchronism and loss of excitation, etc.* Despite additional load shedding, the frequency continued to decrease and when it reached the threshold of 47.5 Hz, the system collapsed (at around 03:28) by tripping of the remaining units.

Nearly all of the northern part of Italy was energized before 08:00, the central part around 12:00 and the remaining parts of mainland Italy at 17:00. Sicily was fully energized at 21:40.

1.1.5 Greece, July 12, 2004 [GRE04]

This incident happened just before some transmission projects planned to reinforce the transmission system, in order to improve voltage stability and increase transfer capacity, were integrated. In addition, several transmission elements and generating units were unavailable on this day due to various failures, repairs and maintenance.

The sequence of events leading to the blackout started with the *loss of a generation unit,* situated in a weak area of the system, *due to auxiliaries failure*. Due to further problems during the startup the unit was synchronized only after approximately 5 hours. During this time the load was increasing and the voltages were constantly dropping. The voltage stopped declining as soon as the generator was synchronized and started generating.

However, in the process of achieving the technical minimum the generator was lost again due to high drum level. At this time the system was in emergency state and a load shedding of 100 MW was requested by the system operator. The load shedding took place but it was not enough in order to stop the voltage decline, so another load shedding action of 200 MW was requested.

The second load shedding action had no time to be executed because two more generators were lost in the weak area. *The event which initiated the tripping of the first generator was "unclear"; as for the second one, it was manually tripped in order to protect the unit*. At this moment the voltages collapsed and the Greek system split in two parts. After splitting the remaining generator in the weak area were disconnected by undervoltage protection leading to blackout.

The split of the system saved the Northern and Western parts of the Greek system, which remained interconnected with the rest of UCTE, even though the surplus of generated power created a severe disturbance. The restoration process started few minutes after and in about five hours all the consumers were fully supplied.

1.1.6 UCTE, November 4, 2006 [UCT06]

In the evening of November 4, 2006, in the UCTE interconnected grid there were significant East-West power flows as a result of international power trade and the obligatory exchange of wind feed-in inside Germany. At around 22:10, a serious incident resulting in tripping of several high-voltage lines, which started in Northern Germany, split the UCTE grid into three separate areas (West, North-East and South-East) with significant power imbalances in each area. The power imbalance in the Western area induced a severe frequency drop that caused an interruption of supply for more than 15 million European households.

The main two causes of the incident were identified as:

- *Non fulfilment of the N-1 criterion* in the E.ON Netz grid and on some of its tie-lines to the neighboring TSOs after manual disconnection of the 380-kV double-circuit line Conneforde - Diele;
- *Insufficient inter-TSO coordination.* Even if the initial planning of the double-circuit line switching-off was duly prepared by the directly involved TSOs (E.ON Netz, RWE TSO and TenneT), the actual time for this switching maneuver was communicated by E.ON Netz at a very late moment; it was also not sufficiently prepared and checked in order to ensure secure operation of the system in this area.

Furthermore, no specific attention was given by E.ON Netz to the fact that the protective devices had different settings on both sides of the Landesbergen - Wehrendorf line linking the E.ON Netz network to the RWE one, although this information was critical due to the very high flow on this line after the initial line switching-off. In response to the RWE TSO request to reduce the power flow E.ON Netz made an empirical assessment of corrective switching measures without any load flow calculations for checking the N-1 criterion. The chosen action of coupling the busbars in the E.ON Netz Landesbergen substation was expected to result in power flow reduction. The simulations made in the course of investigations after the incident showed that *this action led to a result which was contrary to what dispatchers expected*; the power flow increased and *the line was automatically tripped due to overloading by the distance relays in the Wehrendorf substation.* This tripping led to cascading line trippings throughout the UCTE area. All lines tripped due to overloading that triggered distance protection.

The very rapid split of the interconnected system could not be stopped once the cascade tripping of the lines had started. Due to the good performance of countermeasures activated at UCTE level in the individual control areas, a Europe-wide black-out was avoided.

1.1.7 Salient features of the incidents

As can be seen from the presented major incidents and blackouts, no two scenarios are the same. The initiating events vary, including human actions or inactions, system topology, and

load/generation imbalances, etc. Other factors include the distance between generating stations and major load centers, voltage profiles across the grid, and the types and settings of protective relays in use.

Nevertheless, all scenarios present a common pattern of degradation causes, namely cascading loss of transmission lines, mainly due to thermal overload, and generation resources, some of them due to system low voltages and/or frequency.

Thermal overload is related to the maximal current allowable through an equipment, for a specific period of time, without damaging it or its isolation irreversibly, nor causing dangerous conductor sag, which may lead to flashover with surrounding system equipments or vegetation. Some important transmission lines (e.g. interconnection tie-lines) or transformers, may be equipped with overcurrent protections. Their tripping is automatic or controlled by the system operator. In both cases the resulting extra power flow will follow different transmission paths, which may result in overloading some other lines. This can lead to cascade line tripping and eventually to power system isolation and blackout (see the U.S. and Italian incidents).

Transmission lines might be tripped not only by overcurrent protections, but also by distance protections which are detecting high currents and low voltages that appear as faults (see the U.S. incident). Moreover, while overcurrent protections leave some time before tripping the transmission line, thereby allowing control actions to be taken to alleviate the overload, in the directional protection case, the trip is instantaneous and cannot be foreseen.

Other unwanted protection system operations/misoperation are due to hidden failures [HPT88, THP96, PT96, KN02]. A hidden failure of a protection system is a permanent defect that will cause a relay or a relay system to incorrectly and inappropriately remove circuit elements as a direct consequence of another switching event. This definition quoted from [PT96] can be extended to the case where a protection does not act while it should. The defect must be capable of being monitored with an appropriate supervision system. The most severe particularity of hidden failures is that their effects appear when the system is already in stressed conditions. In the blackout scenarios previously presented, some of the events which are further aggravating the system conditions could be considered as hidden failures. The damaged isolator producing the double bus bar fault in the Swedish blackout case, the wrong relay setting in the London case and the “unclear” generator loss in the Greek incident, are such examples.

Finally, under the above mentioned stressed conditions the power system might be subject to another threat for power system security: voltage instability. The latter is caused by load restoration mechanisms trying to restore power consumption beyond the capabilities of the weakened transmission and generation combined system. All the incidents previously presented have resulted in either severely depressed voltage and/or frequency profiles or voltage collapse.

1.2 Motivation and objectives of this work

The main objective of this thesis was to develop appropriate system protection schemes against two of the important causes of power system incidents, illustrated by the examples presented above. Namely, long-term voltage instability and cascade line tripping of overhead lines, mainly due to overloading. To this purpose a distributed undervoltage load shedding protection scheme against voltage instability, and a centralized protection scheme meant to alleviate line overload were designed. Both schemes were to be tested in realistic cases.

Of course, there are other causes of power system instability, such as transient (angle) instability, small-signal angle instability, short-term voltage instability, and frequency instability. These are not considered in this work. They would call for specific protection schemes.

Some of the existing system protection schemes are aimed at reacting to specific disturbances as the tripping of well identified transmission lines or generators. However, as illustrated in the previous sections, many incidents resulted from unforseen disturbances. In this respect, it is a challenge to design system protection schemes able to face a large set of possible degraded situations.

To deal with the combinatorial explosion of the number of scenarios, and avoid considering unrealistic combinations of single events, there is a need to identify *plausible* cascading events. The latter should be used to tune the parameters of the system protection schemes and validate their performance.

The algorithm meant to identify such complex sequences of events should encompass hidden failures and the resulting system response. Developing one such practical algorithm was also one objective of this work.

1.3 Structure of the report

The remaining of this report is organized in six chapters.

In *Chapter 2* are presented two major causes leading to power system degradation, namely the thermal overload and voltage instability. In the first part, basic notions regarding voltage stability are introduced, and the main mechanisms leading to voltage instability and corrective/emergency control actions to counteract these phenomena are illustrated on a small test system. In the second part some features of the thermal overload problem and the resulting cascading loss of transmission equipments are recalled, together with the relevant preventive and corrective control actions.

The scope of *Chapter 3* is to develop an algorithm capable to identify plausible severe cascading events. To this purpose we define the criteria used to determine which are the possible next disturbances following an initial perturbation, the way to compute the cascading event probability and the stopping criteria. Furthermore, we propose a filtering method in order to

cut down in computing times. Finally, we present the results obtained on a real-life system and some of the so determined events are analyzed in detail.

Chapter 4 deals with the undervoltage load shedding against voltage instability and the issues raised by its design, in terms of location, delay and amount of load shedding. After reviewing different available load shedding schemes, we propose a new design and show its potential advantage. Preliminary results of this scheme obtained on the NORDIC32 test system are presented.

Chapter 5 focuses of transmission line thermal overload alleviation using a centralized protection scheme. The latter is inspired of model predictive control algorithms. After briefly reviewing the model predictive control principle, we show how this multi-step optimization could be applied to emergency alleviation of thermal overloads. We illustrate the proposed algorithm on a simple academic system, discuss its limits, and outline some remedies.

Chapter 6 deals with detailed testing of both the distributed undervoltage load shedding and the thermal overload alleviation protection schemes on a model of the real-life system considered in Chapter 3. We analyze the system behavior and the functioning of the proposed protection schemes when dealing with some of the cascading events previously identified by the method of Chapter 3.

General conclusions as well as directions for future developments are presented in Chapter 7

1.4 Publications

Most of the work presented in this report has been published in the following articles:

- B. Otomega, and T. Van Cutsem. Fast Contingency Filtering Based on Linear Voltage Drop Estimates. In *Proc. of the IEEE Power Tech Conf.*, Paper 324, St. Petersburg (Russia), 2005.

- B. Otomega, M. Glavic, and T. Van Cutsem. A Purely Distributed Implementation of Undervoltage Load Shedding. In *Proc. of the IEEE PES General Meeting*, Paper 07GM1037, Tampa, Florida (U.S.), 2007.

- B. Otomega, A. Marinakis, M. Glavic, and T. Van Cutsem. Emergency Alleviation of Thermal Overloads Using Model Predictive Control. In *Proc. of the IEEE Power Tech Conf.*, Laussane (Switzerland), 2007.

- B. Otomega, A. Marinakis, M. Glavic, and T. Van Cutsem. Model predictive control to alleviate thermal overloads. *IEEE Power Engineering Society Letter, published in IEEE*

Transactions on Power Systems, Volume 22, Issue 3, Aug. 2007, Page(s):1384 - 1385.

- B. Otomega, M. Glavic, and T. Van Cutsem. Undervoltage load shedding using distributed controllers. *IEEE Power Engineering Society Letter, published in IEEE Transactions on Power Systems*, Volume 22, Issue 4, Nov. 2007, Page(s):2283 - 2284.

- B. Otomega, and T. Van Cutsem. Distributed undervoltage load shedding. Paper accepted for publication in *IEEE Transactions on Power Systems*, Volume 22, Issue 4, Nov. 2007, Page(s):1898 - 1907.

- B. Otomega, and T. Van Cutsem. Identifying plausible cascading events in system stability assessment. In *Proc. of the 3rd International Conference on Energy and Environment CIEM2007*, Bucharest, 22-23 November 2007.

As of writing this document, the following has been submitted:

- F. Capitanescu, B. Otomega, H. Lefebvre, V. Sermanson, and T. Van Cutsem. Prospects of an improved system protection scheme against voltage instability in the RTE system. Paper accepted to be presented at *16th Power Systems Computation Conference*, Glasgow, Scotland, July 14-18, 2008

My research activity in the field of voltage instability started with the studies performed for my final project, carried out at University of Liège with an ERASMUS scholarship, which were reported in:

- B. Otomega, V. Sermanson, and T. Van Cutsem. Reverse-Logic Control of Load Tap Changers in Emergency Voltage Conditions. In *Proc. of the IEEE Power Tech Conf.*, Paper BPT03-450, Bologna (Italy), 2003.

Chapter 2

Voltage instability and thermal overload: an overview

This chapter proposes a short review of voltage instability and thermal overload phenomena. The first part contains voltage instability definitions and classifications, the mechanisms that can create voltage problems and the preventive and corrective control actions that can be taken in order to counteract this phenomenon. Through simple examples, two of the typical long-term voltage instability mechanisms and some of the corrective actions are presented in detail. The second part deals with thermal overloads, cascade line tripping, transmission line thermal uprating and power system controls to prevent or reduce overload. Finally, this chapter outlines the Quasi-Steady State (QSS) approximation, which is the reference model of the time simulation software used throughout this research work.

2.1 Voltage stability

2.1.1 Definition and classification

Major blackouts caused by power system voltage instability, such as the ones presented in the introduction, have illustrated the importance of this phenomenon. In many power systems, voltage instability is considered as a major risk of blackout, as important as thermal overloads and the associated risk of cascade line tripping [VCV07].

Since a power system experiences various physical processes, it is appropriate to classify the various forms of instability that could affect its normal functioning according to the nature of the involved phenomena. Convenient definitions, classifications and short descriptions of various forms of power system instability established by a joined IEEE and CIGRE Working Group are presented in [CTF04]. The definitions given in the sequel are taken, in great extent, from this reference.

Voltage stability concerns the ability of a power system to maintain acceptable voltages at all buses in the system after being subject to a disturbance. Voltage instability results from the inability of the combined generation-transmission system to provide the power required by loads [VCV98] and generally occurs in the form of a progressive voltage fall at some buses. Nevertheless, overvoltage instability, manifesting as a progressive rise of voltages at some buses, may be also encountered in highly compensated power systems [VCM97].

The term *voltage collapse* is also often used to denote the process by which the sequence of events accompanying the voltage instability leads to a blackout or abnormally low voltages in a significant part of the power system.

The load response to voltage changes is usually the driving force for voltage instability. That is why voltage instability phenomenon is called also *load instability*. After an initial disturbance the power consumed by the loads tends to be restored by the action of motor slip adjustment, distribution voltage regulators, load tap-changing transformers and thermostats. However, loads are not the only responsible for instability.

For purpose of analysis, it is useful to classify voltage stability, with respect to the disturbance the system is experiencing, into the following two subcategories:

- *Small-disturbance voltage stability* is concerned with the system's ability to maintain steady voltages following small perturbations such as incremental changes in system load. This form of stability is influenced by the load characteristics and continuous / discrete controls at a given instant of time. Steady-state approaches can be effectively used to study small-disturbance voltage stability [GMK92]. A criterion for small-disturbance voltage stability is that, at a given operating condition for every bus in the system, the bus voltage magnitude increases as the reactive power injection at the same bus is increased. Thus, a system is voltage unstable if, for at least one bus in the system, the bus voltage magnitude decreases as the reactive power injection at the same bus is increased [Kun94].
- Large-disturbance voltage stability refers to the system's ability to maintain steady voltages following large disturbances such as system faults, loss of generation or circuit contingencies. This ability is determined by the system and load characteristics, and the interactions of both continuous and discrete controls and protections. Large-disturbance voltage stability can be studied using nonlinear time-domain simulations.

Determination of voltage stability requires the examination of the nonlinear response of the power system over a period of time long enough in order to capture the performance and interactions of devices such as motors, load tap-changer transformers, and generator field-current limiters. Therefore, the time frame of interest for voltage stability problems may vary from few seconds to tens of minutes. The analysis of voltage stability with respect to time span can be divided into:

- *Short-term voltage stability* which corresponds to a time-frame of several seconds and involves dynamics of fast acting load components such as induction motors, electronically

controlled loads and HVDC interconnections. This is also the time scale of synchronous generators and their regulators and FACTS devices [Cap04].

- *Long-term voltage stability* which corresponds to a time-frame of several minutes and involves slower acting equipments as load tap-changing transformers, thermostatically controlled loads and generator current limiters.

Considering the above voltage stability categories, this work deals with long-term large-disturbance voltage instability problems.

2.1.2 The QSS approximation of long-term dynamics

Extensive details about the QSS approximation and validation with respect to detailed time simulation can be found in [VCM97, VCV98, VC00, VCG06], from where the material of this section is borrowed.

The general model of power system dynamics relevant to voltage stability analysis takes on the form:

$$0 = \mathbf{g}\left(\mathbf{x}, \mathbf{y}, \mathbf{z_c}, \mathbf{z_d}\right) \tag{2.1}$$

$$\dot{\mathbf{x}} = \mathbf{f}\left(\mathbf{x}, \mathbf{y}, \mathbf{z_c}, \mathbf{z_d}\right) \tag{2.2}$$

$$\dot{\mathbf{z}}_\mathbf{c} = \mathbf{h_c}\left(\mathbf{x}, \mathbf{y}, \mathbf{z_c}, \mathbf{z_d}\right) \tag{2.3}$$

$$\mathbf{z_d}\left(t_k^+\right) = \mathbf{h_d}\left(\mathbf{x}, \mathbf{y}, \mathbf{z_c}, \mathbf{z_d}\left(t_k^-\right)\right) \tag{2.4}$$

The algebraic equations (2.1) relate to the network equations written in terms of active and reactive currents, and where $\mathbf{y}$ represents the vector of bus voltages magnitudes and phase angles. Alternatively, rectangular coordinates can be used.

Differential equations (2.2) and (2.3) relate to a wide variety of phenomena and controls. On one hand, the short-time dynamics captured in (2.2), involving the state vector $\mathbf{x}$, refer to generators, turbines, governors, automatic voltage regulators, static var compensators, induction motors, HVDC links, etc. On the other hand, equations (2.3) describe the components with long-term continuous dynamics, such as secondary frequency control, secondary voltage control, load self-restoration, etc. The corresponding variables are grouped into $\mathbf{z_c}$.

Finally, the equations (2.4) represent the long-term discrete-time dynamics that stem from controllers acting with various delays on shunt compensation, generator setpoints, load tap changers, equipment protection such as Over Excitation Limiter (OEL) and system protection schemes against short and long-term instabilities, acting on loads and/or generators. The corresponding variables are grouped into $\mathbf{z_d}$ which undergoes step changes from $\mathbf{z_d}\left(t_k^-\right)$ to $\mathbf{z_d}\left(t_k^+\right)$ at some instants of time t_k dictated by the system dynamics itself.

The QSS approximation of long time dynamics is based on the natural time decoupling between the short and long-term dynamics, and consists in replacing faster phenomena, represented in

(2.2), by their equilibrium conditions instead of their full dynamics:

$$0 \quad = \quad \mathbf{f}\left(\mathbf{x}, \mathbf{y}, \mathbf{z_c}, \mathbf{z_d}\right) \tag{2.5}$$

However, it is possible that large changes in $\mathbf{z_c}$ and $\mathbf{z_d}$ eventually induce an instability of the short-term dynamics, in which case the QSS approximation is not valid any longer [VCG06]. In practice however this usually happens when the system operating conditions are already very degraded (low voltage levels)

This method is at the heart of the ASTRE software, developed at the University of Liège, that has been used throughout this research work.

2.1.3 Long-term voltage instability mechanisms

The most typical instability mechanism is the *loss of equilibrium of the long-term dynamics* driven by load restoration [VCV98]. It is generally considered that, after an initial large disturbance, load restoration hastens the voltage collapse process as it tries to restore the load in the distribution system to almost the pre-disturbance level. The load restoration may result from a load's own trend, depending on load characteristics (e.g. thermostatic loads, inductions motors [Tay94, Kun94]), or as outcome of different control system actions. An example of the latter are load tap-changers acting to restore distribution voltages, and hence restore the corresponding voltage dependent loads.

Another mode in which the long-term dynamics may become unstable is through a *lack of attraction towards the stable long-term equilibrium*. A typical scenario would be a loss of equilibrium of the long-term dynamics followed by a delayed corrective control action which restores a stable equilibrium but not fast enough for the system to be attracted by the stable post-control equilibrium [VCV98].

A third instability mechanism that can be thought of, but has not been observed in a real power system, is through *growing voltage oscillations*.

Load modeling

The load composition makes the modeling of the aggregate load a difficult problem, since each load device has a different characteristic. Furthermore, load characteristics can vary significantly with time of day, day of week, season, and weather [ITF95]. In large-scale stability studies, the load aggregate is very often represented by the *exponential model* [CTF93]:

$$P = P_0 \left(\frac{V}{V_0}\right)^{\alpha} \tag{2.6}$$

$$Q = Q_0 \left(\frac{V}{V_0}\right)^{\beta} \tag{2.7}$$

where the α and β exponents can be defined as the normalized partial derivatives of the active and reactive power with respect to voltage around the reference operating point (P_0, Q_0, V_0). Values for these parameters can be found in the literature for single or aggregated loads with specified nature [ITF93, ITF95]. Note that P_0 and Q_0 are the active and reactive power consumed under the reference voltage V_0.

Nevertheless, a unique pair of (α, β) exponents may not be appropriate to model a cluster of loads due to the possible wide variety of voltage characteristics. An alternative is to use the *polynomial model*[1], which consists in grouping loads having identical or almost identincal exponents, resulting in a linear combination of exponential models:

$$P = P_0 \sum_{i=1}^{n} a_i \left(\frac{V}{V_0}\right)^{\alpha_i} ,$$
$$Q = Q_0 \sum_{i=1}^{n} b_i \left(\frac{V}{V_0}\right)^{\beta_i} ,$$

where $\sum_{i=1}^{n} a_i = \sum_{i=1}^{n} b_i = 1$ and n is the number of different load characteristics.

A particular case is when all exponents are integers, resulting in a load characteristic defined by a polynomial in V. A well known case is the ZIP model, which is made of three components: constant impedance (α = β = 2), constant current (α = β = 1) and constant power (α = β = 0), combined into the following quadratic expressions:

$$P = P_0 \left[a_2 \left(\frac{V}{V_0}\right)^{2} + a_1 \left(\frac{V}{V_0}\right)^{1} + a_0 \right] ,$$
$$Q = Q_0 \left[b_2 \left(\frac{V}{V_0}\right)^{2} + b_1 \left(\frac{V}{V_0}\right)^{1} + b_0 \right] .$$

The exponential model has been largely used in this work.

Load tap changers

From the point of view of efficiency and power transfer capability, the transmission voltages have to be high, but it is not feasible to generate and consume power at these voltages. Transformers are the power system equipments which enable utilization of different voltage levels across the system. In addition to voltage transformation, transformers are often used to compensate for variations in system voltages. To this purpose transformers are equipped with taps in one or more windings in order to adjust the ratio [Kun94]. Two types of tap-changing facilities are provided:

[1] Multi-exponential to be precise.

- off-load tap-changing requires the de-energization of the transformer in order to change the tap. This is used when the ratio is changed to meet long-lasting operating conditions.
- Load Tap-Changing (LTC) is used when tap changes are frequent. This is used to take care of daily variations in system conditions.

The LTC is a slow acting, discrete device changing the tap by one step at a time, if the voltage remains outside a deadband longer than a specified time delay. The LTC controls the distribution side voltage, V_l in the case of Fig. 2.1, by changing in closed loop the transformer ratio r according to the logic shown in Fig. 2.2, in order to keep this voltage within the deadband $[V_l^o - \varepsilon\ ,\ V_l^o + \varepsilon]$. The size of a tap step is usually in the range 0.5% - 1.5%. The deadband must be larger than the tap step size, typically twice the tap step, in order to avoid voltage oscillations induced by tap changing. Another feature of the deadband is to avoid the activation of the LTC for small voltage changes around the setpoint value.

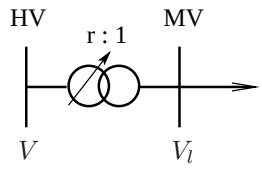

Figure 2.1: Transformer one-line diagram

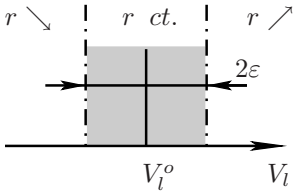

Figure 2.2: LTC control law

Furthermore, in order not to start adjusting the ratio in case of a temporary voltage excursion, an initial time delay is introduced between the moment the voltage exits the deadband and the first tap change. Usually, the initial time delays are larger than the subsequent ones and are adjusted in order to coordinate the cascaded levels of LTCs [OSC03]. Typically, the initial time delay is increasing as the LTC is closer to the load. If the voltage recovers in this time interval, the timer is reset and the action is canceled.

One important constraint of LTCs is the limited regulation range of the variable tap ratio $r^{min} \leq r \leq r^{max}$. Typical values of the lower limit are 0.85 - 0.9 pu and for the upper limit 1.10 - 1.15 pu [VCV98].

Load restoration through LTC action is indirect. When the LTC succeeds to restore the distribution side voltage V_l close to its setpoint value V_l^o, the load power, which depends on bus voltage, is also restored. This property makes the load to appear in the long term as a constant power load.

A large-disturbance long-term stable scenario, involving LTC load restoration, is sketched in Fig. 2.3, where the solid curves represent the pre- and post-disturbance network characteristics, the dotted lines are the short-term load characteristics for different values of r and the dashed vertical line is the long-term load characteristic.

As suggested in the figure, the network characteristic shrinks as a consequence of the disturbance, the system operating point changes from the initial point O (which is the intersection

between the pre-disturbance network characteristic and the long-term load characteristic) to point O' corresponding to the intersection of the short-term load characteristic with the post-disturbance system characteristic. The fact that the load voltage is low results from the voltage reduction experienced by the transmission system and the reduction in voltage dependent load power when moving from O to O'. If the load voltage is outside the deadband, the LTC starts decreasing the transformer ratio r with the intention to restore the load voltage. This causes the short-term characteristics to change as shown in the figure. The operating point moves along the post-disturbance network characteristic until a new operating point is reached, close to the point where the long-term load characteristic intersects the new network characteristic.

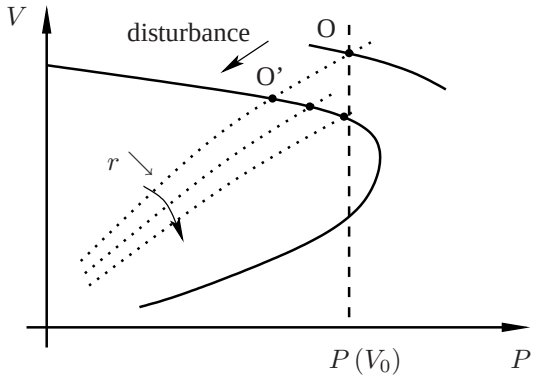

Figure 2.3: Load restoration through LTC

In the sequel, the load restoration is further illustrated using the simple test system shown in Fig. 2.4, which consists of a load fed by two generators through a cascade of transformers with LTCs. The transformers are assumed ideal for simplicity. Let us assume that the disturbance is the loss of one circuit of the transmission line, applied at t = 10 s. The LTCs voltage setpoints are V_4^o = V_5^o = 1 pu with a half-deadband ε = 0.01 pu. LTC operation starts after an initial delay of 20 s for T_1, respectively 50 s for T_2, and continues at a rate of one tap change each 10 seconds.

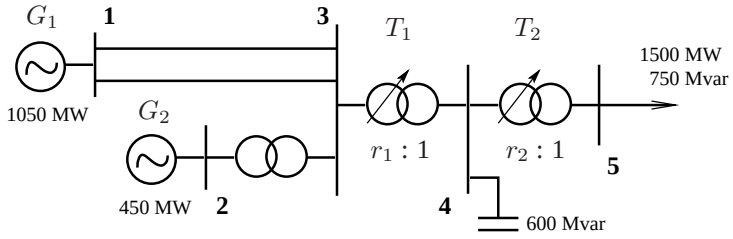

Figure 2.4: One line diagram of the simple test system

The diagram on the left in Fig. 2.5 presents the evolution of the system in the (P_5,V_3) space, while the one on the right shows the time evolution of the transmission voltage V_3, and LTC controlled voltages V_4 and V_5. The dash-dotted lines show the LTC deadbands. The oscillations around the long-term operating point are due to dynamic interactions between the cascaded LTC transformers, as explained hereafter.

Right after the disturbance, both LTC-controlled voltages fall below their respective deadband. Therefore, the LTCs attempt to restore their secondary voltages. The first to initiate the voltage recovery action is the upstream LTC, which has a smaller initial time delay, 20 s. It can be seen that, by reducing r_1 the upstream LTC T_1 is restoring both V_4 and V_5. However, at t = 60 s, after an initial time delay of 50 s, the downstream LTC T_2 starts to act, as the controlled voltage V_5 is still outside the deadband. The effect of combined actions on r_1 and r_2 is a faster recovery of voltage V_5. The opposite effect is seen on V_4, which under the same conditions is decreasing. At t = 80 s, r_2 stops decreasing as V_5 is brought back in the deadband, but this voltage keeps on increasing and eventually exits the deadband on the upper side, under the effect of the still changing r_1. Again, after the initial time delay the downstream LTC starts to increase r_2 in order to reduce V_5, with the effect of increasing both V_4 and V_3. Finally, after another activation of the upstream LTC, both controlled voltages settle down in the deadband.

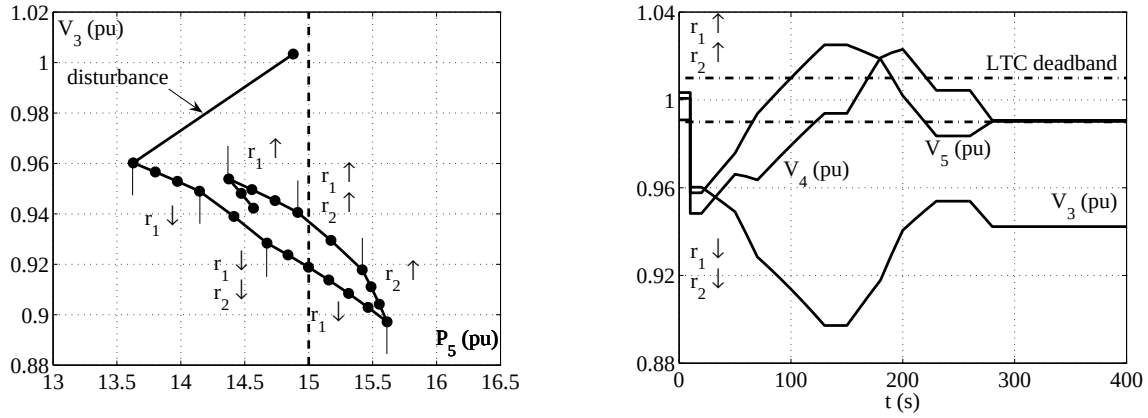

Figure 2.5: LTC load and voltage restoration

Note that the final restored power is different than the initial one and smaller than the long-term load value, dashed vertical line in Fig. 2.5. This is due to the deadband effect, i.e. the LTC stops acting as soon as the controlled voltage enters the deadband. Therefore, the deadband creates a *stable equilibrium area* around the stable long-term equilibrium point.

One important aspect of LTC functioning is that the actions, taken to control subtransmission or distribution voltages, have the opposite effect on the transmission voltages [Cal84]. As can be seen in the example, the transmission voltage V_3 is decreasing when the downstream voltages are increasing and vice versa.

2.1.4 Illustration of long-term voltage instability

In this section, the simple test system, on which the load restoration mechanism was described, is used to illustrate the loss of equilibrium of the long-term dynamics. To this purpose two scenarios are considered.

Loss of local generator

The first instability results from the loss of generator G_2, at t = 10 s. The left diagram in Fig. 2.6 presents the evolution of the system in the (P_5,V_3) space, where the dots represent the intersection between the short-term load characteristic and the post-disturbance network characteristic. The time evolutions of the transmission V_3, subtransmission V_4 and distribution V_5 voltages are shown on the right in the same figure.

As can be seen, under the effect of the disturbance, the network characteristic shrinks and the voltages experience a large decrease. Since the LTC controlled voltages are well outside their deadbands, the LTCs start decreasing the transformers ratio in order to restore their downstream voltages. First the distribution voltage increases, but after some time starts decreasing as the *critical point* of the post-disturbance system characteristic was crossed, as depicted in the left plot of Fig. 2.6. After this point both voltage and load power restoration by the LTCs fail. Eventually the LTCs hit their limits, the transmission voltage settles down to a low, unacceptable value (that in practice will trigger some protections).

It should be mentioned that the final operating point should not be considered stable, as other load recovery mechanisms may continue acting causing further system degradation. Furthermore, there is a point beyond which further decrease of transformer ratio leads to loss of short-term equilibrium, as illustrated in the next example.

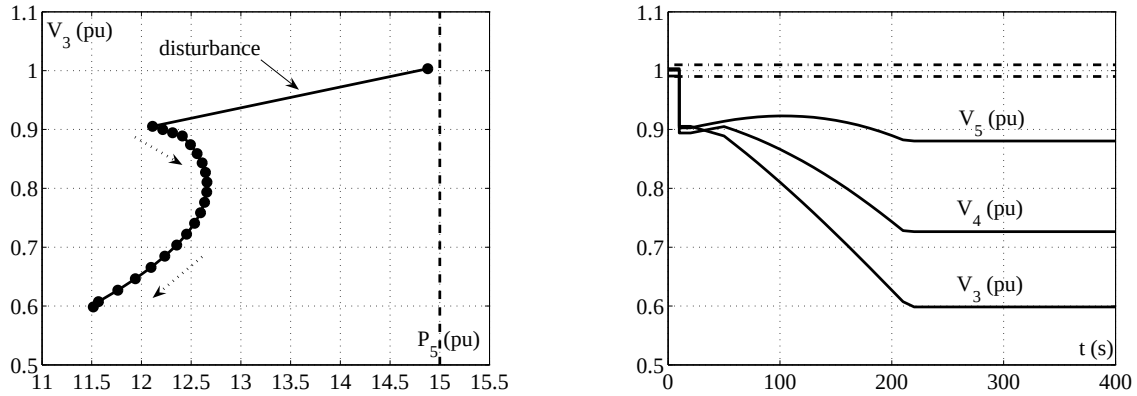

Figure 2.6: LTC driven voltage instability

The nature of instability is revealed by the fact that there is no intersection point between the long-term load characteristic and the post disturbance network characteristic, as can be seen in Fig. 2.6 (left plot).

Loss of line and OEL activation

This case involves the same disturbance used to illustrate load restoration by LTCs, as well as the activation of the Over Excitation Limiter (OEL) of generator G_2.

As in the previous case, soon after the disturbance the LTCs start acting, voltage restoration being possible, since a long-term equilibrium point exists (see left diagram in Fig. 2.5). However, the slow decrease of transmission voltage V_3, caused by successive ratio changes, forces generator G_2 to produce more reactive power. Eventually, the field current of the latter increases above its limit, and after some temporization the OEL comes into play. Consequently, the network characteristic seen from the load further shrinks, and does no longer intersect the long-term load characteristic. Even more, the operating point is already below the critical point, as can be guessed from both plots in Fig. 2.7.

At t = 90 s, following the successive tap changes, the short-time equilibrium is lost, which is revealed in detailed time simulation by a loss of synchronism of G_2 [VCV98].

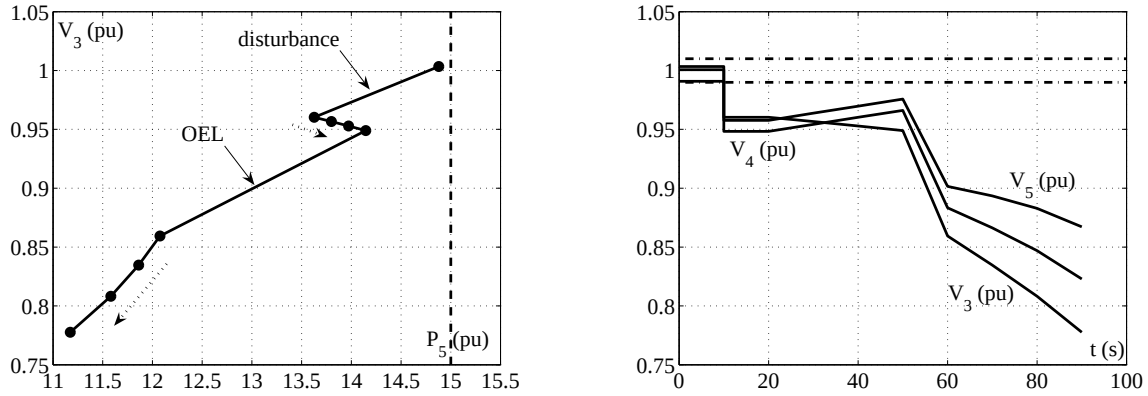

Figure 2.7: LTC and OEL driven instability

The main conclusions that can be drawn from the two shown examples is that emergency controls should act before further degradation of operating conditions (e.g. losing other system equipments due to prevailing conditions), customer voltages become unacceptable and short-term dynamics become unstable. Furthermore, the control actions should be strong enough in order to restore a long-term equilibrium point and to ensure the attraction towards this operating point.

2.1.5 Controls to counteract voltage instability phenomena

In power system operation, a distinction is made between preventive and corrective countermeasures against instability phenomena [CTF95].

Preventive countermeasures are actions which are determined in the power system planning and operation stages, for a set of *credible disturbances*, in order to ensure that no major consequences would follow their occurrence. The control actions are usually operator-initiated and are based on power system security assessment off-line or on-line simulations. The means to improve voltage stability involve mainly shunt compensation switching, LTC modified control, generator voltage control and active power rescheduling, and possibly load curtailment [VC00].

Although preventive countermeasures tend to be reliable and robust, corrective countermeasures are often more effective. The latter are needed to face severe disturbances [CTF95]. Usually these are *non-credible disturbances*, with a small occurrence probability, for which it would be too expensive to take preventive measures.

According to the previous section conclusions the corrective controls can be divided into two categories:

- control actions which stop the system degradation. These mainly act on load restoration mechanisms, such as LTC controllers. To this purpose, several emergency LTC control measures are in use or have been proposed in the literature [VCV07]:
  - *tap blocking* - it consists simply of deactivating the control mechanism that is normally restoring the distribution side voltage of the power delivery transformer. In this way load restoration is canceled, or, in the worst case, delayed;
  - *tap locking* - is the action of assigning a specific tap position, where the LTC will move and then lock;
  - *tap reversing* - consists in changing the control logic, so that the LTC is controlling the transmission side voltage instead of the distribution side.
- control actions which restore a long-term equilibrium. This can be achieved through:
  - *fast increase of generator voltages* - an increase in generator voltages may contribute to system stabilization, provided that the maximum deliverable power becomes larger than the power that the loads attempt to restore[2];
  - *shunt compensation switching* - automatic action in response to low voltages;
  - *reducing load consumption* - this is the ultimate countermeasure and it can be implemented either directly as load-shedding or indirectly through a decrease in LTC voltage setpoint.

In the sequel, some of the above mentioned long-term voltage instability countermeasures are illustrated on the previously introduced simple test system. The original voltage unstable case considered is the one presented in Fig. 2.6, where the initial disturbance is the loss of generator G_2.

LTC tap blocking

From the customer point of view, in an unstable situation the best blocking position is the one corresponding to the highest distribution voltage, thus to maximum restored power. This operating point corresponds to the *critical point* of the post-disturbance system configuration,

[2]Thereby restoring an intersection point between the network characteristic and the long-term load characteristic.

i.e. the tip of the PV curve in Fig. 2.6. However, in real-life systems, the on-line determination of this point remains a challenge, mainly due to the difficulty of running state estimation fast and reliably enough [VM01].

In the case illustrated in Fig. 2.8 both cascaded LTC transformers are blocked when the transmission voltage V_3 falls below 0.8 pu. It must be emphasized that after this action the system degradation is only slowed down or stopped (in our case). If no other corrective control action is taken, in order to give to the system a new long-term equilibrium operating point, and the LTCs are unblocked the instability process would proceed.

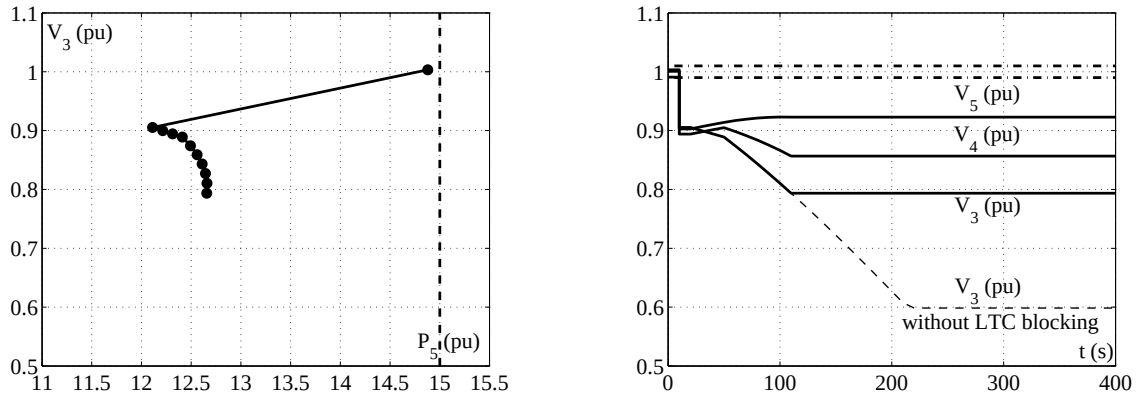

Figure 2.8: Example of LTC blocking

Another drawback of this technique is that other load restoration processes may keep on depressing transmission voltages. Such a case is illustrated in Fig. 2.9 where we consider that only the downstream LTC is blocked[3] when the transmission voltage V_3 falls below 0.8 pu, the upstream one continuing to control its secondary side voltage. In comparison with the case presented in Fig. 2.8, the transmission voltage decrease is only slowed down, and stops when the LTC hit his limits.

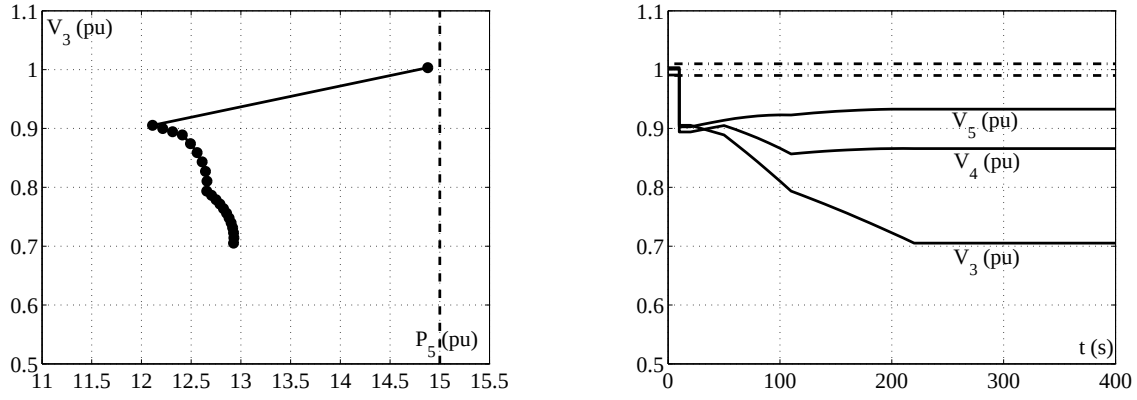

Figure 2.9: Example with only downstream LTC blocked

[3]In real-life power systems the blocking scheme is applied to both levels of transformers in cascade.

The other LTC related techniques, tap locking and voltage setpoint decrease, raise the same problem with respect to other load restoration processes. Furthermore, a single tap position or modified setpoint may not suffice to face all possible scenarios. In all the cases, the LTCs on which to act, must be identified.

LTC tap reversing

The technique that we present in this subsection is not implemented to our knowledge. It is an improved LTC control that we proposed in [OSC03], where the interested reader may find more details and explanations as well as an application to a large-scale system.

As outlined before, the long-term instability mechanism is caused by the "blind" action of the LTC below the critical point. This can be counteracted by changing the LTC control law so that the transmission voltage V is prevented from falling below some setpoint value V^o.

The modified logic is shown graphically in Fig. 2.10. As long as the transmission voltage V remains above $V^o + \varepsilon'$ the LTC operates according to the usual logic. On the contrary, as soon as V falls below $V^o - \varepsilon'$, the LTC increases r in order to decrease the load voltage (and power), and hence increase V. This modified control is referred to as *reverse logic* in [OSC03]. The deadband $[V^o - \varepsilon' , V^o + \varepsilon']$ prevents from oscillating in between the two logics.

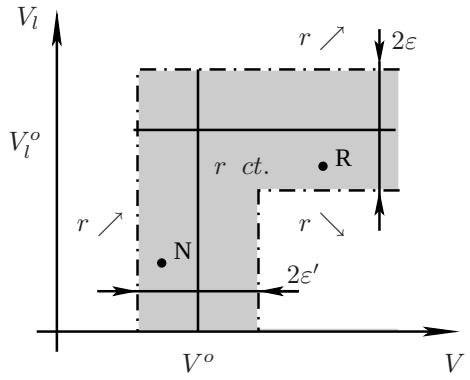

Figure 2.10: LTC reverse control law

This modified control presents a *closed-loop* behavior, extensively illustrated in [OSC03]. Once the reverse logic has been activated, and as long as the LTC is not limited, r will be automatically adjusted so as to prevent V from falling below $V^o - \varepsilon'$. This occurs when another load restoration process or an increase in demand is taking place. This behavior cannot be obtained with the previously mentioned LTC related techniques. Moreover, the closed-loop nature of the control guarantees the robustness of this emergency control scheme with respect to the inevitable uncertainties on the load behavior.

Following a disturbance, the final operating point will be either:
- like R in Fig. 2.10, where the load voltage and power are restored (except for the deadband effect), or

- like N in the same figure, where load voltage has been decreased to prevent V from falling below V^o
- in the non-grayed areas of Fig. 2.10, only if the LTC hits a limit.

As with the usual control logic, there must be a coordination between the multiple LTCs in cascaded layers. In emergency conditions, the objective being to quickly stop the system degradation, the tapping delay of each transformer should be as short as possible (taking into account mechanical constraints) as soon as it enters reverse logic, irrespective of the layer and whether it is the first step change or not. Thus, the initial time delay can no longer be used for LTCs coordination purposes. In this case the voltage setpoint values are used as coordination method. The simulation results reported in [OSC03] indicate that the voltage setpoint should increase as the LTC is closer to the load. Therefore, the downstream LTCs actions are favored.

Figure 2.11 shows the successful operation of the LTC reverse logic, for the considered simple test system and disturbance. Both LTCs are monitoring V_3 in reverse logic, the considered setpoint values being $V^o_{T_1}$ = 0.85 pu and $V^o_{T_2}$ = 0.90 pu as detailed in Fig. 2.12.

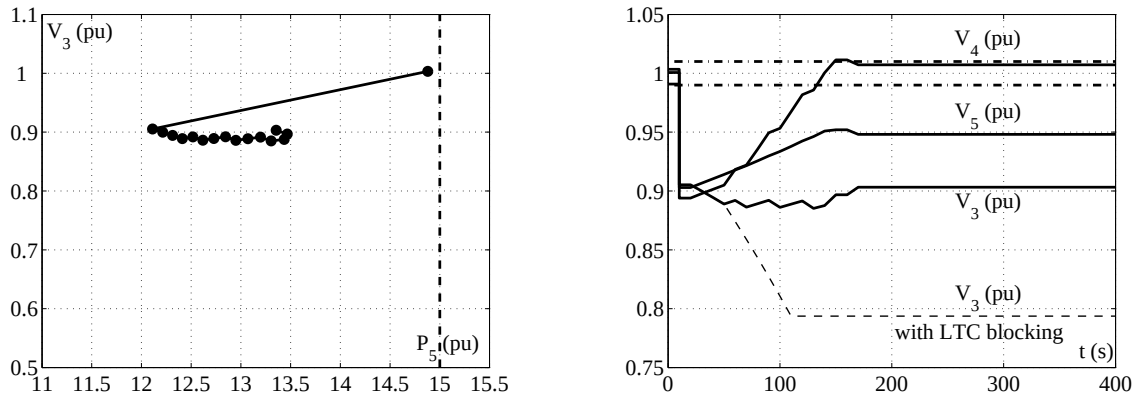

Figure 2.11: Example of LTC reverse logic

Figure 2.12 also illustrates the closed-loop behavior of the proposed scheme, as long as voltage V_3 is outside the deadband, the downstream LTC is increasing r_2 in order to preserve the transmission voltage.

In a real system, by restoring V_4 voltage to its setpoint value, the reactive losses of subtransmission network would decrease and the capacitive support of shunt compensation would increase, which would decrease the reactive power drawn from the transmission system. This, in turn, would allow the load voltage to be eventually somewhat increased, and more load to be restored. A similar conclusion regarding the control of intermediate voltages was drawn in [CCM96], although in a slightly different context.

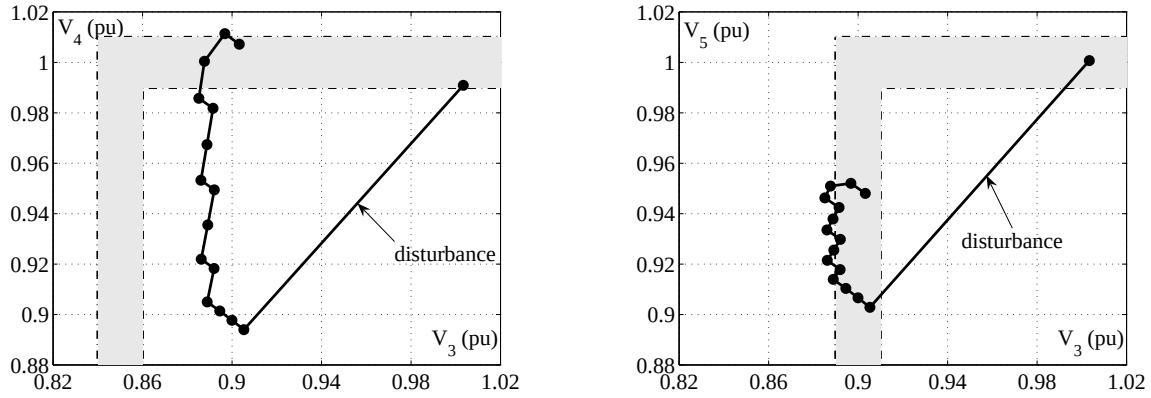

Figure 2.12: LTC reverse logic in voltage space

Generator voltage increase

Proceeding with our example, Fig. 2.13 shows the benefit of quickly raising the voltage setpoint of G_1 by 0.1 pu at t = 100 s. After the generator voltage increase, the new network characteristic intersects the long-term load characteristic, indicating that a new long-term equilibrium has been restored. After a period of oscillations, due to LTC interactions, both sub-transmission V_4 and load voltage V_5 regain their pre-disturbance values.

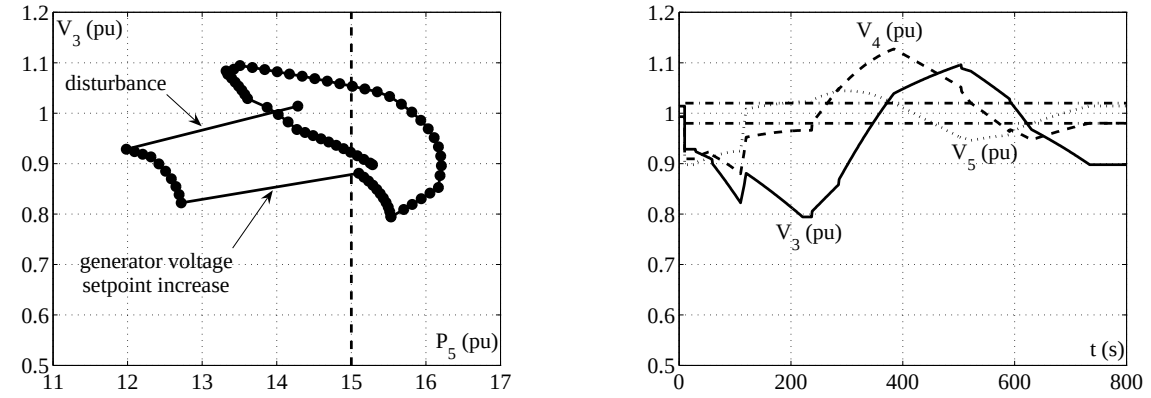

Figure 2.13: Example of generator voltage increase

Load shedding

It is well known that load shedding is a cost effective countermeasure against long-term voltage instability triggered by large disturbances [Tay94]. One argument for undervoltage load shedding is that load will be lost anyway when exposed to abnormal voltage; hence it is better to have the load shedding action under the control of a system protection scheme, with known trip settings and time delays.

Time, location and amount are three important and closely related aspects of load shedding against voltage instability. An extensive discussion of these aspects is presented in Chapter 4.

For the sake of completeness, an illustrative example is presented in Fig. 2.14, where after the initial disturbance applied at t = 10 s, a load shedding action takes place at t = 140 s. The latter consists in reducing the load by 300 MW and 150 Mvar. As in the previous case, the instability mechanism is stopped and a new long-term equilibrium point is restored.

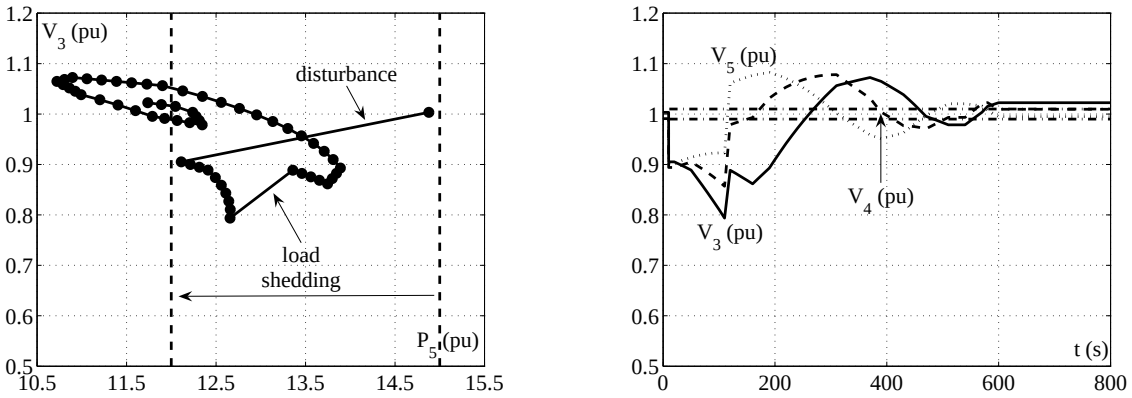

Figure 2.14: Example of load shedding

2.2 Thermal overload problems

Thermal limitations are the most common constraints that limit the capability of a transmission line, cable, or transformer to carry power. The actual temperatures occurring in the transmission line equipment, due to *Joule effect*, depend not only on the current but also on ambient weather conditions, such as temperature, wind speed and direction, which are influencing the dissipation of heat into the air. Thermal ratings for transmission lines are usually expressed in terms of current densities, rather than actual temperatures, for ease of measurement.

Historically, utilities have operated transmission systems conservatively in order to provide high reliability through moderate transmission line loading and redundancy [HD88]. However, environmental, regulatory, and economic pressures have forced utilities to increase line loadings such that some of them operate close to their static ratings or their maximum allowable ratings.

Thermal limits are imposed because overheating leads to two possible problems:

- the transmission line loses strength because of overheating reducing the expected service life of the material. Operating underground cables or power transformers at excessive temperatures also shortens their service lives considerably due to damage to their insulation;

- the transmission line expands and sags. Because overhead transmission lines operate at high voltages and have no electrical insulation, certain legal ground clearances must be ensured for obvious safety reasons [BB83]. Furthermore, if the temperature is repeatedly too high, an overhead line may permanently stretch, which causes its clearance from the ground to be less than required.

Nevertheless, because this overheating is a gradual process, higher currents can be allowed for limited periods of time. A study of relevant data [VVR86] reveals that the time for which a line can be loaded to a particular level is inversely proportional to the square of the loading level and is of the form shown with solid line in Fig. 2.15. In practice, at least two ratings are defined, illustrated with dashed line in the same figure:

- thermal "normal" rating: the current level which can be supported indefinitely;
- thermal emergency ratings: are levels the line can support for specific periods of time, for example, several minutes or hours (e.g. long-term emergency rating - 4 hours, short-term emergency rating - 20 minutes [DL03]).

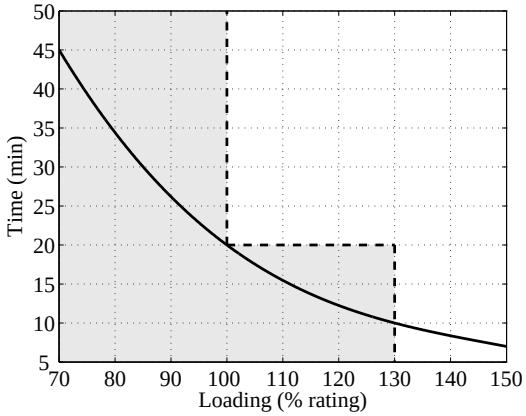

Figure 2.15: Relationship of transmission line loading and maximum time

2.2.1 Cascade tripping

In an unstressed power system and with normal operating protective systems, one component failure has little influence on other components, but in a system that is highly stressed the failure of one component can increase the likelihood of other subsequent component failures.

For example, a line tripping or a generator outage will force power flows to follow some other paths, and in already stressed conditions some other components may approach limits or get overloaded. When a transmission component gets overloaded, it may eventually trip and again the carried power is redistributed over the remaining transmission equipments. This property may lead, in case of subsequent component overload, to cascade tripping.

The remaining components which are not overloaded become progressively more loaded as the cascade tripping proceeds. The extent of the cascade depends on the initial individual system component loadings.

2.2.2 Methods to increase transmission line thermal rating

The *ampacity* is the electric current which a device can carry within specified temperature limitations and in a specified environment in terms of: ambient conditions (temperature, wind, etc.), power loss and heat dissipation.

Transmission circuits include sections exposed to different ambient conditions. Therefore, the overall ampacity of a transmission circuit is given by the section with most restrictive ampacity limit. If any transmission circuit is loaded above the ampacity limit of the most restrictive section, it is said that the entire circuit is loaded beyond its ampacity [WFM82]. Thus, modest increase in the overall thermal rating of the transmission circuit can sometimes result form replacing an inexpensive element, such as a switch or circuit breaker. The thermal limit may be also raised by making similar the thermal limits of all line sections [DL03].

When utilities calculate the static thermal rating, they must assume worst-case ambient conditions, i.e. usually the highest summertime temperatures and solar intensity, low winds, and no rain, which results in higher conductor temperatures and greater sag. This approach has seriously limited the efficient use of the transmission facilities, because the assumed conservative conditions rarely occur [WFM82]. Most of the time the considered thermal ratings are much lower than the true capacity of transmission lines.

As a result, many transmission lines have significant “hidden” capacity that could be used if dynamic thermal rating technology was employed. For this, a real-time ampacity program is necessary in order to predict the transient temperature of the conductor during emergency conditions when line currents may vary significantly over relatively short periods of time [BB83]. This temperature variation results not only from the transmission line loading, but also due to weather conditions, air temperatures and wind velocity and direction which are varying in a seemingly random pattern. The knowledge of the real-time cooling conditions allows a real-time line loading assessment. Furthermore, with the knowledge of the transmission line temperature history, the static rating can be re-assessed without excessive sag or loss of strength [CBJ02].

Among the expensive methods to increase the line thermal rating we can cite the line conductors replacement (e.g., bundling the original conductor with another one or replacing it by a more conductive one) and the transmission circuit voltage upgrade (e.g., from 225 to 400 kV) [DL03]. Both require substantial reinforcement of the tower structures in order to support the increase in weight and transverse loading. Furthermore, the change in voltage level require greater clearances and string of insulators increase, not to mention the expense in substation equipment.

Nevertheless, line uprating does not mean in all the cases an increase in system security. A

small illustrative example is given in Fig. 2.16, where starting from an initially N-1 secure system (a.), the line rating is increased from 300 to 400 MW (b.). As the generation is cheaper in G_1, economics will push the system towards its new, larger N-1 security limit [Kir07]

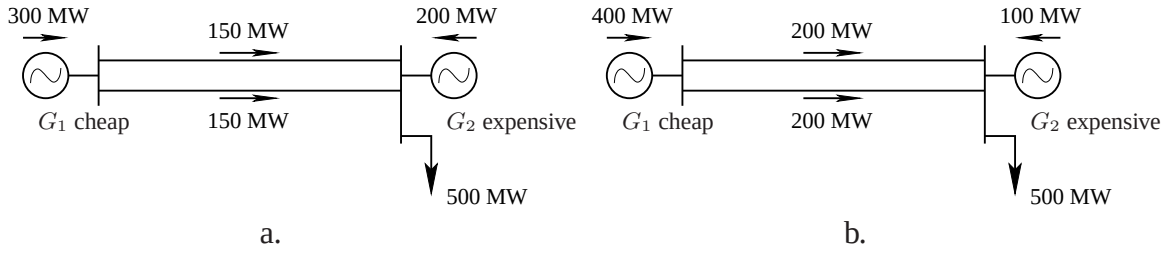

Figure 2.16: N-1 secure system with line limit of (a.) 300 MW and (b.) 400 MW

2.2.3 Controls to prevent or alleviate thermal overload

Line current is influenced by both active and reactive power flows. The key parameters affecting the active power flow in any transmission line are: the line terminal bus voltages, line impedance, and relative phase angle between the sending and receiving ends, as recalled in Fig. 2.17.

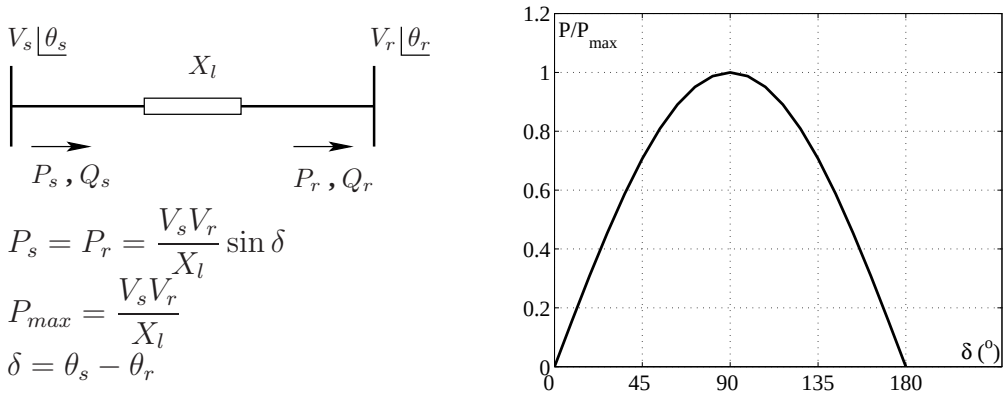

Figure 2.17: Line transmission power characteristic

Since voltage magnitudes must be kept within narrow limits, their variation for power flow control is not significant. Thus, line reactance and voltage phase angle difference are the only practical alternatives for power flow control, even more since there are less restrictions on these parameters [OCG03].

Variation in generated powers and loads can modify the phase angles. Traditionally, generation rescheduling is the most used control method, by power system operators, to reduce or eliminate line overload conditions. Such generation shifts are generally in conflict with the economic generation dispatch. Any deviation from this predetermined schedule results in increased production and transmission costs [Bro88]. Moreover, some line overload situations

cannot be alleviated by generation rescheduling alone. In emergency conditions a proper combination of generation rescheduling and load shedding may alleviate such overloads [MBS79].

Another method is line and bus-bar switching. This does not greatly change the transmission penalty factors, thus the economic dispatch is less affected. In practice, bus-bar switching is preferred to line switching, even though it is more complicated, because it causes smaller disturbances. Nevertheless, when dealing with line overload problems, system operators must be helped by real-time software to identify the appropriate bus-bar or line switchings, and make sure that these actions will indeed relieve the system and will have no adverse effects elsewhere [Bro88].

Series compensation with fixed capacitors has been used for a long time to decrease the line reactance, thereby decreasing the angular difference between sending and receiving end voltages. However, their cost must be justified by other aspects such as dynamics.

The phase-shifting transformer is one of the principal control devices used for a long time in power systems to help direct electricity flows in local parts of the transmission network and to provide possible relief of overloaded facilities in both preventive and corrective modes [BK97, TSO74]. In order to control the active power flows in an efficient way, operators must be provided with some means of determining optimum phase shifter settings and limits for specific system configurations.

With the development of power electronics, other devices with high-speed response and unlimited number of operations, known under the name of Flexible AC Transmission Systems (FACTS) became available. These controllers can dynamically control line impedance, line terminal voltages, active and reactive power flows. From the point of view of their main function FACTS devices could be divided into [Ere97]:

- dynamic voltage control devices: Static VAR compensator (SVC) and the Static Compensator (STATCOM);
- dynamic current flow control devices: Thyristor Controlled Series Capacitor (TCSC) and Static Synchronous Series Compensator (SSSC);
- power flow control devices: Thyristor Controlled Phase Angle Controller (TCPR) and Unified Power Flow Controller (UPFC);

Using FACTS devices control for relieving overloads and voltage violations caused by system disturbances, offers economic advantages compared with the corrective control strategies presented above, since it has low operational costs and no additional costs resulting from changes in generation and/or load. Nevertheless, it is not likely that FACTS devices will be installed for the sole purpose of redirecting power flows, as their investment cost is still high. Their use is mainly motivated by power system dynamic improvement.

Chapter 3

Identifying plausible cascading events

After recalling fundamentals of cascading events, protection systems and hidden failures, an implementation of the event tree approach is proposed to determine possible sequences of cascading failures with severe impact on a given power system. The algorithm takes into account protection systems hidden failures and transmission system equipment overloads. At each level of the event tree development, the sequence probability order is computed, and a linear approximation method is used to identify possible harmful sequences. These are furthermore analyzed with a time domain simulation tool in order to assess their impact on the power system. The proposed algorithm was tested on a real-life model and the overall results as well as the power system behavior for some of the so-discovered cascading scenarios are presented. The emergency control of these scenarios will be further considered in Chapter 6

3.1 Cascading events

Under heavy load conditions, combined with inappropriate protection system action, losing a critical system equipment can represent the initiating disturbance of a cascading event. The latter can be defined as an uncontrolled disconnection of power system components caused by power system parameters degradation [Eli03, PD00].

During a cascading event, the loss of power system components exhibit a clustering behavior, i.e. the loss of one component raises the probability of losing another component. The latter can be more or less close to the initiating disturbance area, due to the impact on the power system (e.g., transient oscillation, power flow increase in the remaining components, voltage excursions) and component protection systems. Protection systems participate to the development of a cascade event through their connection structure (e.g., components connected to the same faulted bus), correlation between protection schemes (e.g. protections that act together to clear the same fault) and protection hidden failures.

Such sequences of cascading disturbances can propagate through interconnections producing

significant load loss, potential islanding of transmission networks and in extreme cases blackouts, such as the ones presented in Chapter 1.

The occurrence probability of such events is very low, but the impact on customers and the damage on power system are important. Knowing that preventive controls against cascading outages are too expensive, enhanced emergency controls are needed to face this kind of events.

The forecasting of such events is very difficult. Furthermore, the analysis of these scenarios is also difficult due to the large number of possible cascading events for different system topologies and stress conditions. Hence, a specific analysis procedure is required, to determine the most likely disturbances, and a filtering tool is needed to discard the events with little impact on the power system.

3.2 Protection systems and hidden failures

Recent studies of US power transmission grid major disturbances have shown that over a long time interval, more than 70% (75% reported in [PT96]) involved relaying systems, not necessarily as the initiating event, but contributing to the cascading nature of the event [NERC, CTD03].

Protection systems are designed to initiate switching actions to rapidly and reliably isolate faults. Standard designs ensure the reliability of a fault isolation at the expense of some small likelihood of false trips. This approach minimizes component system damage and is appropriate when the system is in a normal operating state.

The main drawback is that, in general, these relays take actions to protect a localized region of the network without considering the impact on the whole network [TCM01]. For example, under stressed conditions, due to outages or excessive loading, additional switching to isolate faults will cause additional stress that may contribute to widespread system failures. Moreover, if the switching is due to an incorrect relay operation, the protection system contributes to power system weakening.

A protection system detects fault conditions by continuously monitoring system variables such as current, voltage, frequency and impedance. The following requirements are the basis of protective systems design criteria:

1. *Reliability* - provide both dependability and security, as recalled in Section 3.2.1;
2. *Speed* - relays should respond to abnormal conditions in the least time possible;
3. *Selectivity* - the relay property to operate only for the type of faults for which is designed;
4. *Simplicity and economy*.

3.2.1 Reliability concept

Reliability represents the degree of certainty that a piece of equipment will perform as intended. In the protection system case reliability refers to the action of the relays. There are two modes in which the relays can be unreliable: fail to operate when they suppose to, and operate when is not expected to. Thus, the reliability encompasses two notions [LG01, HP95]:

- *dependability*: certainty that a relay will respond correctly for all faults for which it is designed and applied to operate;
- *security*: certainty that a relay will not operate incorrectly for any fault.

Security is defined in terms of protection zones for which a given relay or protective system is responsible. The relay will be considered secure if it responds only to faults within his protection zone. The protection zone has two important characteristics: all the equipments must be part at least of one protection zone and protection zones must overlap to ensure that all system components are entirely protected. Moreover, vital equipments are covered by at least two protection zones.

Most protection systems are designed for high dependability, in a way that faults to be always cleared at the expense of some false trippings, thus lower security. In these days when the systems are operated closer to their security limits this philosophy may no longer be viable; a compromise between dependability and security must be found.

An electric power system is divided into protection zones for each power system equipment. The division is such that zones are given adequate protection while keeping service interruption to a minimum. A one-line diagram of a part of a power system with its zones of protection is presented in Fig. 3.1 [HP95]. Note that zones overlap in order to avoid unprotected areas.

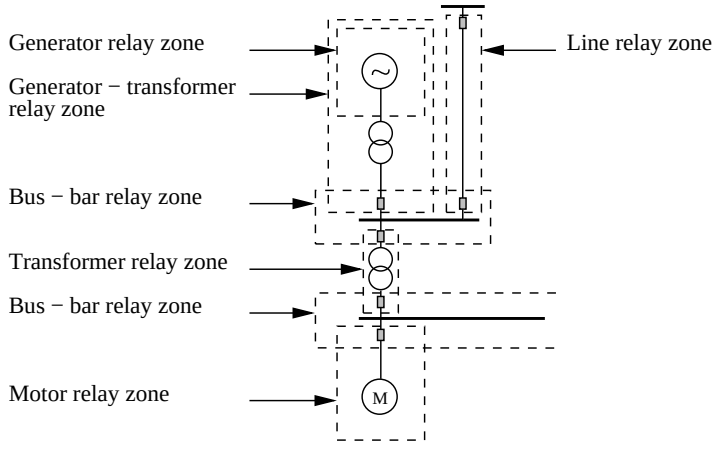

Figure 3.1: Typical power systems protection zones

The main protection system for a given zone of protection is called the primary protection system, and it is set to operate in the fastest time possible and to remove the least amount of equipment from service. On extra high voltage systems it is common to use duplicate primary protection systems in case a component in the primary protection chain fails to operate. These are backup protections which are required to operate only when the primary protection has failed to clear the fault. Furthermore, the backup function should not interfere with the primary function. The tripping logic of the backup protection system is the same as for the primary one, but the relays are set up to be slower and may remove more system elements than necessary in order to clear the fault.

There are two different back-up protection systems:

- *local backup*, when the relays are installed in the same substation and are using some of the equipments of the primary protection. When needed, the backup scheme trips only the protected equipment. The drawback is that both primary and backup protection may fail together if the faulty component is common to both;
- *remote backup*, when the relays are located in a separate place and are completely independent of the main relays, transducers, batteries and circuit breakers that they are backing up. For complex systems the backup may not "see" all the faults for which it is supposed to act. Also, as mentioned above, remote backup may disconnect more equipments.

3.2.2 Protection zone

In order to define the protection zone the notions of underreaching and overreaching protections must be introduced [SDE76]:

- *underreaching protection*: relays at a given terminal do not operate for faults at remote locations on the protected equipment. Thus the relays are set not to see faults beyond a given distance;
- *overreaching protection*: relays at one terminal operate for faults beyond the next terminal of the protected equipment. They may be constrained not to operate until a signal from the remote terminal has been received indicating that the fault is inside the protected line section. The constraining signal is used in order to coordinate the protection systems action.

Fig. 3.2 illustrates the protection zones for a distance relay (located at bus A) used to protect transmission lines, which responds to the impedance between the relay location and the fault location. The dotted line represents the zone of the transmission line to be protected. All the faults in this area must be cleared without delay.

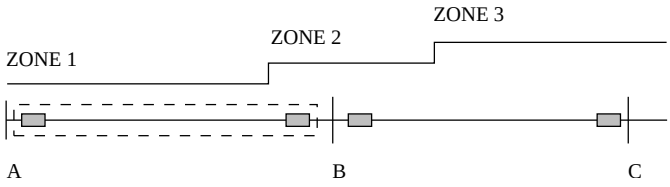

Figure 3.2: Protection zone for distance relay

This zone is mainly covered by the protection Zone 1, which due to uncertainty in measuring the apparent impedance, is set to 85 - 90% of the line length, in order not to overreach the remote end of the transmission line.

As protection Zone 1 alone does not protect the entire line length, for the remaining distance the relay is equipped with another zone which overreaches the remote end. This is known as the distance relay Zone 2, which has a delay in order not to act on faults that must be cleared by the Zone 1 distance protection of the line beyond the remote end. This coordination delay is usually of the order of 0.3 seconds.

The reach of Zone 2 is generally set to 120 - 150% of the protected transmission line length. Therefore protection Zone 2 covers the remote end and acts as a backup for the protection Zone 1 of the neighboring lines beyond the remote end, e.g. line BC in Fig. 3.2. Nevertheless, the Zone 2 of distance relay of one specific line must not overreach the Zone 2 of another line distance relay, otherwise some faults in Zone 2 of both relays may lead to unnecessary tripping of both lines.

In order the relay, in our case from bus A, to be used as a backup for the entire neighboring line, it is customary to provide another zone of protection. This is known as Zone 3 of protection, which extends to 120 - 180% of the next line length. This zone must be coordinated with Zone 2 of the neighboring circuit, the coordination delay is of the order of 1 second.

The main difficulty with this protection is the impossibility to clear a fault situated close to one end, instantaneously from both ends. This is due to the fact that measurements are taken separately at each remote end and delays are necessary between different protection zones. A solution to this problem is the differential comparison protections which uses measurements and controls the breakers from both remote ends. Because of high costs (of measurements and communication) and transmission errors this protection type is used only for transformers and short transmission lines.

Another way to solve this problem is to use *pilot protections*. These require a communication channel between the remote ends of the transmission line. The communication channels generally used are: power line carrier, microwave, fiber optics and communication cable. In this case, in order to act, the breaker must receive the proper signal from the protection scheme at the remote end. If the signal is received, the transmission line is tripped without delay from both ends.

Based on communication between different protections, *functional groups* can be defined. These represent groups of components that operate and fail together due to their connection structure and protection scheme [CTD03, Che04].

3.2.3 Failure mode classification

The failures of generating units, transmission lines, transformers and other power system components can be grouped into the following categories [GB74]:

- *independent outages*, when the outage of each equipment is caused by an independent fault and does not depend on what previously happened in the power system. Independent outages of two or more elements are referred to as simultaneous independent outages. The probability of such an event is calculated as the product of individual equipments failure probability. An example of independent outages is a plant failure followed by a network fault.

- *dependent outages*, when the outage is the result of the occurrence of one or more other outages. Dependent outages are protection systems responses to changes in system parameters caused by previous events in the power system. The probability of such combined outages can be approximated, due to their low probability, with the product of the failure probabilities of each equipment as if they were independent events. An example of dependent outages is the unappropriate trip of the second circuit of a double-circuit transmission line, due to a faulted relay detecting the increase in power flow caused by the independent outage of the first circuit line.

- *common-cause outages* are outages having an external cause with multiple failure effects, where the effects are not consequences of each other. The effect of common-cause outages on reliability indices can be significant and comparable with the effect of N-2 or higher-order outages. The probability of a common-cause outage is larger than the probability of independent outages resulting in a similar event. An example is the primary protection failure followed by the back-up protection clearing, which disconnects more equipments.

- *station originated outages* can occur due to a ground fault on a breaker, a stuck breaker, a bus and other faults or a combination of these outages. This can produce the outage of two or more transmission elements and/or generating units, which are not necessarily on the same right-of-way. As in the case of common-cause outages, the probability of these outages is larger than the probability of independent outages resulting in a similar event. The bus-bar fault is one of the well-known station originated outages, all transmission or generation components connected to that specific bus-bar being tripped.

3.2.4 Hidden failures

Among the incorrect relay operations, a common scenario exists: the relay has an undetected defect that remains dormant until abnormal operating conditions are reached. This is often referred as *hidden failure* [THP96].

In [PT96] the protection system hidden failure is defined as a permanent defect that will cause an individual relay or a relay system to incorrectly and inappropriately remove system components as a direct consequence of another switching event. In order a relay failure to be considered as hidden failure, one must be able to monitor the defect which led to relay misoperation with an appropriate supervision system. A failure that results in an immediate trip without any prior event is not considered a hidden failure. The consequence of such event is minor in so far as the power system is designed to withstand the loss of any component (N-1 criterion).

Hidden failures can be classified into [Pha01]:

- *software failures*: the protection system settings are inappropriate or outdated for the prevailing system conditions. Consequently, although the relay functions correctly, in effect it has a hidden failure because of the inappropriate setting. This category may include human errors or negligence [ERP01, Eli03]. This kind of failures could be overcome by more frequent reviews of settings performed by relay engineers;
- *hardware failures*: actual equipment failure in relays. This kind of failures is to be expected in any device and its occurrence can be reduced by proper maintenance.

From the point of view of protection systems, there are two types of failure events that can occur in a terminal station and cause one or several lines or generator units to be outaged simultaneously [BM81, AA82]:

- active failures: faults cleared by the relevant primary protection, which can simultaneously disconnect more than one healthy line and/or generator unit. This kind of failures depend upon the protection scheme, but it can also be associated with hidden failures such as wrong settings or relay failure. In terms of protection system reliability this type of failure can be seen as lack of security;
- passive failures: primary protection failure which triggers the action of other protections in order to clear the fault. This may cause a greater number of disconnected lines/generator units. It can be triggered by hidden failures like stuck breaker condition or relay failure. In terms of protection system reliability this type of failure can be seen as lack of dependability.

There are different modes in which hidden failures can be detected and managed. For hidden failures in software, one may be able to perform self-checking and self-curing. For hardware failures, sensors are needed to detect device status. Since a hidden failure is not a critical problem under light load or no contingency conditions, when hidden failures are discovered under

abnormal conditions, the protection system could be automatically adjusted to an emergency mode which guards against false tripping more strictly than against failure to trip [DKH00].

Such a protection system which can adjust the operating characteristics of the relays with respect to power system conditions is called *adaptive protection*. In [HPT88] a more general definition is given as "Adaptive protection is a protection philosophy which permits and seeks to make adjustments to various protection functions in order to make them more attuned to prevailing power system conditions". Based on this definition there are two operating modes for such a wide-area adaptive protection system:

- one anticipates vulnerabilities and positions the system to be more robust in the event of a threat. This means that optimal and condition dependent relay settings must be found, in order to satisfy different load conditions (adjust relay parameters during heavy loading to guard against the impact of hidden failures);
- another mode is to respond to the failure by modifying the protection system to defend against future events in case of a component failure (learn from previous relay actions).

A more ambitious response mode might identify a developing emergency and respond to diminish its impact, for example by creating islands with balanced generation and load. This mode implies the need for high speed computation facilities and transmission of new operating parameters [DKH00].

In the sequel, normal functioning and hidden failures modes for some protection schemes are presented in detail. In great extent the material is borrowed from references [HP95, Eli03, Ned03].

Directional comparison blocking protection scheme

The directional comparison blocking scheme is one of the most popular protection schemes for protecting HV and EHV transmission lines. The one-line diagram and schematic control logic of such a scheme is presented in Fig. 3.3

The usual sequence of actions for a fault in the protected area (F_1) is the following: the directional relays D_A and D_B are picking the fault and close their normally open contacts. The fault detectors FD_A and FD_B do not see the fault; thus they do not activate their respective transmitter T_A and T_B, aimed at sending blocking signals. Hence, the receiver relays R_A and R_B remain closed. Consequently, the line is instantaneously cleared from both ends by opening the respective circuit breakers CB_A and CB_B.

For a fault situated outside the protected line (F_2), the fault detector picks up the fault and gives the permission to transmitter T_A to send the blocking signal; the receiver R_B opens his normally closed contacts and avoids opening the circuit breaker CB_B.

A hidden failure leading to an inadvertent action of this scheme may occur if [PT96]:

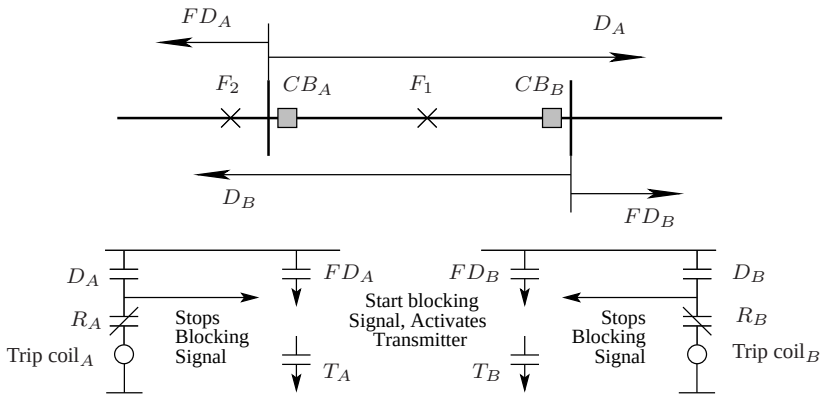

Figure 3.3: One-line diagram and schematic logic of the directional comparison blocking

- the appropriate fault detector cannot be activated to start transmitting a blocking signal;
- the stop blocking signal has a permanent failure, which overrides the blocking signal transmission for an external fault;
- the transmitter cannot transmit, which allows a false trip for all external faults;
- the receiver relay cannot be activated, which allows a false trip when the associated directional relay operates;
- a receiver relay is continuously activated, which will block the circuit breaker to act for all faults in the protected zone.

If the transmission line protection system is subject to any of these hidden failures, and an external fault occurs, this will result in unduly transmission line trip from one end. In the case illustrated in Fig 3.3, the circuit breaker CB_B trips when F_2 occurs.

The above mentioned hidden failures are the ones leading to undue transmission line trip. However, there are other hidden failures leading to normal but unwanted system component trip. An example is the failure to clear a fault inside the protected area due to, for example, mechanical failure of the circuit breaker. The fault will be cleared by the backup protection which will disconnect more system components (see station originated outages in Section 3.2.3).

Directional comparison unblocking protection scheme

In the directional comparison unblocking scheme case, Fig. 3.4, for a fault in the protected area, the directional relays D_A and D_B are closing their normally open contacts and start sending unblocking signal. This permits to R_A and R_B to close their contacts and clear the fault from both ends instantaneously.

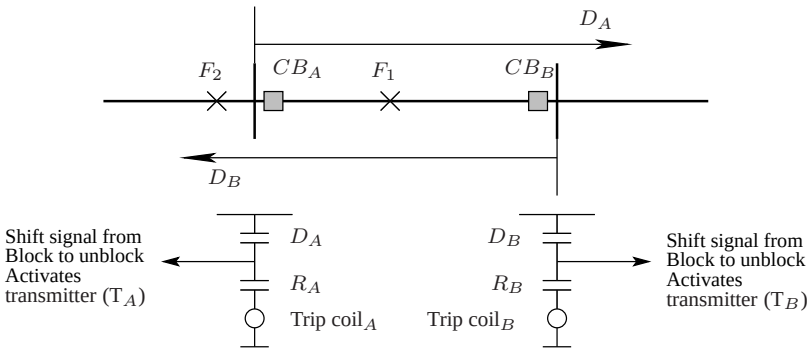

Figure 3.4: One-line diagram and schematic logic of the directional comparison unblocking scheme

If the fault is outside the protected area, only one of the directional relays is picking up the fault, but the circuit breaker action is blocked due to the fact that no unblocking signal is received from the other remote end (in the case of fault F_2, D_B closes its contacts but R_B remains open).

A hidden failure leading to an inadvertent action of this scheme may occur if:

- a directional relay is continuously activated, unblocking signal is continuously transmitted;
- the transmitter transmits continuously unblocking signal;
- the receiver relay is continuously activated.

As in the case of the directional comparison blocking protection scheme, if subject to one of the above hidden failures, the transmission line will be unduly tripped from at least one end. Indeed, if one directional relay is continuously activated, when the directional relay from the remote end picks up a fault outside the protected area the line is tripped instantaneously from both ends.

Underreaching transfer-trip protection scheme

In the case of the underreaching transfer-trip protection scheme, Fig. 3.5, the directional relay is underreaching the remote bus, which is covered by the overreaching fault detector relay. Thus, the action of the circuit breaker can be triggered directly by the directional relay or by the fault detector action correlated with the trip signal received from the remote bus.

For a fault outside the protected area the fault detector picking up the fault is closing its contacts, but the circuit breaker is not acting because the trip signal is not received from the remote end.

A hidden failure leading to an inadvertent action of this scheme may occur if:

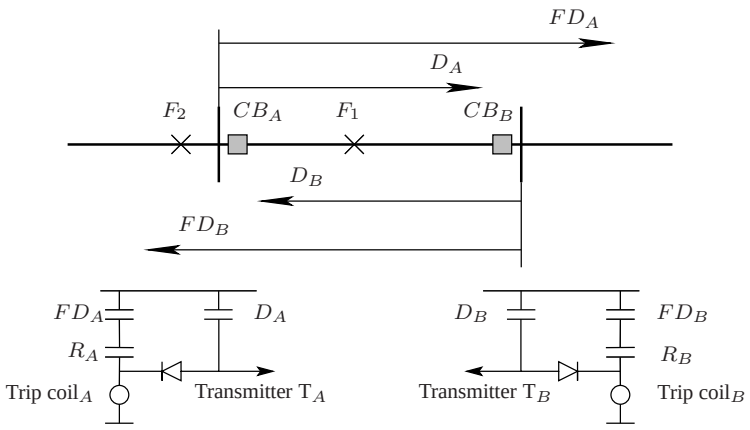

Figure 3.5: One-line diagram and schematic logic of the permissive underreaching transfer trip scheme

- the directional relay is activated in the absence of a fault, which will trigger the circuit breaker action;
- the transmitter transmits continuously tripping signal, which allows a false trip for all external faults;
- the receiver relay is continuously activated, which allows a false trip when the associated fault detector relay operates.

3.2.5 Vulnerability region

For each hidden failure of a component, a *vulnerability region* can be established, associated with the type of protection scheme. If an abnormal event or a fault occurs in the vulnerability region, and the protection component is subject to a hidden failure, this could cause the relay to incorrectly remove system components from service.

In Fig. 3.6 the shaded areas represent the vulnerability region corresponding to side B fault detector of the directional comparison blocking protection scheme (see Fig. 3.3). For a fault inside this region, if the fault detector in B is subject to a hidden failure, the circuit breaker from the remote side A will open its contacts unduly. Such vulnerability regions can be determined for all types of hidden failures.

The probability of an inadvertent tripping in case of a hidden failure is increasing with the size of the vulnerability region, and can be computed as the sum of all failure probabilities of the equipments included in the vulnerability region. As recalled in Section 3.2.2, the maximum distance that is covered by a protection system depends on protection functionality and relay settings. The latter have to be adjusted in order to assure system observation and a good coordination with the other protections in the area. For example, the vulnerability region for a directional protection scheme may extend over one line behind and one line beyond the

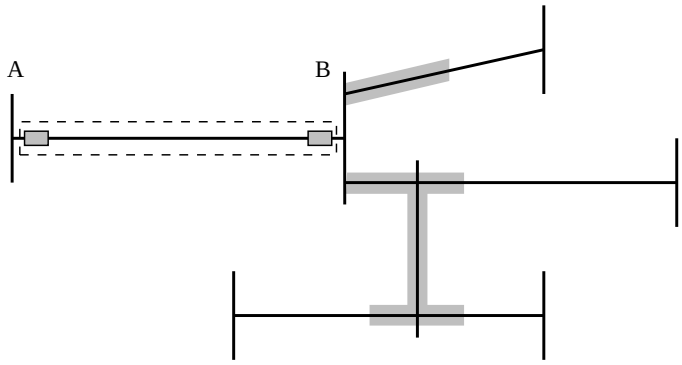

Figure 3.6: Vulnerability region for the fault detector in B

protected line. In the case of a back-up protection scheme the vulnerability region depends on the settings of the Zone 2 or Zone 3 relays (see Section 3.2.2).

3.3 Using event trees to model cascading outages

Event trees are structures which starting from an “undesired initiator” (loss of critical supply, component failure, etc.) can describe a chronological sequence of events. Each new event depends on what previously happened and for each new possible event considered, a new branch and node are added to the tree, with an associated probability. Each path from the root to end nodes represents a possible scenario, arising from the initial event, with the associated probability and consequences.

The functioning of protection systems as well as the development of a cascading outage can be described by a sequence of dependent events. In the first case the sequence is governed by the time delays used to initiate/inhibit protection actions. In the second case, the sequence of power system equipment disconnections also depends on intermediate operating states of the system. In both cases the event tree is a suitable structure to model the sequence of events.

Such event tree structures were used in order to model the protection failure scenarios, including stuck breaker events [CM05] or hidden failures [KN02, Ned03]. Also, the algorithm presented in [DCN03, DCN04] can be seen as an event tree for power system equipment overloads.

3.3.1 Cascading outage event tree

An event tree structure describing cascading outage sequences can be developed as presented in Fig. 3.7. Where each each node represents a power system state and each branch represents the loss of at least one power system component. Indeed, as mentioned before, if the primary

protection fails to clear the initial fault the back-up protection may remove from service more components than the initial faulted one[1]. A probability of occurrence can be associated with each branch.

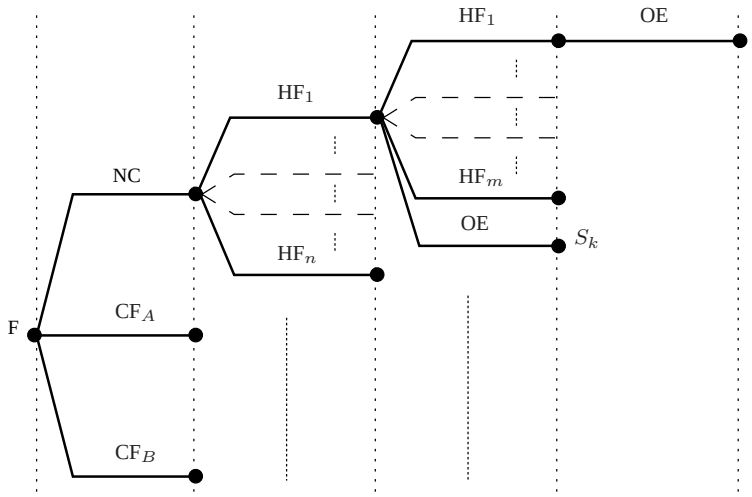

Figure 3.7: Cascading outage event tree

As illustrated in the figure, starting from the initial fault the first actions to be considered are the primary protection ones. The protection system behavior is reduced to two main events. The first one includes the sequence of relay actions leading to the Normal Clearing (NC) of the initial fault. The second one contains all possible hidden failures resulting in protection system Clearing Failure (CF) grouped under the same branch. The CF event includes besides the failure of the primary protection, the action of the back-up protection. Since to clear the fault the protection systems from both ends of the faulted line are concerned, two branches are needed to count for clearing failure cases (in our case CF_A and CF_B).

The events taken into account when expanding the event tree, after the action of the primary protection, could be classified into:

1. Protection system Hidden Failures (HF), which include both hardware and software failures. For example we consider inadvertent trip, due to inappropriate settings, of:

   - transmission lines with current approaching (but not exceeding) the thermal rating;
   - generator with rotor current approaching (but not exceeding) the limit enforced by the overexcitation limiter.

   We also consider the inadvertent action of relays whose vulnerability area includes the initial fault location (e.g. Zone 2 and 3 relays). Depending of the hidden failure type, the associated probability, $p(HF)$, can be determined using linear or exponential probability functions or approximated with the standard component unavailability [Ned03];

[1] See also station originated outages.

2. Overloaded Equipments trip (OE): this category includes the tripping of transmission lines due to high current, and reactive power limited generators due to low voltage, as a result of the initial and/or subsequent events. As these events are part of the power system response (probability $p(OE) = 1$) their representation in the event tree could be skipped. Nevertheless, their inclusion in the sequence is appropriate in order to emphasize the system degradation.

Figure 3.8 presents the evolution of the lowest transmission voltage for a sequence S of events in the Nordic32 test system whose data are given in [CTF98] and further considered in Chapter 4. $S^{(1)}$ refers to the voltage evolution after the disconnection of initially faulted equipment. Evolution $S^{(2)}$ corresponds to a scenario where after the normal clearing of the initial fault another transmission line is inadvertently tripped due to a hidden failure. As can be seen the voltage evolution is still acceptable. However, three generators are hitting their overexcitation limits. The voltage evolution $S^{(3)}$ corresponds to the scenario including the line trips and the trip of one of the limited generators. As can be seen, after losing the generator, the voltage is reaching low unacceptable values.

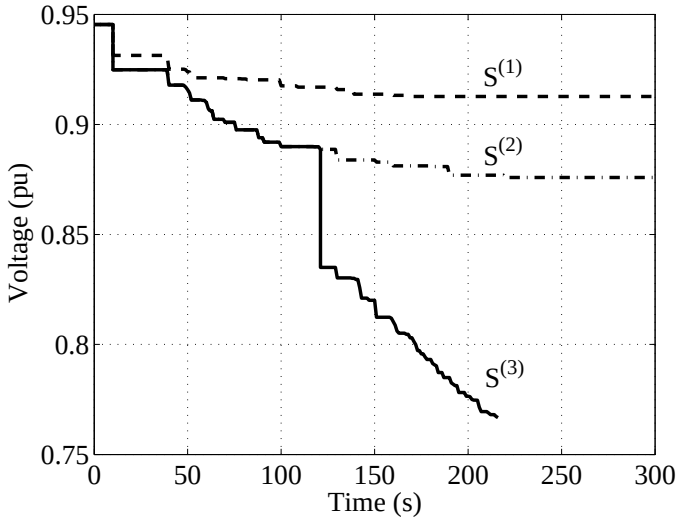

Figure 3.8: Evolution of lowest voltage for successive power system states

3.3.2 Cascading outages probability

As stated in the introduction of this chapter, loss of elements in power systems exhibit a clustering phenomenon, i.e., the loss of one element raises the probability of losing another element due to impact on power system parameters and protection schemes [CM04]. The more severe the first event, the more likely an additional event will follow. The elementary events are no longer independent, the succeeding events depend on what previously occurred in the event tree sequence. Thus, the more we advance in the development of the event tree, the more difficult it is to determine the probability of each sequence. In the same time the probability of one sequence is decreasing as one progresses in the event tree.

The probability to have a hidden failure is given by:

$$p(HF) = p(HF \cap F) + p(HF \cap \neg F) \ . \tag{3.1}$$

By definition, hidden failures happen only after a fault F, i.e., they have no effect until a fault has to be cleared by the protection, therefore:

$$p(HF \cap \neg F) = 0 \ .$$

In other words the probability to have a fault aggravated by a hidden failure is equal to the product between the initiating fault probability and the probability of having a hidden failure revealed by this fault.

$$p(HF) = p(HF \cap F) = p(F) \cdot p(HF/F) \ . \tag{3.2}$$

The probability of a specific sequence of events, sequence S_k from Fig. 3.7 for instance, is given by:

$$\begin{aligned} p(S_k) &= p(F \cap NC \cap HF \cap OE) \\ &= p(F) \cdot p\left((NC \cap HF \cap OE)/F\right) \\ &= p(F) \cdot p(NC/F) \cdot p\left((HF \cap OE)/(F \cap NC)\right) \\ &= p(F) \cdot p(NC/F) \cdot p\left(HF/(F \cap NC)\right) \cdot p\left(OE/(F \cap NC \cap HF)\right) \end{aligned} \tag{3.3}$$

As the probability of an overloaded equipment to be tripped does not depend of the sequence that led to this overload we can write:

$$p\left(OE/(F \cap NC \cap HF)\right) \simeq 1 \tag{3.4}$$

Considering (3.4) into (3.3) we obtain:

$$\begin{aligned} p(S_k) &= p(F) \cdot p(NC/F) \cdot p\left(HF/(F \cap NC)\right) \\ &= p(F) \cdot (1 - p(CF/F)) \cdot p\left(HF/(F \cap NC)\right) \\ &= p(F) \cdot p\left(HF/(F \cap NC)\right) - p(F) \cdot p(CF/F) \cdot p\left(HF/(F \cap NC)\right) \end{aligned} \tag{3.5}$$

Rare event probability approximation

The main idea behind the rare event probability approximation is that, if the probabilities of the events considered in a sequence have very small values, the high-order terms of a sequence probability polynomial expression can be omitted. Thus, $p(S_k)$ from Eq. (3.5) can be approximated by:

$$p(S_k) = p(F) \cdot p\left(HF/(F \cap NC)\right) \tag{3.6}$$

Furthermore, if we consider that all probabilities have approximately the same magnitude order, $p(F) = p\left(HF/(F \cap NC)\right) = p$, a *probability order* can be associated to each term of the entire polynomial expression. The probability order, depends on how many factors are in the

significant product terms of the polynomial expression after applying the rare event probability approximation. In our example, the probability of the cascading event can be approximated by $p(S_k) = p^2$. Thus, the probability order of the sequence is 2.

The so determined probability order can be used, together with an analysis of system behavior, as a stopping criterion of the event tree expansion, to discard less probable scenarios.

Overloaded component trip probability

References [DCN03, DCN04] considered that after an initial contingency, all the lines have the same probability to trip if their loading has overstepped a specified threshold. In [CTD03], it is considered that each line has a different load-dependent probability of incorrect trip that is modeled as an increasing function of the line load flow seen by the line protection relay. The probability is low when the line loading is below the line limit, and increases linearly to 1 when the line loading reaches 1.4 times the line limit, see Fig. 3.9.

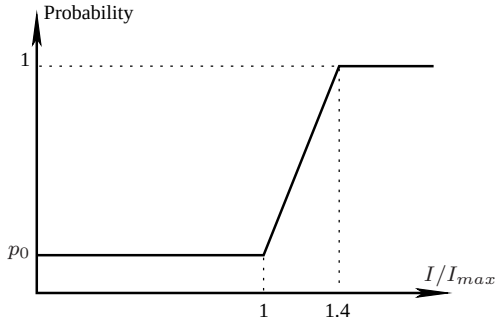

Figure 3.9: Trip probability of a line (taken from [DCN04]

If at a given node of the event tree being developed there are multiple system components overloads, it is assumed that the component experiencing the largest overload is tripped first, since it has the largest probability to be tripped. This assumption is in accordance with the fact that the period of time for which the overload is allowed usually decreases with the magnitude of the overload, see Fig. 2.15.

Furthermore, the component loading versus trip probability diagram of Fig. 3.9, can be updated in order to take into account the hidden failures related to inappropriate or outdated protection settings leading to inadvertent tripping events.

Such a diagram is illustrated in Fig. 3.10, where l is a loading level above which the probability of inadvertent tripping due to hidden failures becomes greater. When the current exceeds the rated value the trip probability is increasing linearly and is reaching the value 1 when the emergency rating is reached. This probability approximation can be extended to all power system components subject to limits.

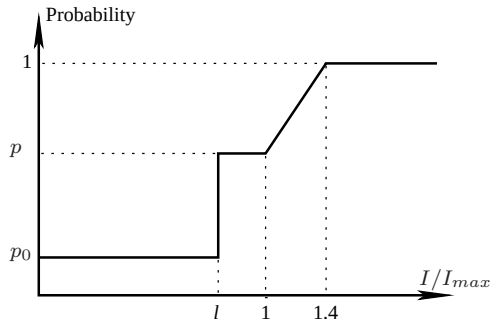

Figure 3.10: Power system component inadvertent tripping probability

This is the probability characteristic that we used in the cascading outage algorithm described in the next section. Furthermore, in the development of the event tree we considered only equipments approaching or reaching their limits as a result of the sequence of events considered up to that level. This assumption is made in order to avoid the trip of equipments already close to their limits, but not affected by the cascading event.

3.4 Cascading outage determination procedure

Considering the cascading outage event tree model, Fig. 3.7, the following algorithm to identify plausible cascading events was developed and coupled with the ASTRE software:

1. Apply the initiating disturbance to the initial state of the power system and draw up the list of next possible disturbances due to hidden failures. They are of two types:

   - hidden failures directly related to the initiating disturbance, i.e. involving protections whose vulnerability region includes the initial fault location. These failures can only be revealed by the initial fault. They are determined only once for all sequences that result from the considered initiating disturbance;
   - hidden failures causing unwanted trip of system components approaching (but not exceeding) their operating limits due to wrong/outdated protection settings or human errors. Note that equipment loadings depends on the sequence of events and hence they have to be checked while the event tree is being expanded. However, we assume that the system is initially N-1 secure, so that no component is overloaded after normal clearing of the initial fault.

2. Apply a disturbance from the list determined at the previous step. Priority is given to equipments exceeding limits (overloaded lines, reactive limited generators reaching low voltages), if any, as these are considered as deterministic events. More than one disturbance will be applied at once only if they have a common cause (e.g., the back-up protection action or the station originated outages).

As already mentioned, if the list with next possible disturbances includes more than one overloaded equipment, we consider that the one experiencing the largest overload is tripped first. This assumption is in concordance with the fact that the larger the overload, the shorter it can be tolerated. Nevertheless, the overload must result from the sequence of events assumed up to that level;

Due to their very low probability the number of hidden failures considered in one sequence can be considered as stopping criterion.

3. Classify the sequences into harmless or potentially harmful. To this purpose we use a procedure based on voltage drop and branch currents estimates computed with linear approximation methods, detailed in Appendix A. The sequences are flagged as potentially harmful if the post-contingency voltage drops are larger than a specified threshold value δ_V or if at least one equipment is exceeding its limits.

4. Using the linear approximation method, determine for the harmless sequences the line currents approaching limits and generator field currents approaching limits or limited due to the events considered in the sequence up to that state. These system components are added to the list with next possible disturbances due to hidden failures.

5. Analyze the potentially harmful sequences more accurately with QSS time simulation in order to assess the sequence severity. This simulation includes the actions of protections on overloaded transmission lines and limited generators with low voltages, which are tripped as part of the system response. The criterion to accept a post-cascading-outage evolution is that the system remain connected[2] and all transmission voltages remain above a specified value V^{crt}.

   If the system behavior is unacceptable or if the system was split into islands the development of that specific sequence is stopped.

   If the system behavior is acceptable, overloaded lines and reactive limited generators with low voltages, observed during time simulation, are added to the list of possible disturbances (with probability 1 of occurrence), as well as the transmission lines approaching limits and generators approaching or reaching limits (with probability $p(HF)$). Afterwards, when a sequence involving such tripping is analyzed with QSS simulation, the equipment is tripped only after it gets overloaded or limited, with or without a temporization.

6. For the sequences flagged as harmless (in step 3) and those with acceptable system behavior (after step 5) compute the probability order of the sequences using the rare event probability approximation. If the probability order is smaller than a predefined threshold n_{max}, then the algorithm proceeds with Step 2, else the sequence development is stopped.

Figure 3.11 gives the flowchart of the inner loop of the algorithm (steps 2 to 5) which generates one branch of the event tree. As can be seen there are three stopping criteria of a cascading sequence, as follows:

[2] In a more refined analysis, one could check the viability of the islands resulting from a network split, for instance from frequency viewpoint.

- the sequence contains the maximum number of hidden failures per sequence and there is no overloaded component;
- the sequence probability order is equal to the chosen threshold;
- the QSS time domain simulation of the cascading sequence is violating the specified criteria.

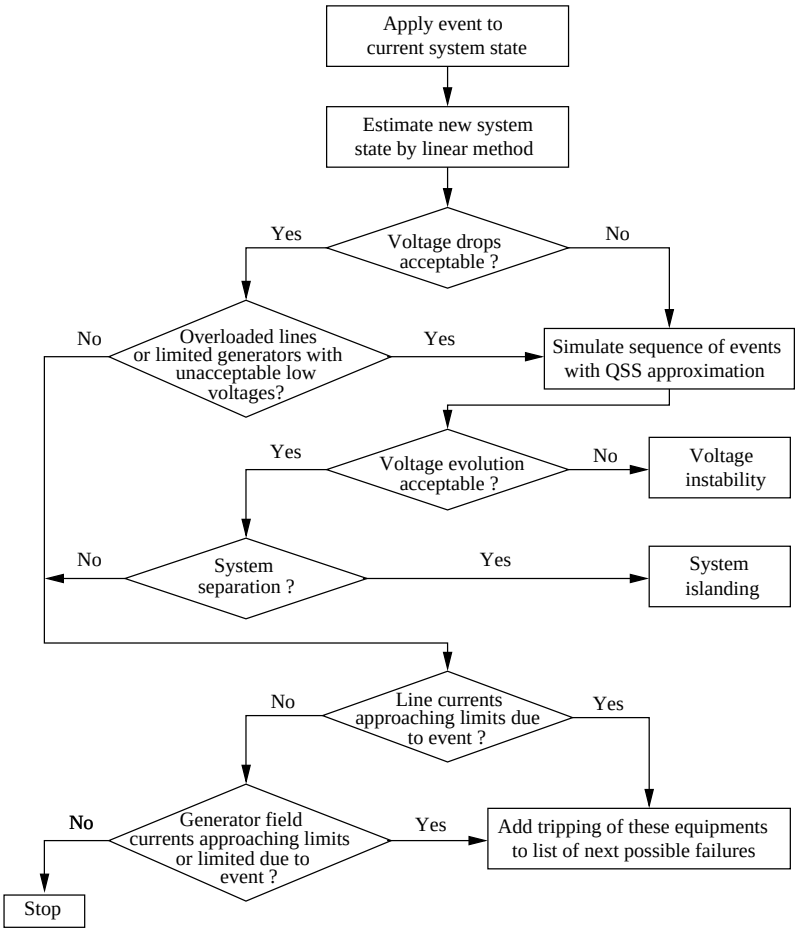

Figure 3.11: Event tree algorithm

Finally, the resulting cascading events can be divided with respect to system response into two categories:

- system behavior is acceptable: we can determine the security margin left to the system by the cascading sequence;
- system behavior is unacceptable: we can determine either the corrective actions (e.g. amount of load shedding) or the impact of the cascading sequence on the system (e.g. amount of load power that is not supplied).

This additional analysis can be used to rank the contingency sequences, to determine the area of influence of an initiating disturbance, to identify weak areas and, last but not least, to tune system system protection schemes, as considered in the next three chapters.

3.5 Preliminary results and presentation of determined cascading outages

3.5.1 The simulated system

The proposed algorithm has been tested on a detailed planning model of a the western region of the French transmission system, operated by RTE [SMC98], where security is on some occasions constrained by voltage stability as well as cascade tripping of overhead lines by overcurrent protections. A one-line diagram of the transmission (380 and 225-kV) grid is shown in Fig. 3.12.

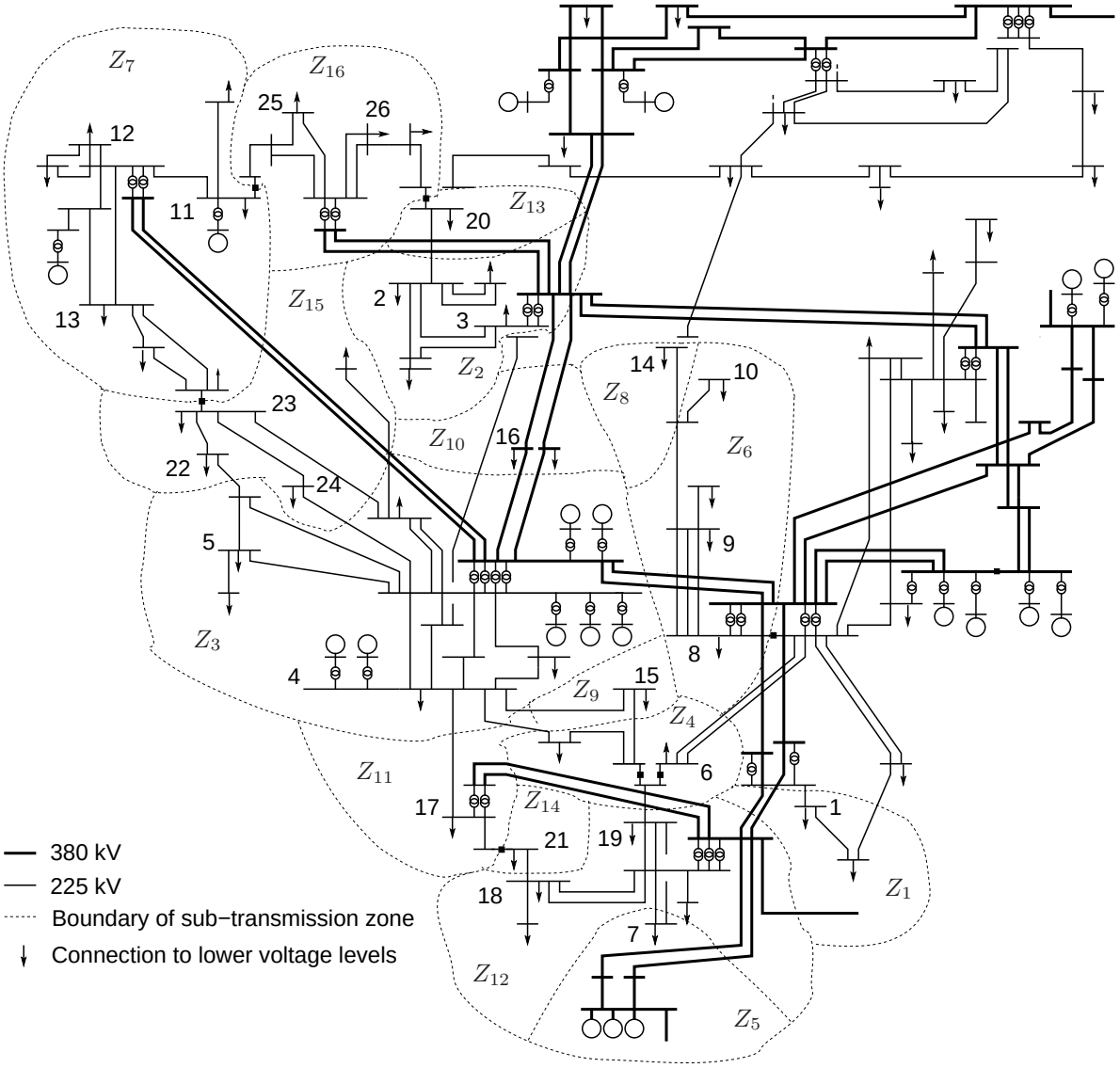

Figure 3.12: One-line diagram of the studied region within RTE system

The model includes 1244 buses, 1090 lines and 541 transformers. This involves the main

transmission grid of France and, for its Western region, a detailed representation of the (90 and 63-kV) sub-transmission networks as well as 341 transformers feeding 20-kV distribution buses. Part of the main 380 kV and 225 kV buses were modeled with their actual bus-bar configuration (detailed topology) in order to identify realistic cascading event sequences.

The sub-transmission system is subdivided into 16 non connected zones, whose boundaries are shown with dotted lines and labeled $Z_1, \ldots, Z_{16}$ in Fig. 3.12. In the same figure, the arrows indicate connections to lower voltage levels (mainly sub-transmission except for a few loads directly fed from transmission).

Loads are connected at the distribution buses and represented by the well-known exponential model, Eqs. (2.6 - 2.7).

Following a disturbance, the long-term dynamics are driven by 341 load tap changers with various delays, by overexcitation limiters of generators, and by 11 secondary voltage regulators controlling "pilot nodes" [PLT87]. Two levels of tap changers control sub-transmission and distribution voltages (the 380/225 kV transformers having fixed ratios). Furthermore, the main lines of the transmission system are equipped with overcurrent protection systems with various delays depending on the considered emergency rating. In our tests we have considered a an overcurrent protection allowing a 140 $\%$ overload to last for at most 60 s.

The voltage drop used to classify the sequences into harmless or potentially harmful (with the linear method of Appendix A) was taken $\delta_V = 0.09$ pu. In the tests presented in [OVC05] this value was found to be a good compromise in terms of harmless scenarios flagged as potential harmful. Furthermore, the system (long-term) evolution is considered unacceptable if any transmission voltage reaches the value V^{crt} = 0.8 pu, which makes sense considering the nuisance for customers and the lack of reliability of load models below this value. In addition, it was checked that no field-current limited generator had its voltage below the value imposed by plant auxiliaries.

Even if the procedures presented in [THP96, PT96] consider the possibility of more than one hidden failure per sequence, due to their very low probability[3], we limited ourself to a single one, as in [KN02]. Therefore, if a specific sequence already includes a hidden failure and the list of possible disturbances does not contain an overloaded equipment the sequence expansion is stopped. Thus, the maximum probability order was set to $n_{max} = 2$

Considering the above parameters, a set of 54 cascading events creating instability problems were identified. Some of the so determined cascading events were already known as potentially dangerous and dedicated protection schemes are already in service.

Note that some scenarios include the same disturbances but their order in the sequence is different. In other words the initiating event is different but the subsequent disturbances involved in the sequence and hence the final outcome is the same. Thus, the above figures could be corrected in order to count equivalent sequences only once. Nevertheless, these are considered

[3]Breaker active failure rate = 0.0066 failures/year, Breaker passive failure rate = 0.0005 failures/year, Fault probability of one power system component $< 1\%$ per year.

as distinct scenarios as different phenomena may be involved, thus different types of protection schemes are needed to prevent system instability.

In the sequel some of the so determined cascading event are presented. Emphasis is put on phenomena discussed in Chapter 2. These disturbances will be used in Chapter 6 to test the behavior of the system protection schemes proposed in Chapter 4 and 5.

3.5.2 Pure voltage instability scenario

A severe disturbance, denoted D1 in sequel, is applied at t = 10 s, including the loss of a transmission line inside zone Z_7 followed by the trip of a transmission line connecting Z_7 to Z_3, see Fig. 3.12. The voltages are decreasing under the effect of load restoration, and eventually they settle down at low levels, below the 0.8 pu threshold. The voltage drop stops when load tap changers hit their limits. The small final increase in voltage is due to secondary voltage control.

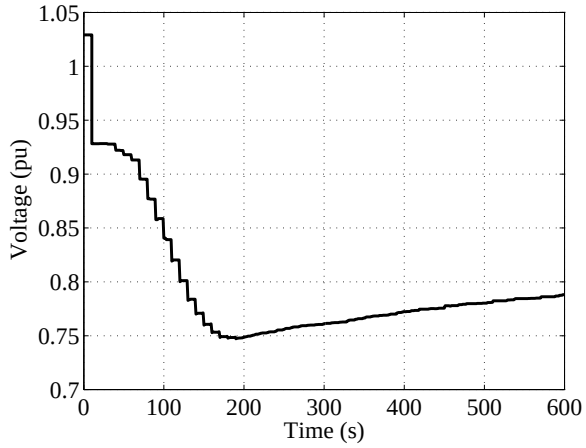

Figure 3.13: Disturbance D1: evolution of lowest voltage

3.5.3 Pure thermal cascading scenario

The disturbance, denoted as D2, involves the loss of a transmission line inside zone Z_3 followed immediately by the trip of a transmission line connecting Z_{15} to Z_3. As illustrated in Fig. 3.14.a, after the two line outages, another line inside Z_3, part of the transmission path feeding Z_{15}, gets directly overloaded and is tripped by an overcurrent protection after a 60 s delay. The voltages in the affected area after the initial disturbance are acceptable, but they drop to very low values just after the third line tripping, as shown Fig. 3.14.b.

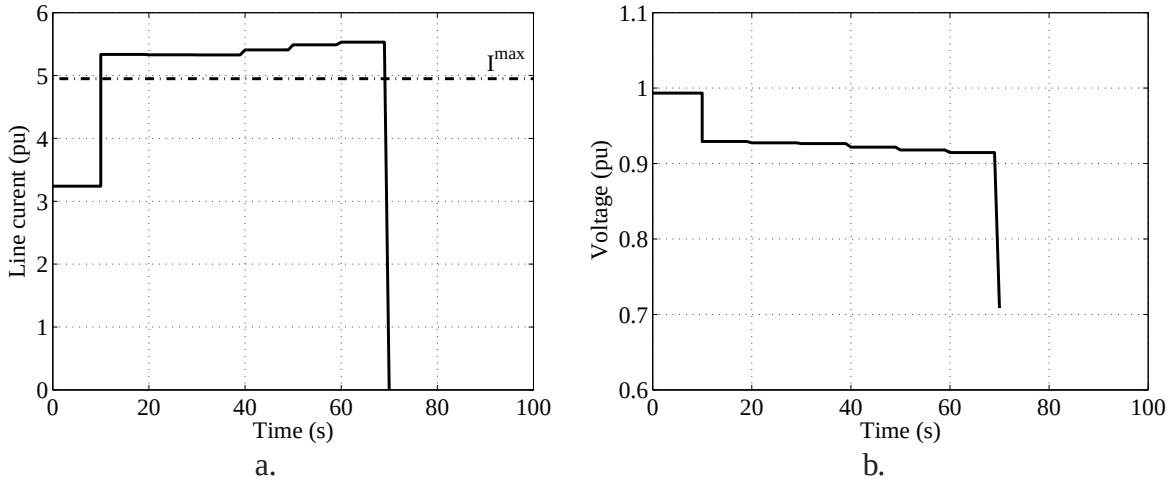

Figure 3.14: Disturbance D2: line current and evolution of lowest voltage

3.5.4 Voltage instability aggravated by overloaded line tripping

The considered disturbance, D3, is the loss of two transmission lines connecting Z_7 to Z_3 with automatic reclosure of a switch between Z_7 and Z_{15}. Figure 3.15 shows the evolution of the lowest transmission voltage in the affected area. As can be seen, after the initial drop caused by the disturbance, the voltage is falling under the effect of load restoration, driven by load tap changers. The last voltage drops are caused by the tripping of overloaded lines, leading the system to very low voltage. In fact, voltages have already reached the 0.8 pu limit well before this line tripping takes place. If there was no over-current protection in operation this case would be like D1.

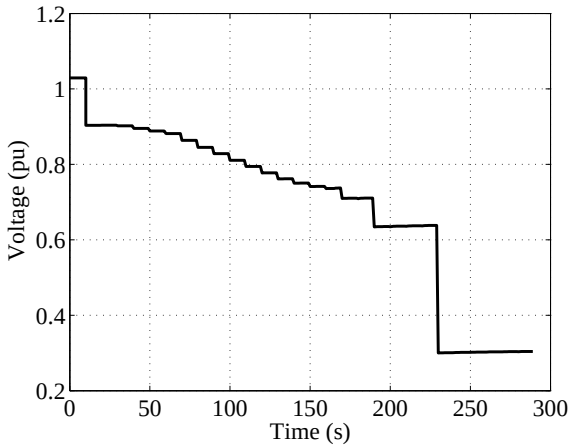

Figure 3.15: Disturbance D3: evolution of lowest voltages

A similar case is depicted in Fig. 3.16, where the considered disturbance, D4, is the loss of two transmission lines connecting load zone Z_{15} to Z_3.

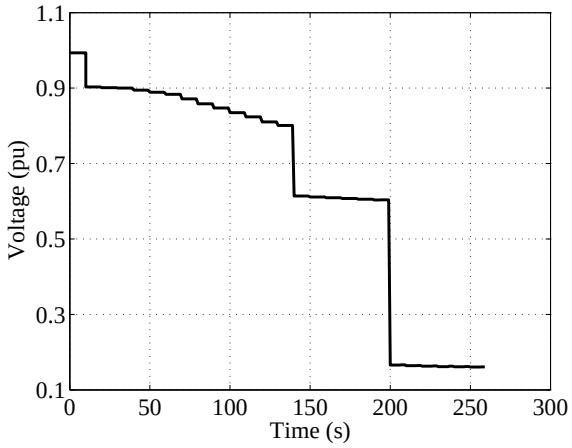

Figure 3.16: Disturbance D4: evolution of lowest voltages

3.5.5 Combined voltage and thermal problems

In some cases load restoration causes both line currents and voltages to become unacceptable. We present here a sample of three representative simulations:

- Disturbance D5: includes the loss of two transmission lines, feeding zone Z_{15}. As can be seen in Fig. 3.17, after the initial disturbance the system settles down, but with a transmission line slightly overloaded. As the system has no corrective control to alleviate the overload, the line is tripped, which causes the voltage to cross the 0.8 pu limit.

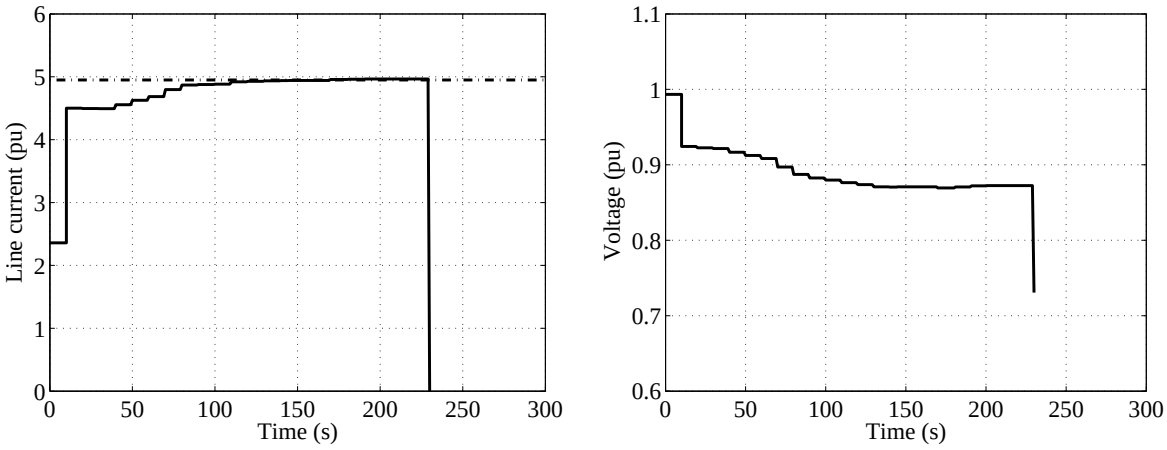

Figure 3.17: Disturbance D5: line current and lowest voltage evolution

- Disturbance D6: includes the loss of two transmission lines in zone Z_{12}. This case is a severe one. Right after the disturbance, the affected area remains connected through a single transmission line, which under the effect of load restoration gets overloaded. After the 60 s delay the line is tripped and the affected area is blacked out. Note that the final voltage shown in Fig. 3.18 is the one just before the tripping of this line, since a singularity is met in the QSS simulation.

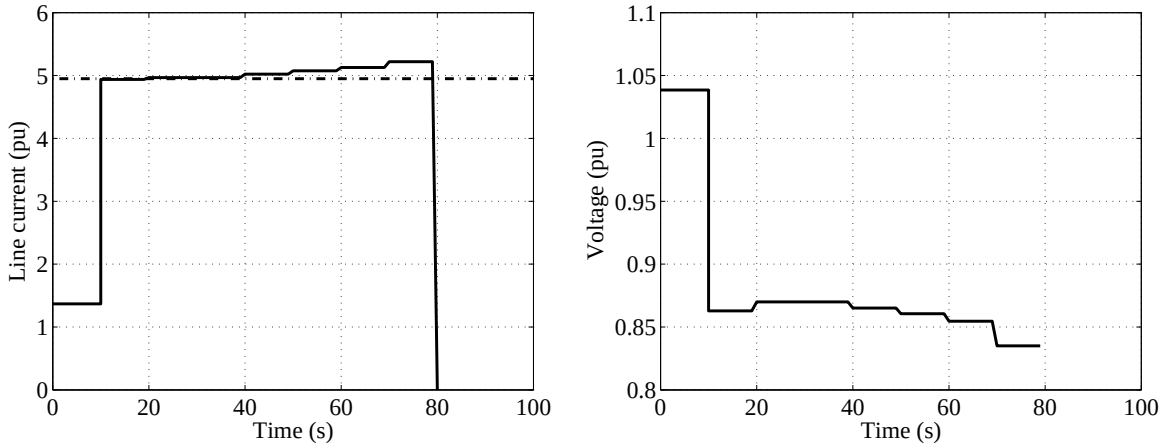

Figure 3.18: Disturbance D6: line current and lowest voltage evolution

- Disturbance D7: involves the loss of two transmission lines connecting Z_{16} to Z_2. As in the previous cases, the load restoration is the driving force leading to both transmission line overload and low voltages, as shown in Fig. 3.19.

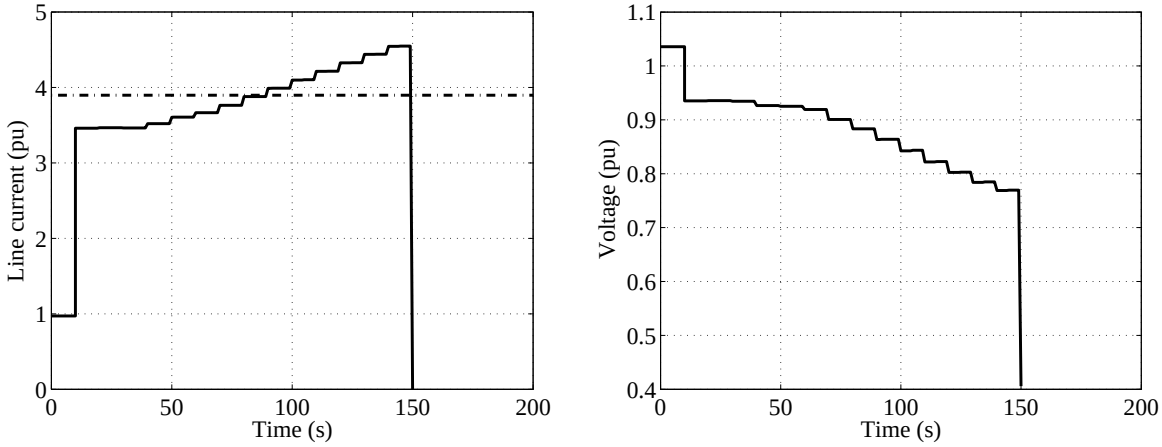

Figure 3.19: Disturbance D7: line current and lowest voltage evolution

3.6 Concluding remark

An algorithm based on the cascading outage event tree model, aimed at identifying plausible cascading events was developed and coupled to the ASTRE software. The events considered in the development are hidden failures directly related to the initial fault or revealed by the sequence of events and overloaded equipments trippings. The resulting cascading scenarios can be used in system stability assessment studies as well as to devise system protection schemes.

Chapter 4

Distributed undervoltage load shedding

A new design of load shedding against long-term voltage instability is proposed. It uses a set of distributed controllers, each monitoring a transmission voltage and controlling a group of loads. Each controller acts in closed-loop, shedding amounts that vary in magnitude and time according to the evolution of its monitored voltage. The whole system operates without information exchange between controllers, the latter being implicitly coordinated through network voltages. The operation, design and robustness of the proposed scheme are illustrated through a small but realistic example.

4.1 System protection schemes against voltage instability

Load shedding is the ultimate countermeasure to save a voltage unstable system, when there is no other alternative to stop an approaching collapse [Tay94, VCV98]. This countermeasure is cost effective in the sense that it can stop voltage instability triggered by large disturbances, against which preventive actions would not be economically justified (if at all possible) in view of the low probability of occurrence [Tay92]. Load shedding is also needed when the system undergoes an initial voltage drop that is too pronounced to be corrected by generators (due their limited range of allowed voltages) or load tap changers (due to their relatively slow movements and also limited control range).

As load shedding action results in high costs to electricity suppliers and consumers, power systems should be designed to require such action only under very rare circumstances.

Load power may be shed either *manually* or *automatically* depending on the rate of voltage drop. Manual load shedding can be thought of in response to load increases (if equipments are unavailable). This type of action, however, should have preplanned guidelines and procedures for the system operator to implement load shedding efficiently.

System studies can provide sensitivity analysis from which the critical voltage can be determined to start load shedding. Another option to assist system operators is to preprogram blocks

of loads on the dispatcher control console. Dispatchers can select a particular block of load in a specific area requiring load shedding to control the voltage drop. Nevertheless, this remains a heavy decision for an operator and it is widely agreed that it should be performed by a (carefully tuned) system protection scheme [CTF01].

More importantly, when voltage instability is caused by a sudden loss of critical transmission or generation equipment, manual load shedding is not conceivable because it places a severe burden on system operators to take appropriate actions in timely manner especially for few seconds to few minutes order phenomena. Therefore, automatic load shedding must be used to quickly arrest a fast voltage decay and trigger its recovery to an acceptable level before collapse can occur.

Thus, the automatic load shedding proposed in this work belongs to the family of System Protection Schemes (also referred to as Special Protections Scheme) (SPS) against long-term voltage instability. An SPS is a protection designed to detect abnormal system conditions and take predetermined corrective actions (other than the isolation of the faulted elements) to preserve as far as possible system integrity and regain acceptable performances [CTF01].

The main design requirements of an SPS (similar to component protection) are:

- *dependability* - the protection must act when needed;
- *security* - the protection must not act when not needed;
- *reliability* - the protection is both dependable and secure;
- *selectivity* - the size of the action must fit the severity of the disturbance;
- *robustness* - the protection must be able to face the widest range of possible scenarios which could be encountered.

Considering the input variables that initiate the load shedding action the SPS can be classified into *response-based* and *event-based*. A response-based SPS relies on measurements of electric quantities through which the consequences of an event can be observed. Event-based SPS are designed to operate upon recognition of a particular combination of events. They are accordingly faster than response-based SPS, which have to wait for the system response to a specific event before acting. Response-based SPS are, however, more robust, since they work by observing the consequences of disturbances. Therefore, they can face different events that were not considered in the design phase.

Furthermore, the SPS against voltage instability can be roughly classified into *algorithmic decision-based* and *rule-based*.

An algorithmic decision-based SPS could exploit the ability of simulating system evolution faster than real-time, when long-term voltage instability is of concern and provided a fast simulation technique such as the quasi steady-state approximation is used [VCV98]. Assuming that the disturbance has been identified, the minimal post-disturbance load shedding could be

efficiently determined using a method of the type described in [MC99]. This is, however, an open-loop approach that cannot compensate for inevitable modelling inaccuracies (due mainly to uncertainties in load behavior) as well as possible unexpected component failures [Reh01].

A rule-based SPS relies on simple rules of the type "if voltage drops below some threshold V^{th} for some duration τ, shed some power ΔP". Being much simpler, it is less exposed to failures originating from telecommunications, erroneous models, etc.

Rule-based load shedding usually relies on the detection of low transmission voltages. Clearly, the detection of a low voltage situation is meaningful by itself, as an indication of customer nuisance. Nevertheless, efforts have been paid to develop alternative criteria, having hopefully more anticipation ability.

Other input signals than voltage magnitudes may be monitored. Reactive reserve (or field current) on key generators has been considered [ILK96], for instance to deal with situations where voltages drop abruptly after the activation of OELs. An alternative consists in trying to detect a condition that corresponds to loss of stability, instead of observing its consequences, the objective being to obtain an earlier emergency signal. This is the purpose of the voltage instability predictor initially proposed in [BVN99] and improved in [BM03, ZLK05]. The latter relies on the identification of a Thévenin equivalent from local measurements.

No matter the input signal several issues need to be addressed regarding the use of this predictor after a severe disturbance (instead of during a smooth load increase) and its anticipation capability compared to low voltage detection.

Nevertheless, the simplicity of the above rules does not allow the SPS to adjust its action to the severity and location of the disturbance. A step towards better design was made in [LMC03] where the parameters involved in the rules were optimized over a set of scenarios, and an additional rule made the protection operate in closed loop.

As an alternative to the above rule-based scheme, some researchers have proposed a more involved analysis of a real-time model of the system to control generator voltages, shunt compensation and load shedding in emergency conditions. Among them, let us quote the approaches inspired of Model Predictive Control [LK03, WWT04, ZA03, HG06]. Some strengths and limitations of this approach are discussed in [GVC06]. More investigations are needed to ascertain that these more complex and computationally intensive schemes meet the reliability and robustness requirements of an SPS.

As already mentioned, an SPS can work in *closed loop* or in *open loop*. Closed-loop SPS are allowed to operate many times if needed, automatically adjusting their action to the severity of the disturbance, as far as the size of successive controls has been fixed to a reasonable value. This behavior increases the SPS robustness against modeling uncertainties at the design stage [Weh99].

Finally one may distinguish between *distributed* and *centralized* load shedding. A distributed scheme has each protective relay closely coupled to a cluster of loads to be shed. If the voltage conditions of a relay enter the region where collapse is predicted, load assigned to that relay

is shed. A centralized scheme has measurements taken at one or more key busses within one specific region, and trip signals transmitted to shed load at various locations within the region. Since voltage instability may be recognized by low voltages across the region, the basis of centralized measurement lies in the notion that if the voltage is low at certain key locations, it is likely to be also low in the neighborhood of these locations. This scheme requires communications but may naturally embed other measurements than voltages. This is a step forward towards wide area protection [RB02, ZLK05, CTF07].

In a distributed system, load shedding is concentrated and localized to the areas where the effects of the instability are felt most strongly. The main advantage of the distributed load shedding scheme is the increased reliability due to diversification. Failure of one component of the distributed system will not directly or detrimentally affect the operation of other components of the load shedding system. Failure of the centralized system results in complete failure of the scheme, and could result in large blocks of load being unnecessarily shed or failure of the scheme to shed load when required. The reliability of the centralized system can be increased by applying redundant, or voting measuring schemes.

Another advantage of the distributed model is that it does not depend so much on communication systems for its operation. If the local relays and breakers are operable, load shedding will occur even if one of the communication facilities fails. The centralized scheme is heavily dependent upon communications, both for making the shedding decision, and for implementing it. This can make the scheme more expensive than a distributed scheme. If communications are required anyway for system restoration by supervisory control, then this advantage of the distributed scheme is not as important.

Undervoltage load shedding SPS is not yet very common in the electric power industry. Among the existing SPS, some are using centralized controllers receiving information like undervoltage, high reactive output, loss of power plants or lines from remote substations, and sending load shedding orders to substations [LBC04, MEC04, WEC99], others are part of an Emergency Management System [SPC, KH04] and one is using decentralized undervoltage relays installed in substations [MDJ93].

Considering the above mentioned SPS characteristics, the design chosen in this work has the following features:

- *response-based*: load shedding will rely on voltage measurements which reflect the initiating disturbance (without identifying it) and the actions taken so far by the SPS and by other controllers, of the same type or not, acting in the power system;
- *rule-based*: load shedding will rely on a combination of rules of the type:

$$\text{if } V < V^{th} \text{ during } \tau \text{ seconds, shed } \Delta P \text{ MW} \tag{4.1}$$

  where V is a measured voltage and V^{th} a corresponding threshold value;
- *closed-loop automatic operation*: an essential feature of the scheme considered here is the ability to activate the rule (4.1) several times, based on the measured result of

the previous activations. This closed-loop feature allows the load shedding controllers to adapt their actions to the severity of the disturbance. Furthermore, it increases the robustness with respect to operation failures as well as system behavior uncertainties [LMC03]. This is particularly important in voltage instability, where load plays a central role but its composition varies with time and its behavior under large voltage drops may not be known accurately;

- a *distributed* scheme is proposed for its ability to adjust to the disturbance location, as will be explained and illustrated in the following sections.

4.2 Essential aspects of load shedding

It is well-known that the *timing*, the *location* and the *amount* are three important and closely related aspects of load shedding against voltage instability [AAH97].

When designing an undervoltage load shedding scheme, the consideration given to the timing of the load shedding action is very important. The motivation for delaying load shedding are: (i) ascertain that the system is indeed going to be unstable, and (ii) let other "inexpensive" controllers (such as shunt compensation and secondary voltage control) attempting system recovery. On the other hand, the time available for shedding is limited by the necessity to avoid [VCV98]:

- reaching the collapse point corresponding to generator loss of synchronism or motor stalling;
- further system degradation due to undervoltage tripping of field current limited generators, or line tripping by protections;
- the nuisance for customers of sustained low voltages. This may require to act fast, even in the case of long-term voltage instability, if the disturbance has a strong initial impact [LMC03].

As far as long-term voltage instability is concerned, if none of the above factors is limiting, one can show that there is a maximum delay beyond which shedding later requires shedding more [VCV98, MC99]. On the other hand, it may be appropriate to activate other emergency controls first so that the amount of load shedding is reduced.

In [Moo02] it is shown that there would be an advantage in letting shunt reactors trip, so that less load is shed, although it is not always possible to wait. For example, an undervoltage load shedding scheme implemented in an area feeding a lot of induction motors has to rely on an SPS that is able to react within seconds of the onset of the disturbance. As this case has to do with short-term voltage instability[1] there is no advantage of delaying the load shedding action.

[1]The concern of this report is long-term voltage stability.

In this case, locally positioned SVCs, synchronous condensers or generation excitation system controls would react to attempt voltage recovery and exhausting these resources would then trigger the load shedding action.

The shedding location matters a lot when dealing with voltage instability: shedding at a less appropriate place requires shedding more. In practice, the region prone to voltage instability is well known beforehand. However, within this region, the best location for load shedding may vary significantly with the disturbance and system topology [SMC98].

Many methodologies have been proposed to ascertain the amount of load that is appropriate to shed under given conditions. Tripping less load than necessary will obviously not be effective in stopping voltage instability. Tripping too much load may result in transitioning the system from an under-voltage to an over-frequency condition as the resulting system will have more generation than load [LR04]. Furthermore, load characteristics play an important role in determining the ability of the system to recover stability after a disturbance. The incorrect presumption of load characteristics in load-flow and dynamic studies may reduce the selectivity of the undervoltage load shedding scheme.

There are proven sensitivity techniques to identify which parameters have most influence on load power margin [Dob92]; they can be straightforwardly applied to load shedding. Furthermore, this analysis can be coupled to time simulation in order to find the best corrective actions in a post-disturbance unstable situation [GMK92, VCT95, MC99, FAM00]. More recently Ref. [CVC05] proposed a simple sensitivity computation encompassing unstable as well as low but stable voltage situations. Once a ranking of loads has been set up, the minimal amount of power to shed can be easily computed [MC99].

While easily performed off-line, for predefined contingencies, the above computations can hardly be embedded in an SPS facing an unknown disturbance. Instead, the latter must be provided with a possibly sub-optimal but simple and robust logic to choose the shedding location. The distributed scheme proposed here tends to act first where voltages drop the most. Even if it may lead to shedding some more load, as it was found out in [BPA98], this criterion makes sense in terms of reducing the nuisance caused to customers by low voltages.

In an actual power system, the “granularity” with which load can be shed is limited due to practical considerations. In general, the smallest block of load that can be shed is the load served through one substation-class distribution breaker since this is employed in order to interrupt the load. Furthermore, the distribution feeders served out of a particular substation in most cases have different aggregate load characteristics and demand profiles, which makes the predetermination of the actual amount of load available for shedding challenging. This means that the design of an undervoltage load shedding scheme should incorporate the impact of errors stemming from differences between the load that is presumably shed and the load that is actually shed.

4.3 Proposed load shedding scheme

4.3.1 Overall principle

The proposed scheme relies on a set of controllers distributed over the region prone to voltage instability. Each controller monitors the voltage V at a transmission bus and acts on a set of loads located at distribution level and having influence on V. A sub-transmission network may exist in between the monitored and the controlled buses, as sketched in Fig. 4.1. Note that not all transmission buses need to be monitored, and not all loads need to be controlled.

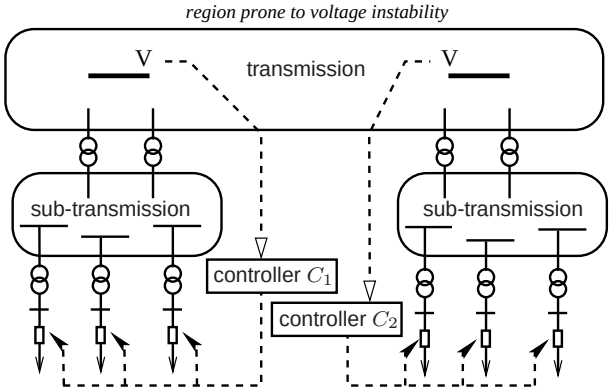

Figure 4.1: Overall structure of the proposed scheme

Each controller operates as follows:

- it acts when its monitored voltage V falls below some threshold V^{th};
- it can act repeatedly, until V recovers above V^{th}. This yields the already mentioned closed-loop behavior;
- it waits in between two sheddings, in order to assess the effect of the actions taken both by itself and by the other controllers;
- the delay between successive sheddings varies with the severity of the situation;
- the same holds true for the amount shed.

4.3.2 Individual controller design

The operation of an individual controller is described in Fig. 4.2 in the form of an automaton.

As long as V remains above the specified threshold, the controller is idle, while it is started as soon as a (severe) disturbance causes V to drop below V^{th}. Let t_0 be the time where this

change takes place. The controller remains started until either the voltage recovers, or a time τ is elapsed since t_0. In the latter case, the controller sheds a power ΔP^{sh} and returns to either idle (if V recovers above V^{th}) or started state (if V remains smaller than V^{th}). In the second case, the current time is taken as the new value of t_0 and the controller is ready to act again, provided of course that there remains load to shed. If the available load to shed is exhausted, $\Delta P^{sh}_{max} = 0$, the controller returns to idle state.

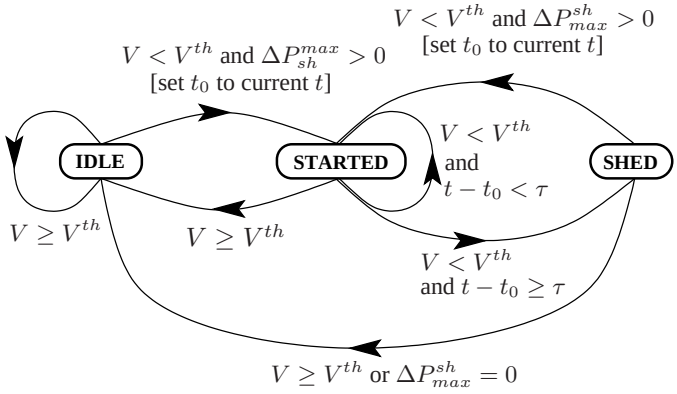

Figure 4.2: Logic of an individual load shedding controller (within brackets: action taken when the transition takes place)

The delay τ depends on the time evolution of V as follows. A block of load is shed at a time $t_0 + \tau$ such that:

$$\int_{t_0}^{t_0+\tau} \left(V^{th} - V(t)\right) dt = C \ , \tag{4.2}$$

where C is a constant to be adjusted. Figure 4.3 is a graphical representation of the integral used to determine the time delay. As soon as the area between the voltage threshold and monitored bus voltage evolution equals C, the load shedding action takes place.

This control law yields an inverse-time characteristic: the deeper the voltage drops, the less time it takes to reach the value C and, hence, the faster the shedding. The larger C, the more time it takes for the integral to reach this value and hence, the slower the action.

Furthermore, the delay τ is lower bounded:

$$\tau_{min} \leq \tau \ , \tag{4.3}$$

in order to take into account the communication time and breaker mechanical constraints, respectively to prevent the controller from reacting on a nearby fault. Indeed, in normal situations time must be left for the protections to clear the fault and the voltage to recover to normal values. In consequence, if the value of τ resulting from Eq. (4.2) is smaller than τ_{min}[2] the controller will trigger the load shedding action at time instant $t_0 + \tau_{min}$.

[2]This might happen if C is very small, for instance C = 0, or if the voltage drop is very large.

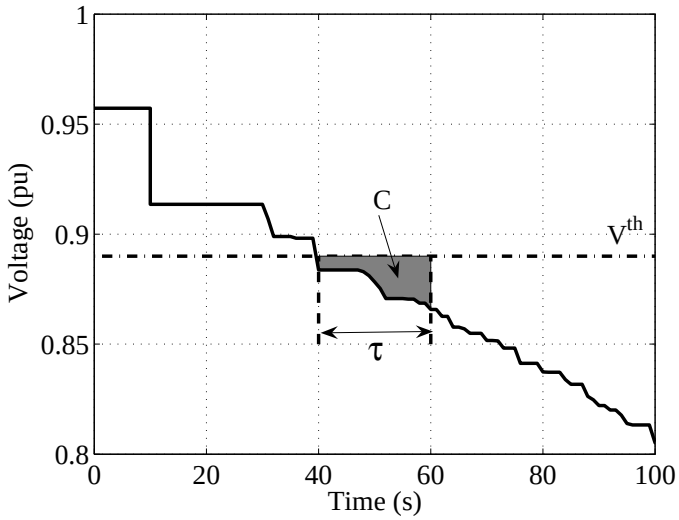

Figure 4.3: Illustration of time delay determination

Similarly, the amount ΔP^{sh} of power shed at time $t_0 + \tau$ depends on the time evolution of V through:

$$\Delta P^{sh} = K \cdot \Delta V^{av} \ , \tag{4.4}$$

where K is another constant to be adjusted, and ΔV^{av} is the average voltage drop over the $[t_0\ t_0 + \tau]$ interval, i.e.,

$$\Delta V^{av} = \frac{1}{\tau} \int_{t_0}^{t_0+\tau} \big(V^{th} - V(t)\big)\, dt \ . \tag{4.5}$$

The above relationships, illustrated in Fig. 4.4, transpose voltage drop severity into load shedding amplitude: the larger $V^{th} - V$, the larger ΔV^{av} and, hence, the larger the amount of load shed. The same holds true when the gain K increases.

As already mentioned, the controller acts by opening distribution circuit breakers and may disconnect interruptible loads only. Hence, the minimum load shedding corresponds to the smallest load whose breaker can be opened, while the maximum shedding corresponds to opening all the manoeuvrable breakers. Furthermore, to prevent unacceptable transients, it may be appropriate to limit the power disconnected in a single step to some value ΔP^{sh}_{tr}. The above limitations are summarized as follows:

$$\min_k P_k \leq \Delta P^{sh} \leq \Delta P^{sh}_{max} \ , \tag{4.6}$$

$$\text{with} \ \ \Delta P^{sh}_{max} = \min\big(P_{int}(t),\ \Delta P^{sh}_{tr}\big) \ , \tag{4.7}$$

$$\text{and} \ \ P_{int}(t) = \sum_k P_k \ , \tag{4.8}$$

where $P_{int}(t)$ represents the part of the load still interruptible at time t, P_k denotes the individual load power behind the k-th circuit breaker under control, and the minimum in (4.6) and the sum in (4.8) extend over all manoeuvrable breakers still connected at time t. It results that, for

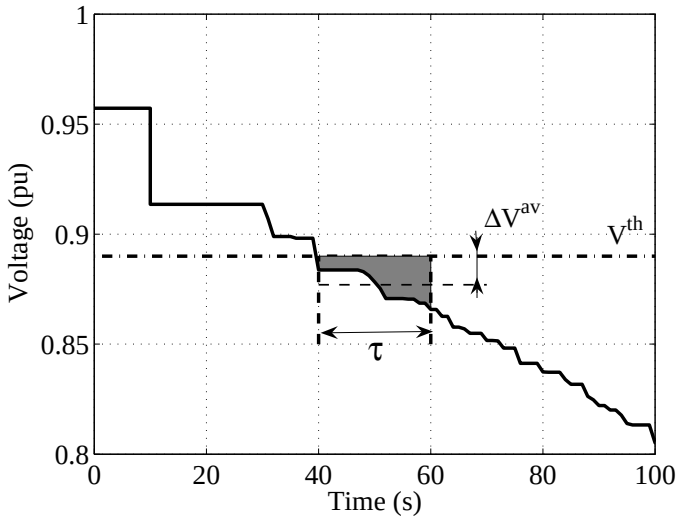

Figure 4.4: Illustration of voltage average determination

small values of K, for instance K = 0, resulting in an amount of load shedding ΔP^{sh} smaller than $\min_k P_k$ the controller has to shed the smallest load power behind a circuit breaker.

The control logic focuses on active power but load reactive power is obviously reduced together with active power. In the absence of more detailed information on load composition, disconnected by each manoeuvrable breaker, we assume that both powers vary in the same proportion, i.e., the reactive change is given by:

$$\Delta Q^{sh} = \Delta P^{sh} \frac{Q_{int}(t)}{P_{int}(t)} \ , \tag{4.9}$$

where $Q_{int}(t)$ is the interruptible reactive power, at time instant t.

4.3.3 Tuning the controller parameters

The tuning of the controllers should rely on a set of scenarios combining different operating conditions and disturbances, as typically considered when planning an SPS [LMC03].

Considering the SPS basic requirements presented in Section 4.1, the parameter settings of the proposed undervoltage protection scheme have to provide:

1. dependability: all unacceptable post-disturbance system responses are saved by the SPS, possibly in conjunction with other available controls;

2. security: the SPS does not act in a scenario with acceptable post-disturbance system response. This is normally the case following any N-1 contingency;

3. selectivity: as few load power as possible is interrupted.

The tuning mainly consists of choosing the best values for V^{th}, C and K. The bounds τ_{min} and ΔP_{tr}^{sh} can be chosen by engineering judgement.

First, attention must be paid to V^{th}. This threshold should be set high enough to avoid excessive shedding delays, which in turn would require to shed more and/or cause low load voltages. On the other hand, it should be low enough to obey requirement 2 above. It should thus be set a little below the lowest voltage value reached during any of the acceptable post-disturbance evolutions.

Next, C and K should be selected so that, for all scenarios:

- the protection sheds as few load as possible and
- some security margin is left with respect to values causing protection failure.

Using the same C and K values for all controllers makes the design definitely simpler. In the tests we performed so far, there has been no evidence that individual values would yield substantial benefits. Therefore, this simplification is adopted throughout the remaining of the thesis.

4.3.4 Cooperation between controllers

The various controllers interact in the following way.

Let us consider two close controllers: C_i monitoring bus i and C_j monitoring bus j ($j \neq i$). Let us assume that both controllers are started by a disturbance. When C_i sheds some load, this causes the voltages to increase not only at bus i but also at neighboring buses, in particular at the monitored bus j. Since V_j increases, the integral $\int \left(V^{th} - V_j(t)\right) dt$ grows more slowly with time, thereby leading to a larger delay τ before C_j can act. For the same reason, ΔV^{av} decreases and C_j will shed less load once its delay τ is elapsed. For larger voltage increases, V_j may even become larger than V^{th} making C_j return to idle state. In other words, when one controller sheds load, this slows down or inhibits the controllers that compete with him to restore voltages in the same area. This cooperation avoids excessive load shedding.

Moreover, the whole system will tend to shed first where voltages drop the most. This location changes with the disturbance. Hence, the proposed scheme automatically adjusts the shedding location to the disturbance it faces.

Note that the above features are achieved without resorting to a dedicated communication network. The controllers do not exchange information, but are rather informed of their respective actions through the power system itself. This is made possible by the fact that voltages have no “inertia”: the effects of shedding are felt almost instantaneously. Neither do the controllers

require a model of the system. This and the absence of communication makes the protection scheme definitely simpler and hence more reliable.

4.3.5 About system partitioning into load areas

From our tests it was found that simple geographical considerations can be used to assign loads to different monitored buses. However, if this was not deemed satisfactory, one could resort to more elaborate techniques like the ones outlined hereafter.

The notion of *Voltage Control Areas* (VCA) [SHC91] could prove useful in defining the load shedding areas. A VCA is a group of buses in a geographically dense area responding similarly (as far as voltage magnitude is concerned) to external disturbances.

VCAs can be built from electrical distances which are a measure of voltage interaction between different buses of the system [LSL89]. The latter are obtained from a sensitivity matrix $[\partial \mathbf{V}/\partial \mathbf{Q}]$ whose elements reflect the propagation of voltage variation following reactive power injection at a bus. More precisely, the degree of voltage coupling between two buses i and j is given by the α_{ij} factor involved in the relation:

$$\Delta V_i = \frac{\frac{\partial V_i}{\partial Q_j}}{\frac{\partial V_j}{\partial Q_j}} \Delta V_j = \alpha_{ij} \Delta V_j \ ,$$

In general, $\alpha_{ij} \neq \alpha_{ji}$. In order to retain symmetry in the distance concept, the electrical distance between buses i and j is defined as:

$$D_{ij} = D_{ji} = -log\left(\alpha_{ij} \times \alpha_{ji}\right) \ .$$

The boundaries of the VCAs could be determined from the electrical distances between any load bus and the transmission buses monitored for undervoltage load shedding. In order a load bus to be included in one area only, it is appropriate to assign each load bus to the ”closest” monitored bus (in the sense of the above defined distance).

Alternatively, it has been proposed to determine VCAs from terms of a properly normalized $[\partial \mathbf{Q}/\partial \mathbf{V}]$ Jacobian matrix, by eliminating smaller off-diagonal elements [SHC91, LSR93, AS03, VS05].

If should be noted, however, that a fundamental limitation of sensitivity or Jacobian matrices lies in the fact that their terms may significantly vary with operating conditions or after a network topology change.

4.3.6 Analogy with multi-agent systems

The proposed scheme shows a strong analogy with Multi-Agent Systems (MAS). MAS have received much attention in various engineering disciplines (e.g. [SV00]), including power sys-

tem engineering [CR03, DH05]. In fact, there is no general consensus on what an agent is [SV00, CR03, DH05, RN95]. Its meaning is strongly biased by the background field (engineering, artificial intelligence, cognitive science, computer science, software engineering, etc.), although the perception in software engineering and artificial intelligence tends to prevail [CR03]. Similarly, there is no clear borderline between distributed computing and multi-agent technology.

In [SV00] a MAS is defined as a loosely coupled network of problem-solving entities (agents) that work together to find answers to problems that are beyond the individual capabilities of each entity. Where an agent is a *computational (intelligent) system* that inhabits some complex dynamic environment, *senses* and *acts autonomously* in this environment, and by doing so *fulfills a set of goals or tasks* for which it was designed [Mae95].

In the spirit of these general definitions, the following analogy between the distributed load shedding controllers and MAS can be made.

Each controller possesses some of the distinguishing characteristics of an agent: it senses the power system behavior through the measurement inputs, each controller is autonomous (it operates without direct intervention of another controller or supervisor) and has some degree of intelligence (in the form of "if ...then ..." rules and Eqs. (4.2 - 4.6)). Therefore, the proposed scheme can be seen as a MAS. In the remaining of the thesis the term *controller*, will be used to designate a load shedding controller.

As sketched in Fig. 4.5, MAS fall into two basic categories [DFJ97]: *independent* and *cooperative*.

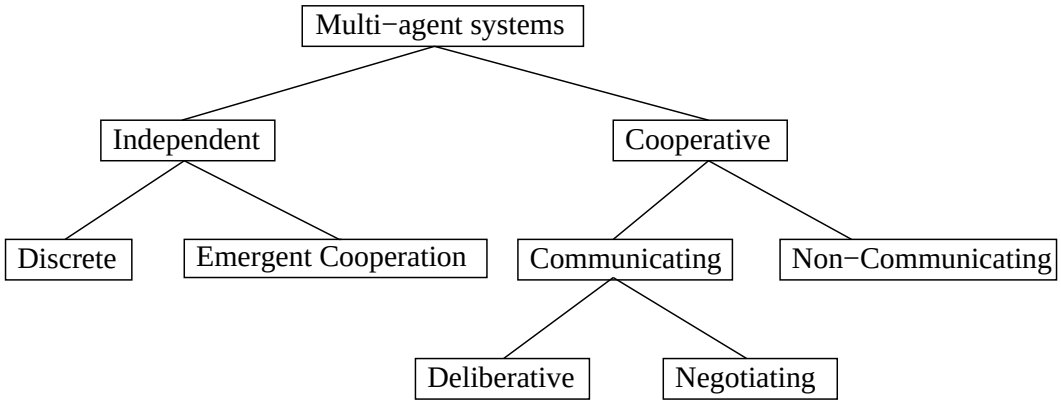

Figure 4.5: Multi-agent systems classification

In independent MAS, the individual agents pursue their own goals independently of the others. They can be further classified into MAS with *discrete agents*, if the goals of the agents bear no relation to one another, or MAS with *emergent cooperation*, if agents cooperate "with no intention of doing so" and cooperation emerges from the consistency of their individual goals. An example of the latter is the combination of secondary voltage control and undervoltage load shedding.

On the other hand, cooperative agents have the same goals, domain knowledge and possible actions. The only difference among individual agents is their sensory inputs, i.e. they are situated at different places in the environment. The cooperation within a MAS can be realized in three ways:

- explicit design - the agents are designed to cooperate;
- adaptation - the agents learn to cooperate;
- by evolution - individual agents cooperation evolves through some kind of evolutionary process.

Cooperative agents can be further classified into *communicating* and *non-communicating*. In the former case, the agents are intentionally exchanging signals; to this purpose, they usually rely on a dedicated communication system, which is considered from the MAS design stage. In the non-communicating case, the agents coordinate their cooperative activity by observing and reacting to the behavior of others.

Intentional communication can take at least two forms: *deliberation* or *negotiation*. In deliberative MAS the agents jointly plan their actions so as to cooperate with each other in order to achieve their goals. The coordination of their respective actions is not mandatory. Negotiating systems are similar to the deliberative ones, except that there is a competition among the agents.

The proposed load shedding scheme can be categorized as a cooperative non-communicating MAS. Indeed, in the proposed scheme, there is an implicit communication and coordination between agents, through system voltages, as explained in the previous section.

4.4 Preliminary results on a small test system

4.4.1 Nordic32 test system

The Nordic32 test system is the LF32-029 version of the test system used by CIGRE Task Force 38.02.08 [CTF98]. It includes 80 buses, 23 generators and 22 loads fed through transformers equipped with LTCs. The one-line diagram is shown in Fig. 4.6. The test system consists of four parts, the main power transfer is from the “North” area, where important hydro plants are located, to “Central” area, where the main load area and some thermal plants are located. Taking into account that only the Northern hydro generators participate to frequency control, when a generator is lost in the Central area, the power deficit is added to the North to Central transfer. The transmission capacity from North to Central areas is limited by transient stability and voltage stability. Overexcitation limiters and LTCs play an important role [CTF98].

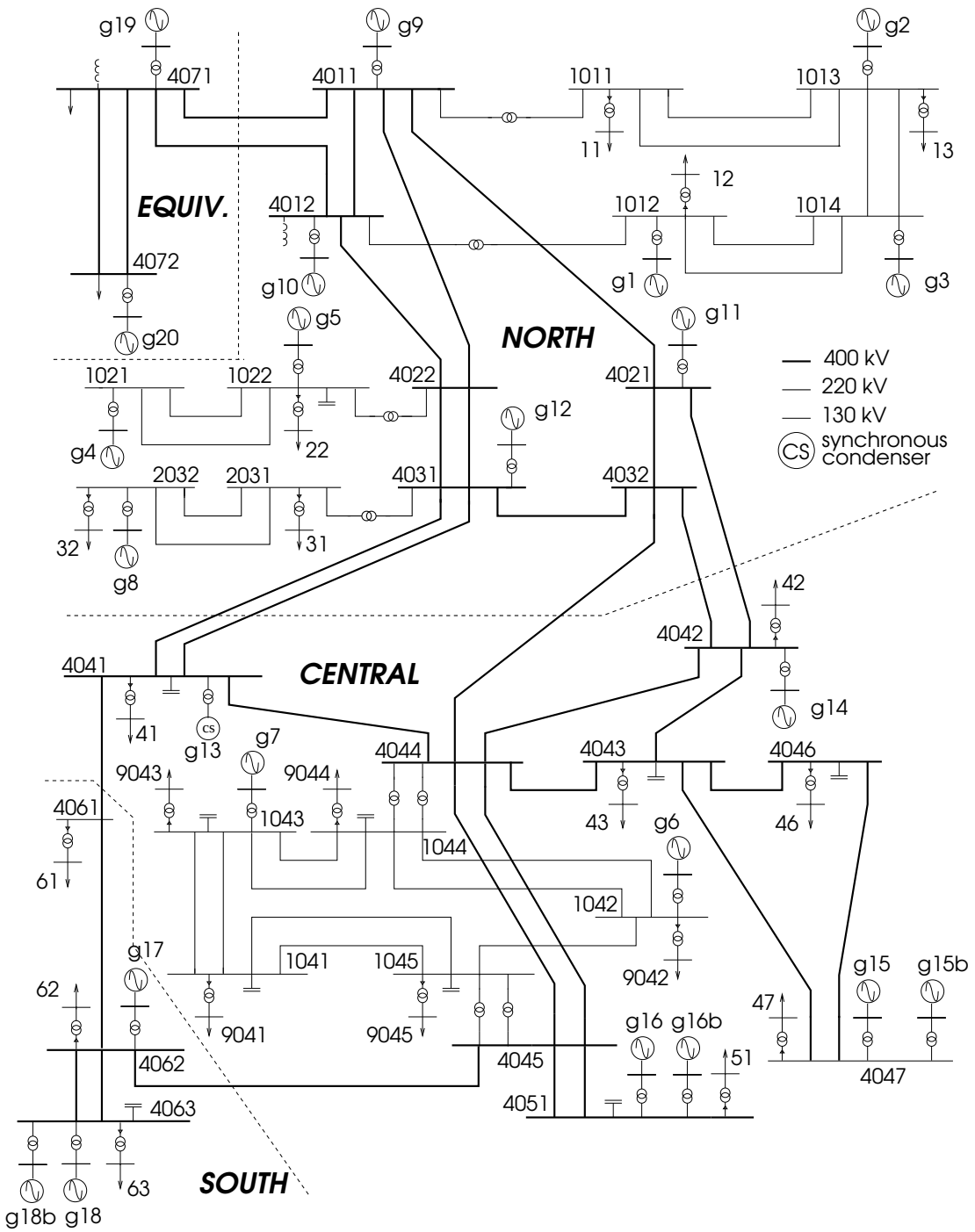

Figure 4.6: Nordic32 test system

In order to illustrate the controller tuning and behavior, we have considered the following four severe contingencies requiring load shedding (more disturbances should be considered in practice):

N1: loss of line 4032-4044 and generator g14

N2: loss of lines 4032-4044 and 4041-4044

N3: loss of double-circuit line 4031-4041

N4: loss of lines 4042-4043 and 4042-4044

The system responses have been obtained by QSS simulation, using a time step of 1 second and a simulation interval of 600 seconds.

4.4.2 Load shedding controller location

The "Central" region is the one where voltage problems are experienced. Therefore, this area has been provided with five controllers, as detailed in Table 4.1. In this simple system, each controller monitors the voltage of one transmission bus and controls the load on the distribution side of the transformer connected to that bus. In a real-life application, however, each controller would act on a set of loads located at different buses, as sketched in Fig. 4.1.

Table 4.1: Considered controllers

Controller name	Monitored bus	Controlled load bus	Available power to shed (MW)
C_{1041}	1041	9041	600
C_{1042}	1042	9042	300
C_{1043}	1043	9043	230
C_{1044}	1044	9044	800
C_{1045}	1045	9045	700

4.4.3 Choosing the voltage threshold

As previously mentioned, the voltage threshold V^{th} should be chosen low enough in order the protection not to act in acceptable post-disturbance situations (typically for N-1 contingencies) but high enough to prevent load voltages from reaching unacceptable values.

To this purpose, we consider all N-1 (line or generator tripping) contingencies, for which post-disturbance evolution is accepted. The criterion is that all transmission voltages remain above 0.85 pu. This value corresponds to unacceptable customer voltages as well as a high risk of field-current limited generators to lose synchronism. Note that, according to standard practice, all N-1 contingencies should be involved; however, the operating point of the Nordic32 test system, at which the undervoltage protection scheme was implemented, is very stressed and cannot withstand the single loss of generator g6, g14, g15, g15b or g16. Furthermore, when

generator g7 is lost the system experiences low voltages but the criterion is not violated. Therefore, these six contingencies are not included in the list (i.e. load shedding will be allowed). The lowest voltages reached at the five buses monitored by controllers, following any of the above contingencies, are given in Table 6.1.

Table 4.2: lowest voltages after N-1 contingencies

bus	min. volt. (pu)
1041	0.90
1042	0.98
1043	0.93
1044	0.94
1045	0.95

One can see that the voltage threshold could take a value in between 0.85 pu, the lowest acceptable voltage, and 0.9 pu, so that no load is unduly shed following any of N-1 contingencies considered. Nevertheless, V^{th} should be set high enough in order to leave some time for the controllers to act, as illustrated in the sequel.

4.4.4 Sensitivity to parameters V^{th}, C and K

Figures 4.7.a and b illustrate the control scheme performance for various values of V^{th}, C and K, for contingencies N1 and N2, respectively. We considered τ_{min} = 3 s, $\min_k P_k$ = 10 MW and ΔP_{tr}^{sh} = 250 MW.

The stars indicate settings for which the post-disturbance evolution is accepted. The dots indicate failures, i.e. cases where the 0.85 pu voltage was temporarily or permanently crossed. Expectedly, the lower V^{th}, the less time the controllers have to prevent voltages from reaching 0.85 pu, and hence a smaller C has to be chosen. This can also be compensated by a larger K[3].

Taking a 0.01 pu tolerance for security, we set V^{th} to 0.89 pu and use this value in the remaining of the procedure.

4.4.5 Assessing the protection scheme selectivity

To assess the selectivity of the load shedding scheme we considered the *total amount of load shed*. This is obviously the sum of the amounts ΔP_i^{sh}, shed by all controllers, until all monitored voltages recover above V^{th}, for a specific disturbance:

$$P^{sh} = \sum_i \Delta P_i^{sh}$$

[3]The controller has to act faster or to shed more load.

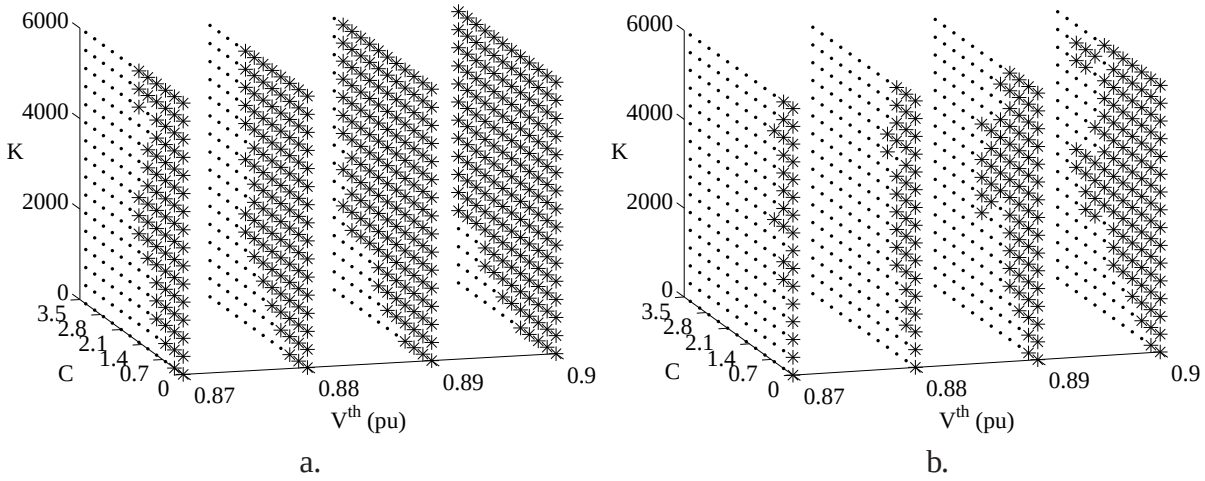

Figure 4.7: Performance of load shedding scheme for different settings

The plot in Fig. 4.8 shows the total amount of power shed, for various values of C and K, under the chosen V^{th}, for contingency N1. The gray parts represent successful protection operation, the darkest points corresponding to the smallest amount of power cut.

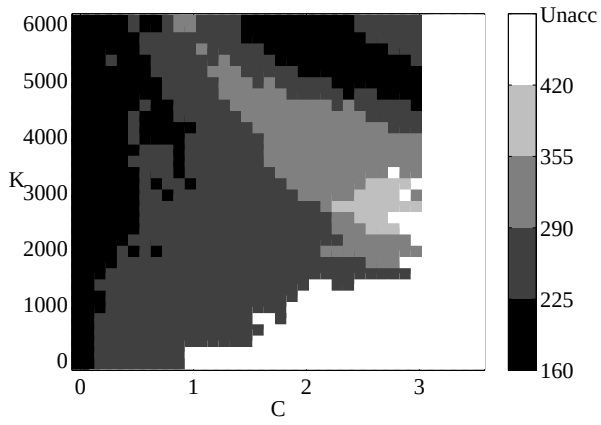

Figure 4.8: Total power shed (MW) for various (C, K) values, with $V^{th} = 0.89$ pu

Our main concern in this work was the minimization of interrupted power, irrespective of voltage recovery at the terminal of non interrupted load. If one would like to incorporate a measure of voltage recovery, and take into account loads magnitude, we would consider the *unserved energy*, determined from the unserved power.

The unserved power is computed as:

$$\Delta P^{unser} = \sum_{k} \left(P_k^0 - P_k \right)$$

where P_k^0 is the pre-disturbance load power at bus k.

If we consider the load model Eq. (2.6), the above equation can be rewritten as:

$$\Delta P^{unser} = \sum_k P_k^0 \left[1 - \left(\frac{V_k(t)}{V_k^0} \right)^{\alpha_k} \right]$$

where the sum extends over the set of buses controlled by load tap changers. However, if voltage V_k lies in the LTC deadband, it is appropriate not to include the load of concern in the sum since $|V_k - V_k^0|$ is a normal voltage deviation [OSC03].

The unserved energy is given by the expression:

$$E^{unser} = \int_0^{t_s} \Delta P^{unser} dt$$

where t_s is the time simulation interval (in the absence of a more precise information on the restoration time).

As for the total amount of load shedding, plots can be used to show the unserved energy for various (C, K) combinations. Such a diagram is provided in Fig. 4.9, which corresponds to the same contingency and voltage threshold used to determine Fig. 4.8. The simulation time considered was t_s = 600 s.

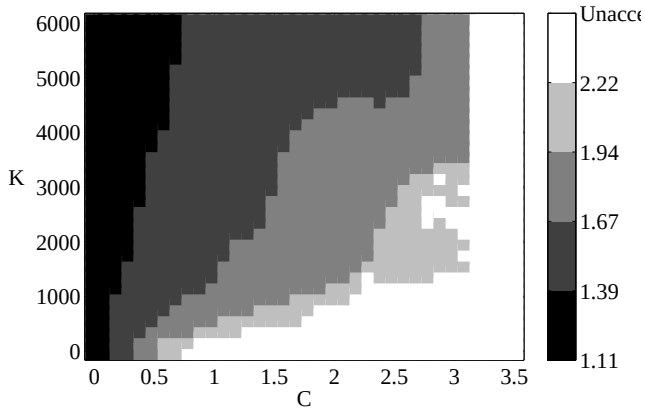

Figure 4.9: Unserved energy (MWh) for various (C, K) values, with $V^{th} = 0.89$ pu

The unserved energy parameter is a more comprehensive measure of the load shedding action as it takes into account the consumer voltage deviation. Indeed, this parameter is directly influenced by the amount of load shed (the more load is shed the better the voltage profile) and the load shedding delay (the faster the load shedding the faster the voltage recovery). Furthermore, it has no information about the amount of load shed.

Therefore, one may also think of considering a general index including the total amount of load power shed and the unserved power over the simulation interval. However, as the shed power and the unserved power have different costs, weighting factors have to be used.

4.4.6 Choosing C and K

After choosing the voltage threshold, the next step is to determine the best (C,K) combination. To this purpose, for each scenario necessitating load shedding, it is appropriate to consider plots of the type shown in Fig. 4.8.

Figures 4.10.a - d correspond to contingencies N1 - N4 (see Section 4.4.1). The figures confirm that choosing a larger C (i.e. a slow responding protection) generally requires to also set K to a larger value, which generally leads to shedding more load. Beyond some value of C, the protection is so slow that it fails, whatever the value of K.

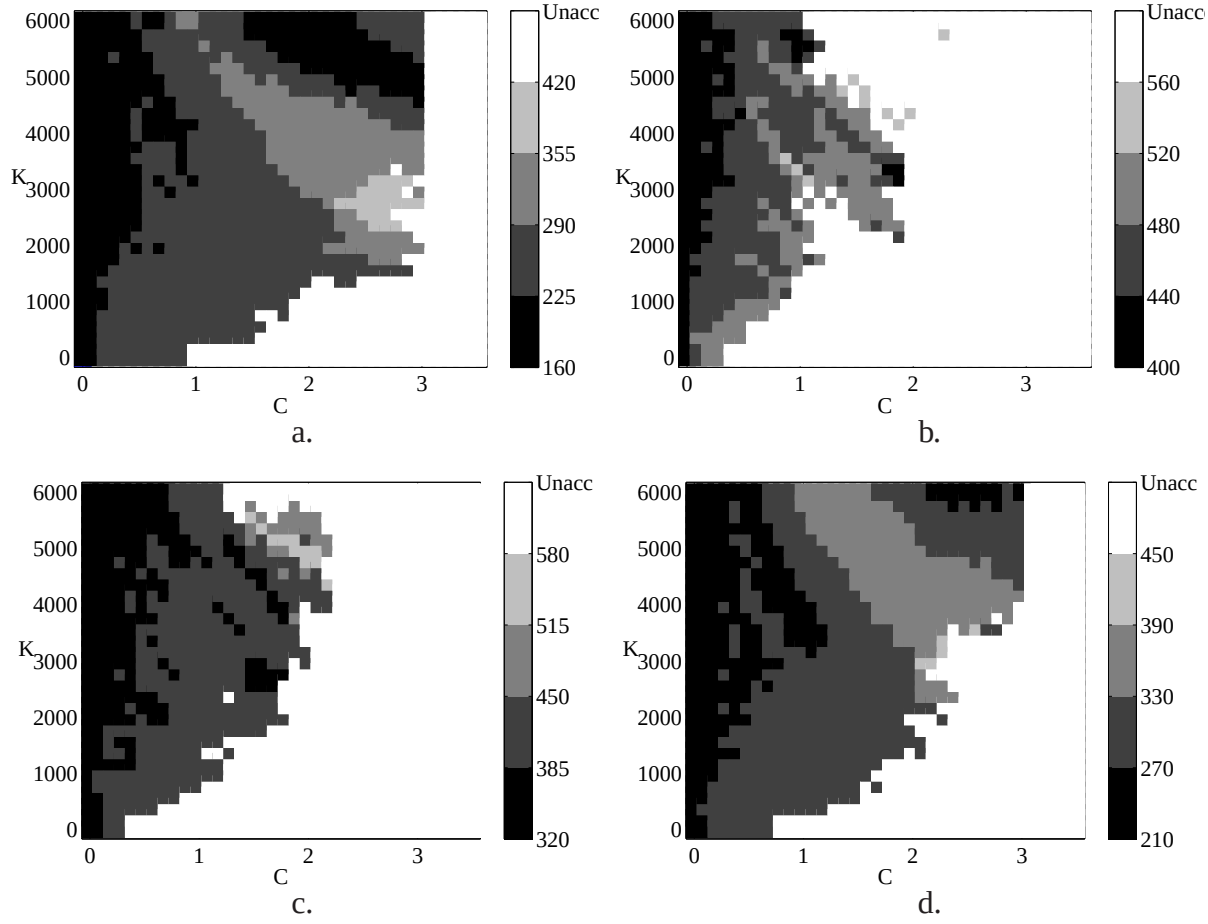

Figure 4.10: Total power shed (MW) for various (C, K) values, with $V^{th} = 0.89$ pu

Note that the zones of equal shedding are not limited by smooth boundaries. This is attributable to the discrete nature of the controllers; a smooth change of a parameter may lead to a different sequence of load shedding actions. This aspect will be further commented in the next section.

Moreover, one can notice that for $C = 0$, all values of K lead to almost the same amount of load shedding. This is explained by the fact that for $C = 0$ the delay is lower limited to τ_{min}; the protection will thus act many times and voltages will recover fast. In this case, it

does not really matter how much of load is shed at each step, because shedding is taking place fast enough so that it is not required to shed more to compensate for shedding more slowly [VCV98, LMC03].

Other aspects (and engineering judgement) have to be taken into consideration when tuning such an SPS. For instance:

- for reliability reasons, it does not sound appropriate to choose a point in the (C,K) space close to the limit of protection failure. With reference to Fig. 4.10, the chosen point should be at a minimum distance of the white areas;
- too small C values are not recommended because the integral in Eq. (4.5) would be computed over a short interval where transients may deteriorate accuracy;
- too small K values are not realistic because it may not be feasible to disconnect small blocks of loads.

From such plots, and the above mentioned recommendations, a (C,K) combination suitable to all scenarios can be identified by minimizing the total load shedding over all scenarios. Other criteria could be considered as well [Moo02, COL08].

These considerations lead to the settings of Table 4.3, which have been adopted for all controllers. According to Eqs. (4.2, 4.4, 4.5), these values of C and K mean that if V settles at 0.87 pu, for instance, 80 MW are shed after 20 seconds.

Table 4.3: Controller settings

V^{th}	C	K	τ_{min}	$\min_k P_k$	ΔP_{tr}^{sh}
0.89 pu	0.4 pu·s	4000 MW/pu	3 s	10 MW	250 MW

4.4.7 Detailed example of performance

To illustrate the performance of the controllers, we consider hereafter contingency N3. The unstable system response experienced without load shedding is shown with dotted line in Fig. 4.11, showing the evolution of voltage at bus 1041 provided by quasi steady-state simulation. The heavy line in the same figure corresponds to the system stabilized by the proposed control scheme.

In this example, controllers C_{1041} and C_{1044} responded to the disturbance. In order to illustrate their interactions, a zoom of the dashed area of Fig. 4.11 is given in Fig. 4.12, while Fig. 4.13 shows the voltage monitored by controller C_{1044} over the same time interval. In both figures, the MW values refer to the power shed by the controller of concern while the circles indicate shedding by the other one.

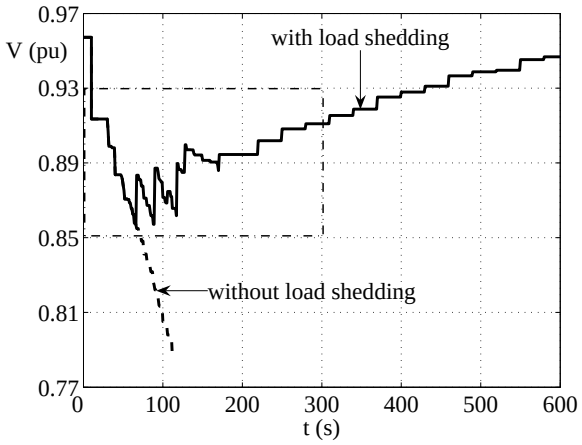

Figure 4.11: Voltage evolution at bus 1041 without and with load shedding

As can be seen, the 64 MW shed by C_{1041} make the voltage at bus 1044 recover above V^{th}, with the effect of resetting C_{1044}. Similarly, the voltage jump experienced when C_{1041} sheds 72 MW delays and reduces the first load shedding by C_{1044}.

Figure 4.13 also illustrates the previously mentioned inverse-time characteristic. The two hatched areas have the same surface C. Since the voltage is lower after the first shedding than after the third one, the controller waits less before the second shedding than before the fourth one.

In the previous section we pointed out the fact that a small change in parameter settings leads to a different load shedding sequence (in terms of time delays and amounts of load shed), due to the interaction between controllers, as explained above. Fig. 4.14 presents the load shedding sequences for three different (C,K) combinations, where the black bar refers to the case presented in Figs. 4.12 and 4.13. As can be seen, an increase of parameter K results in larger amounts of load shed. Similarly, an increase of C leads to a slower but stronger load shedding action. In both cases, the controlled voltages recover faster as more load is shed at the beginning of the load shedding sequence.

4.4.8 Robustness of the control scheme

In order to illustrate the robustness of the proposed design, Table 4.4 shows the power shed by each controller in various scenarios. Case 1 corresponds to the simulation shown in Figs. 4.12 and 4.13 while the other cases correspond to failures, as detailed hereafter.

In Case 2 it is assumed that only 20 % of the load are interruptible at bus 1041. This is compensated by a stronger action of C_{1044} and an intervention of C_{1043}.

In Case 3 we suppose that the voltage measurement used by C_{1041} is 0.01 pu smaller than the correct value, causing this controller to act faster and shed more power. This is compensated

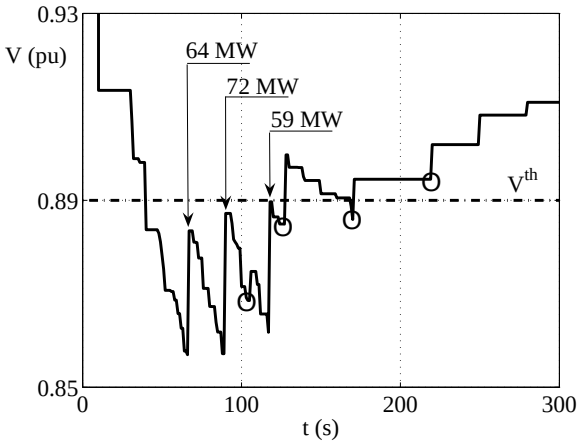

Figure 4.12: Monitored voltage and actions of controller C_{1041}

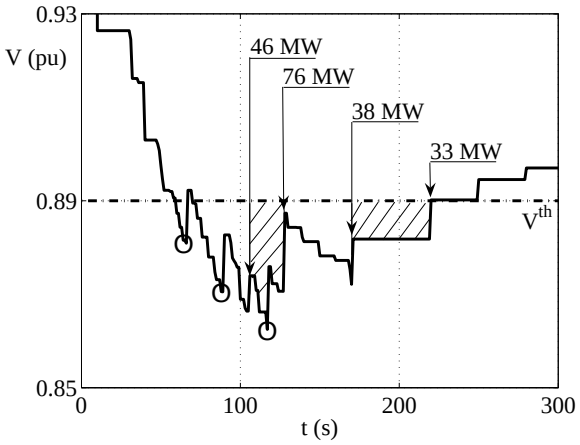

Figure 4.13: Monitored voltage and actions of controller C_{1044}

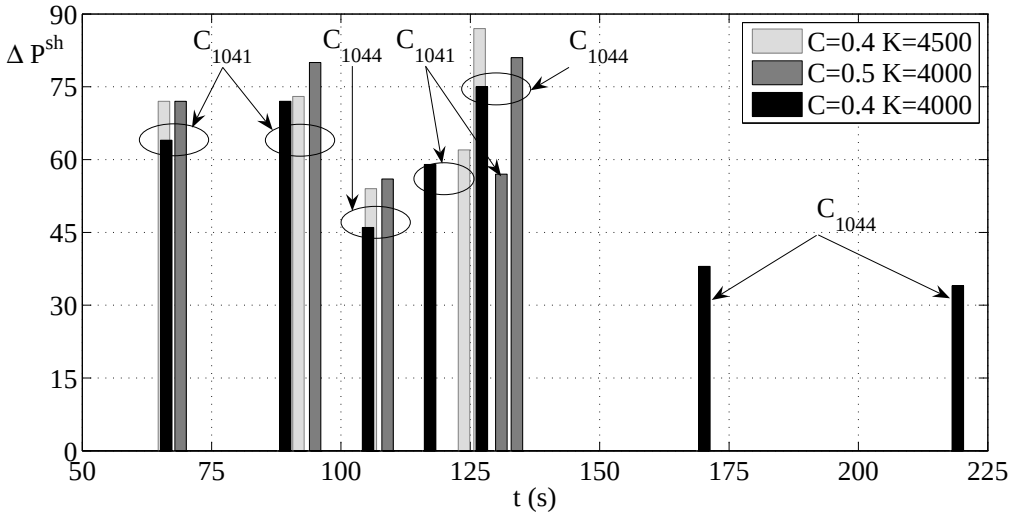

Figure 4.14: Load shedding sequence for different (C,K) combinations

by a smaller action of C_{1044}.

Case 4 simulates a full failure of C_{1041}; this is covered by a stronger action of C_{1043} and C_{1044}. Similarly, Case 5 corresponds to failure of both C_{1041} and C_{1044}, leading C_{1042} and C_{1045} to come into play.

Clearly, this redundancy among controllers makes the protection scheme very reliable. In this example, the total power shed even decreases as more controllers compensate for those that should have responded first to the voltage drops.

Table 4.4: Load shedding amount (MW) in various scenarios

Controller	Case				
	1	2	3	4	5
C_{1041}	195	120	206	-	-
C_{1042}	0	0	0	0	102
C_{1043}	0	39	0	120	229
C_{1044}	193	220	159	244	-
C_{1045}	0	0	0	0	33
Total	388	379	365	364	363

4.5 Concluding remarks

The decentralized implementation of undervoltage load shedding based on voltage measurements was found to behave quite satisfactorily. The controllers are coordinated through the power system itself, without resorting to a dedicated communication network, which adds to simplicity and hence reliability.

The controllers operate in closed-loop, adjusting their emergency action to the severity of the disturbance they are facing. Redundancy guarantees robustness against system behavior uncertainties and operation failures.

However, its ability to adjust to the disturbance location and the coordination with other voltage controls has still to be demonstrated on a larger system. Results regarding these aspects are reported in Chapter 6 where the protection scheme is implemented on a model of a real-life system.

Chapter 5

Wide-area protection against overloaded line tripping

An approach inspired of Model Predictive Control is proposed to determine a sequence of control actions aimed at alleviating thermal overloads in emergency conditions. The algorithm brings the line currents below their limits in the time interval left by protections, while accounting for constraints on control changes at each step. Its closed-loop nature allows to compensate for measurement noise and model uncertainties. Various aspects such as the choice of the objective function, the influence of modeling errors, etc., are discussed and illustrated through a small academic test system.

5.1 Previous work

As illustrated in Chapter 1, some of the recent blackouts involved cascade line trippings due to thermal overloads. In some cases, emergency measures were not taken to quickly prevent some of the overloaded lines from being tripped, thereby leading to cascading effects on the remaining lines.

In such emergency conditions, it is essential to quickly mitigate the consequences of the initial disturbances before protection systems take actions that make the problem more severe [TJH05]. As is well-known, protections may take the overloaded line out of service after some temporization or the line may sag and eventually touch objects, causing a short-circuit, quickly eliminated by distance protections.

The approaches dealing with transmission line overloads, reported in the past, can be roughly classified into: optimization based, non-optimization based and mixed methods.

Optimization based methods, which includes the Optimal Power Flow (OPF) formulation with proper objective and constraints, can be used to determine the best actions [SG90, MZB01,

SV06]. These are accurate methods as they are using the full model of the network. For the same reason they are regarded as computationally expensive and time consuming methods. Many publications have been devoted to improving OPF algorithms, and OPF is available in Energy Management Systems [AS74]. In many control centers, however, the OPF output is only proposed to the operator, who is responsible for implementing the corresponding changes [MKB97].

Non-optimization methods emerged as the need for an efficient and fast method so that system operators can make quick decisions under emergency conditions of the power system [MBS79, BDD99, SV05]. The primary concern in these methods is to obtain a secure state of operation quickly with little or no concern of optimality of the corrected operating point.

A combination of the two approaches has been proposed in several publications [NK94, TSM05]. These approaches aim at combining efficiency and speed of non-optimization methods while at the same time pursuing the solution that is sufficiently close to the optimal one.

Depending on the system, emergency control actions may involve changing the angle of phase shifting transformers [MZB01, CBC02, MC04], rescheduling generation and, in the last resort, shedding load [CS79, MCT05]. Topology changes (line and bus-bar switching) [SG90] and different types of FACTS devices may also prove very efficient [SV06], but are not considered here.

5.2 Computation of optimal corrective control actions to alleviate thermal overload

OPF has been widely used in planning and real-time operation of power systems for active and reactive power dispatch to minimize generation costs and system losses and to improve the voltage profile [SAM87]. It combines economical aspects with power system secure operation aspects.

The research work on OPF can be divided into two parts. The first part deals with the development of efficient algorithms for solving nonlinear OPF problems, such as the reduced gradient method, linear and quadratic programming method [ABP90], Newton method [SAB84] and the interior point method [WSK98]. The second part deals with application scope extension. In recent years there were two main extension areas. One is the application of OPF in electricity market and the other is the application of OPF in preventive control for improving transient or voltage stability margins. The former explored OPF capability of maximizing for instance the social welfare while the latter developed OPF capability of satisfying comprehensive security and stability constraints.

The applications in preventive control for enhancing stability can be divided into OPF with transient stability constraints (TSCOPF) [GTZ00, YKS03] and OPF with voltage stability constraints (VSCOPF) [CRB01, RCQ03, SLK03].

The classical OPF problem can be stated as the following general constrained optimization problem:

$$\min C(\mathbf{x}, \mathbf{u}) \tag{5.1}$$

$$\text{subject to:} \quad \mathbf{g}(\mathbf{x}, \mathbf{u}) = \mathbf{0} \tag{5.2}$$

$$\mathbf{h}(\mathbf{x}, \mathbf{u}) \leq \mathbf{0} \tag{5.3}$$

$$\mathbf{u}^{min} \leq \mathbf{u} \leq \mathbf{u}^{max} \tag{5.4}$$

where:

- $\mathbf{x}$ is the vector of system state or dependent variables, which are usually bus voltage magnitudes and phase angles,
- $\mathbf{u}$ is the vector of control or independent variables (e.g., active generators power, phase shifter angle, load power, etc.),
- $\mathbf{g}$ denotes the load flow equations,
- $\mathbf{h}$ denotes the operational constraints such as bus voltage and branch thermal limits
- inequality constraints (5.4) represent the upper and lower limits of control variables (e.g. generator active/reactive power, OLTC transformer ratio, phase shifter angle, etc.),
- $\mathbf{C}(\mathbf{x}, \mathbf{u})$ is the cost function.

When dealing with line overload alleviation, time is important in two, somewhat contradictory respects. On one hand, there is some time left to alleviate overloads, thanks to thermal inertia of equipments. Progress has been made in the real-time estimation of the time left before the conductor material is damaged or the line sag leaves insufficient insulation distance [BDD99]. On the other hand, there are limits on the rate of change of some of the above mentioned controls: for instance, it takes time to change the tap position of a phase shifting transformer, the rate of change of power plant production is limited, etc.

In order to take into account the rate of change of different controls and the available control time, the traditional one-step optimization should be replaced with a multi-step optimization problem, which would provide an "optimal" time sequence of control actions. This multi-step optimization problem can be stated as follows:

$$\min_{\mathbf{x}^j, \mathbf{u}^j} \sum_j C^j(\mathbf{x}^j, \mathbf{u}^j) \tag{5.5}$$

$$\text{subject to:} \quad \mathbf{g}^j(\mathbf{x}^j, \mathbf{u}^j) = \mathbf{0} \tag{5.6}$$

$$\mathbf{h}^j(\mathbf{x}^j, \mathbf{u}^j) \leq \mathbf{0} \tag{5.7}$$

$$\mathbf{u}^{min} \leq \mathbf{u}^j \leq \mathbf{u}^{max} \tag{5.8}$$

$$\Delta\mathbf{u}^{min} \leq \mathbf{u}^j - \mathbf{u}^{j-1} \leq \Delta\mathbf{u}^{max} \tag{5.9}$$

where $j = 1, \ldots, J$ represents the control step number, and J is the total number of steps.

However, the number of equality and inequality constraints of the single-step optimization is now multiplied by J; therefore the optimization problem becomes even more computationally complex and time consuming. Hence, to keep the approach tractable, some simplifications of (5.6) and (5.7) are desirable. One such simplification is used in the sequel.

Furthermore, this single "optimal" control sequence is determined for the available system model and the given initial conditions. Thus, the open-loop nature of this optimization would not allow to compensate for inaccuracies originating from modeling uncertainties, measurement noises and unexpected reactions of some components. Therefore, it is desirable to resort to closed-loop control, relying on system response in the course of applying corrective actions.

To this purpose, we propose an optimization procedure that bears the spirit of Model Predictive Control (MPC).

5.3 Introduction to MPC

MPC techniques have been used for years in process industry [QB97], and they are to the greatest extent theoretically understood [MRR00]. Nevertheless, up to now this control technique seems to have not received enough attention from power system researchers and practitioners, although recent references show a growing interest for this approach [LK03, ARH03, TJH05, HG06, ZA06].

Standard MPC is a class of algorithms to control the future behavior of a system through the use of an explicit model of the latter [Mac02, FA02]. In general, the MPC problem is formulated as solving on-line a finite horizon open-loop optimal control problem subject to system dynamics and constraints involving states and controls.

Figure 5.1 shows the basic principle. Based on measurements obtained at time t_0, the controller predicts the future open-loop dynamic behavior of the system over a prediction horizon T_p and determines the control sequence over a control horizon $T_c \leq T_p$, such that a performance objective is optimized.

If there were no disturbances and no model mismatch, and if the optimization problem could be solved, then one could apply the control sequence determined at time t_0 to the system for all times $t \geq t_0$. However, this is not possible in general: due to disturbances, modeling errors and measurement noise, the real system behavior could be different from the predicted behavior.

In order to incorporate some feedback mechanism, the so obtained open-loop control sequence will be implemented only until the next system measurements become available. Although the sampling period of measurements can vary, often it is assumed to be fixed, i.e. measurements are gathered every Δt sampling time-units. Using the new measurements at time $t_0 + \Delta t$, the whole prediction and optimization is repeated to find a new control sequence with the control and prediction horizons moving forward. Since predictive control involves on-line

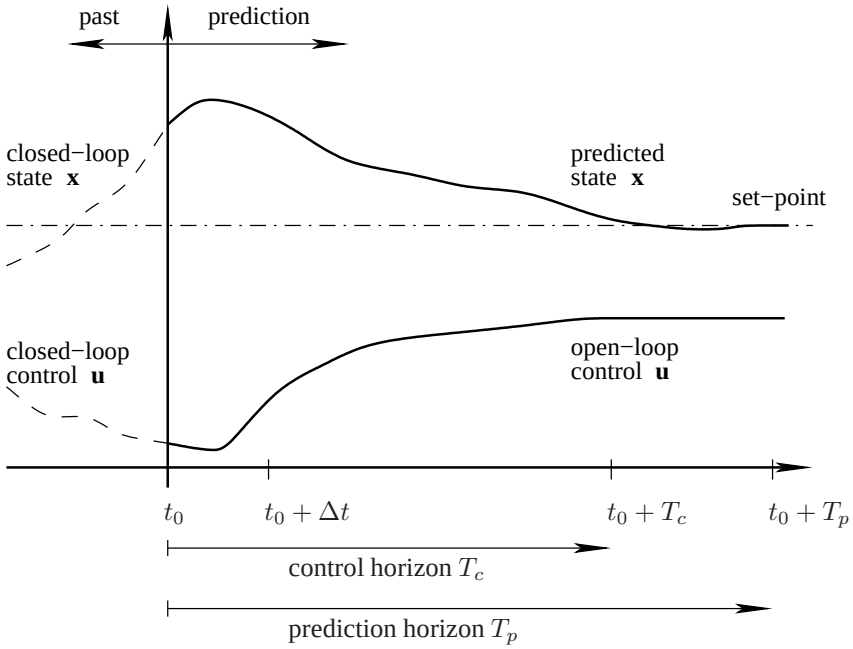

Figure 5.1: Principle of model predictive control

optimization, depending on the complexity of the explicit system model, a computational delay may be necessary, and should be taken into account [Mac02].

Notice that in Fig. 5.1 the control action is depicted as a continuous function of time. For numerical solutions of the open-loop optimal control problem it is often necessary to discretize the control action in an appropriate way. Thus, the control action is approximated as piecewise constant over the sampling time Δt, see Fig. 5.2. This allows the inclusion of constraints on states and controls as well as the optimization of a given cost function. One of the main assets of MPC is precisely the easy handling of constraints.

The optimization problem solved at each step is basically (5.5 - 5.9) which can be rewritten in terms of control changes as:

$$\min_{\mathbf{x}^j, \Delta\mathbf{u}^j} \sum_j C^j(\mathbf{x}^j, \Delta\mathbf{u}^j) \tag{5.10}$$

subject to:

$$\mathbf{g}^j(\mathbf{x}^j, \Delta\mathbf{u}^j) = \mathbf{0} \qquad j = 1, \ldots, J \tag{5.11}$$

$$\mathbf{h}^j(\mathbf{x}^j, \Delta\mathbf{u}^j) \leq \mathbf{0} \qquad j = 1, \ldots, J \tag{5.12}$$

$$\mathbf{u}^{min} \leq \mathbf{u}^j \leq \mathbf{u}^{max} \qquad j = 1, \ldots, J \tag{5.13}$$

$$\mathbf{u}^j = \mathbf{u}^{j-1} + \Delta\mathbf{u}^j \qquad j = 1, \ldots, J \tag{5.14}$$

$$\Delta\mathbf{u}^{min} \leq \Delta\mathbf{u}^j \leq \Delta\mathbf{u}^{max} \qquad j = 1, \ldots, J \tag{5.15}$$

The general MPC procedure can be described as follows:

- *initialization*: at each control step, the initial state in the predictive model is set to the

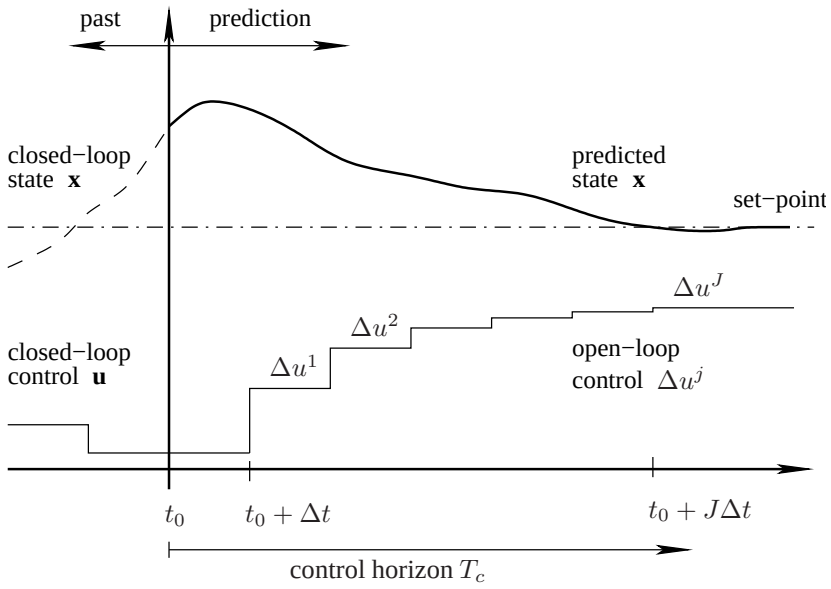

Figure 5.2: Piecewise control action

measured or estimated state of the physical system, the prediction and control horizons are determined and the controls are initialized for the initial control step;

- *computing control sequence*: the optimization produces an optimal control sequence $\Delta u^1 \dots \Delta u^J$;

- *apply control action*: the first control in the sequence Δu^1 is used as control action and applied at the next step to the physical system, all other controls in the sequence are discarded;

- *waiting/settling time*: the control system waits until the next control step, when new measurements are received and the optimal control problem is reformulate. During this period, necessary information for the next control step might be updated, such as state constraints, disturbance information, etc.

An efficient implementation of MPC requires the following issues to be addressed:

- *choice of objective functions*: according to the objective function, Linear Programming (LP) or Quadratic Programming (QP) are often employed;

- *sampling time, prediction and control horizon*: the sampling interval basically depends on the system dynamics. The prediction horizon should be chosen long enough so as to cover the settling time and the control horizon is usually smaller than the prediction horizon and represents the number of possible control moves. Short horizons are desirable from computational point of view, but long horizons are required for closed-loop stability;

- *system model*: it should be both accurate and computationally tractable. It is widely agreed that the closed-loop nature of MPC allows compensating for modeling inaccuracies;

- *stability*: the model and the optimization problem must be tuned to achieve the required objective no matter the difference between the expected and real behaviors of the controlled processes.

As in the multi-step optimization case the computing time is influenced by the degree of detail of the system model (the environment in which the MPC is operating) and length of the control horizon (number of control steps). The system model accuracy has a great effect on the predicted system parameters values, thus on the performance and the stability of the closed-loop system running under predictive control. Therefore, the system model can be considered as another tuning parameter, just as the choices of objective function, control horizon, the number and the limits of the control actions.

MPC stability can be ensured by considering either the *terminal constraint* assumption or the *infinite horizon* assumption [Mac02].

The former assumption forces, for example, the operational constraints to take a particular value at the end of the prediction horizon:

$$\mathbf{h}^J(\mathbf{x}^J, \Delta\mathbf{u}^J) = \mathbf{0} \ . \tag{5.16}$$

This is true only if the optimization problem has a solution at each sample time. General constrained optimization problems can be extremely difficult to solve, and adding terminal constraints may not be feasible. An important generalization, and relaxation, of the terminal constraints is to specify a terminal constraint set, rather than a single point. Finally, the same results are achieved by including in the cost function a terminal cost, penalizing the non-zero states at the end of the prediction horizon:

$$\min_{(\mathbf{x}^J, \Delta\mathbf{u}^j)} \sum_j C^j \left(\left| \mathbf{x}^J - \mathbf{x}^{sp} \right|, \Delta\mathbf{u}^j \right) \ . \tag{5.17}$$

With the infinite horizon assumption stability is guaranteed by making the horizons infinite in the predictive control. Nevertheless, with infinite horizons it is difficult to handle the large number of constraints. It was shown that infinite-horizon constrained control problems could be approximated by finite receding-horizon with terminal constraints problems [Mac02]. The idea is to reparametrize the predictive control problem with infinite horizon in forms of finite number parameters and perform the optimization over a finite-horizon.

We did not consider stability issues in great detail. In our problem, we can say that the system is stable if the controller succeeds bringing the currents in the overloaded transmission lines below their limits before the maximum overload duration has elapsed. This is somewhat similar to imposing a terminal constraint set.

5.4 A centralized scheme for thermal overload alleviation

The objective of the proposed approach inspired of MPC is to bring the currents in overloaded transmission lines below their admissible values before they are taken out of service, which may trigger cascading failures. The actions have to be taken over a finite period of time, compatible with the tolerable overload duration, which depends on the overload magnitude.

Control actions may involve changing the angle of phase shifting transformers, rescheduling generation and, in the last resort, shedding load. The first two controls present limits on the rate of change that have to be taken into account. From this point of view the MPC approach is a good candidate for its ease in handling constraints.

Furthermore, the closed-loop behavior of the MPC scheme, by incorporating measurements gathered at each time step, and adjusting accordingly its next action, is another advantage. The scheme operates in closed-loop mode until the overload has been eliminated, and allows to somewhat compensate for model inaccuracies [Mac02].

5.4.1 Modelling and statement of the problem

A typical control sequence is depicted in Fig. 5.3. The proposed discrete controller acts at multiples of a period Δt. Assume that some line gets overloaded in the interval $[t_0 - \Delta t \;\; t_0]$, thus causing the emergency condition to be detected at time t_0, and the controller to act for the first time at $t_0 + \Delta t$. Let T_{ol} be the duration the overload can be tolerated before the line is tripped. For security, a settling delay M is left after the last control action while the time of overload occurrence is taken as $t_0 - \Delta t$. Thus, the controller has to remove the overload in at most J steps, where J is the largest integer such that:

$$(J+1)\,\Delta t \leq T_{ol} - M \;. \tag{5.18}$$

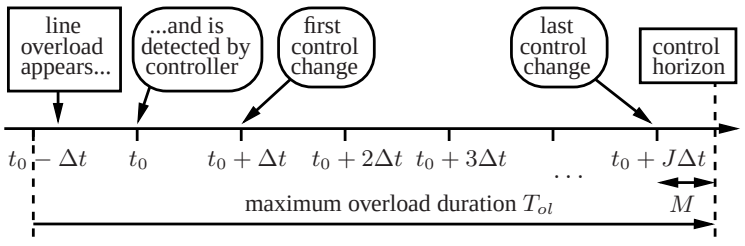

Figure 5.3: Sequence of events and controls

The system model used in the controller is linear: we consider that the vectors of branch currents at successive times $(j-1)\Delta t$ and $j\Delta t$ are linked through:

$$\mathbf{i}^j = \mathbf{i}^{j-1} + \mathbf{S}\,\Delta\mathbf{u}^j \qquad j = 1, \ldots, J \tag{5.19}$$

where $\Delta\mathbf{u}^j$ is the vector of control changes applied at time $j\Delta t$ $(j = 1, \ldots, J)$ and $\mathbf{S}$ is the sensitivity matrix of branch currents to controls. As discussed in Section 5.4.3, the computation of matrix $\mathbf{S}$ is efficient even in the case the controller would monitor a large region. Furthermore, this matrix may be updated only after a change in topology.

The linear approximation is acceptable to the extent that in most real-life situations where cascade line tripping took place, the system was in normal operating conditions when the first line overload(s) appeared; large transients (such as interarea oscillations or frequency swings) appeared in an already degraded situation resulting from a significant number of line outages (leading in extreme cases to network split). Although better modeling is desirable, the closed-loop MPC scheme is expected to compensate for inaccuracies to some extent.

The control objective is to have, at step J, the currents in the overloaded lines brought back within their admissible limits. This is written as:

$$\mathbf{i}^J \leq \mathbf{i}^{max} \,, \tag{5.20}$$

where $\mathbf{i}^{max}$ is the vector of branch current limits. In the previous section it was mentioned that this type of constraint may ensure stability of the MPC algorithm.

As illustrated in Fig. 2.15 the maximum overload duration depends on the overload magnitude. Thus it may happen that two lines, which get overloaded in the same time interval, have different maximum overload duration. Furthermore, other lines may get overloaded due to the control actions taken in order to alleviate the initial overloads. Therefore, for each overloaded line there may be a different number of steps in which the overload problem has to be solved.

In Chapter 3 it was mentioned that line overloading or approaching limits may trigger hidden failures in the protection system detecting the power flow increase. Thus, the overloading of an initially non overloaded line, due to corrective control actions, could lead to incorrect tripping of additional system equipments. For this reason, although it is not mandatory, we introduce the following constraint that prevent lines that are initially within their limits from getting subsequently overloaded by the controller:

$$\mathbf{i}_{no}^j \leq \mathbf{i}_{no}^{max} \qquad j = 1, \ldots, J \tag{5.21}$$

where $\mathbf{i}_{no}^j$ is the vector of initially non overloaded lines.

Another important feature of the proposed algorithm is the possibility of dynamically updating the value of T_{ol} (see Fig. 5.4) and hence the number J of control steps. Indeed, if the overcurrent protections have not been designed with a single, fixed temporization T_{ol}, as the controller starts alleviating line overloads, more time is available before the lines trip. Thus more control steps are available ($J^1 \leq J^2$), which allows replacing expensive fast emergency controls with slower but cheaper ones. Furthermore, this extension of the control window leaves more time for the controller to compensate for modeling errors and increases controller stability (see the infinite horizon approach mentioned in previous section).

In the case of receding control horizon the reference time with respect to which the maximum number of control steps is computed, J^2 in our case, remains the same $t_0 - \Delta t$. This is justified by the fact that the transmission line got overloaded for the first time in the $[t_0 - \Delta t \;\; t_0]$

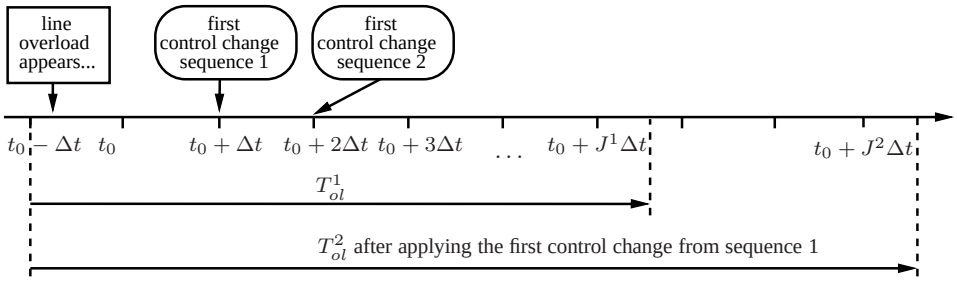

Figure 5.4: Sequence of events and controls with receding control horizon

interval[1] and tolerable overload durations must be counted from the first overload occurrence. The reference time could be also updated if the branch current was smaller than its limits for a specific period of time.

5.4.2 Multi-step optimization

At time t_0, a sequence of J future controls $\left(\Delta\mathbf{u}^1, \Delta\mathbf{u}^2, \ldots, \Delta\mathbf{u}^J\right)$ is computed in order to bring the branch currents from their initial value $\mathbf{i}^0$ to a value satisfying (5.20). This sequence is computed so as to minimize the total "cost" associated with control changes, while keeping the rate of change of the latter within the allowed limits.

The sequence of J future controls is thus obtained as the solution of the optimization problem:

$$\min_{\Delta\mathbf{u}^1, \Delta\mathbf{u}^2, \ldots, \Delta\mathbf{u}^J} \sum_{j=1}^{J} C^j\left(\Delta\mathbf{u}^j\right) \tag{5.22}$$

subject to:

$$\mathbf{i}^j = \mathbf{i}^{j-1} + \mathbf{S}\,\Delta\mathbf{u}^j \qquad j = 1, \ldots, J \tag{5.23}$$

$$\Delta\mathbf{u}^{min} \leq \Delta\mathbf{u}^j \leq \Delta\mathbf{u}^{max} \qquad j = 1, \ldots, J \tag{5.24}$$

$$\mathbf{u}^j = \mathbf{u}^{j-1} + \Delta\mathbf{u}^j \qquad j = 1, \ldots, J \tag{5.25}$$

$$\mathbf{u}^{min} \leq \mathbf{u}^j \leq \mathbf{u}^{max} \qquad j = 1, \ldots, J \tag{5.26}$$

$$\mathbf{i}^j_{no} \leq \mathbf{i}^{max}_{no} \qquad j = 1, \ldots, J \tag{5.27}$$

$$\mathbf{i}^J \leq \mathbf{i}^{max} \tag{5.28}$$

Several objectives can be thought of for the above approach, such as: minimum cost associated to control actions, minimum amount of rescheduling with respect to control base case values or minimum number of control actions. As presented in (5.22), we focus on minimizing the cost of rescheduling control variables with respect to their initial values. Furthermore, linear or quadratic objectives could be employed. The former tends to produce control changes at

[1]Let us recall that, for security reasons, it is assumed to have occurred at $t = t_0 - \Delta$ (as indicated in the previous page).

the end of the control window. The latter tends to produce control changes evenly distributed over the control horizon. The behavior of both objectives is illustrated and compared in the following sections.

Equation (5.23) represents a time sequence of linear predictions of the type (5.19). $\Delta\mathbf{u}^{max}$ in (5.24) is obtained by multiplying the maximum rate of increase of each control by the time interval Δt, and similarly for $\Delta\mathbf{u}^{min}$. The constraints (5.25, 5.26) obviously aim at keeping the controls within their admissible limits, corresponding to $\mathbf{u}^{min}$ and $\mathbf{u}^{max}$, respectively.

The above multi-step optimization relies on the vector $\mathbf{i}^0$ of branch current measurements, gathered at time t_0, and the initial value $\mathbf{u}^0$ of controls. According to MPC principle, only the first control step $\Delta\mathbf{u}^1$ of the so computed sequence is applied, at time $t_0 + \Delta t$. At that time, new measurements are collected in $\mathbf{p}^1$ and a completely new control sequence is computed for the next time steps.

Note that current measurements can be collected at a higher frequency than controller actions. This is probably desirable to filter out transients and focus on the long-term trend of currents.

5.4.3 Sensitivity of branch current with respect to controls

When dealing with thermal overload the best location and controls have to be identified in order to decrease the magnitude of some specific branch currents. To this purpose it is appropriate to rely on sensitivities of branch currents to controls.

An easy method to compute these sensitivities is that of finite differences, which consists in successively applying a certain control action and computing the corresponding branch current variation. This requires to compute the new branch currents for each control change and the procedure must be repeated each time the power system configuration changes. Although this method is very simple, it remains too computationally demanding, especially for on-line applications.

For this reason it is more efficient to rely on sensitivity formulae as detailed hereafter [Cap04].

General sensitivity formula

Let us assume that the power system is described, in steady state, by a set of algebraic equations, which can be written in compact form as:

$$\boldsymbol{\varphi}\left(\mathbf{v}, \mathbf{p}\right) = \mathbf{0}\ , \tag{5.29}$$

where $\boldsymbol{\varphi}$ is a set of *smooth* functions, $\mathbf{v}$ is the vector of algebraic variables and $\mathbf{p}$ is a parameter vector.

Let η be some scalar quantity of interest that can be expressed as function of $\mathbf{v}$ and possibly $\mathbf{p}$. If some changes in parameter $\mathbf{p}$ take place, the system will generally operate at an other

point still satisfying (5.29), and η will also change. For small changes in $\mathbf{p}$ we are interested in determining the sensitivity of η with respect to each component p_i of $\mathbf{p}$:

$$\frac{\partial \eta}{\partial p_i} = \lim_{\Delta p_i \to 0} \frac{\Delta \eta}{\Delta p_i} \; . \tag{5.30}$$

Differentiating $\eta(\mathbf{v}, \mathbf{p})$ according to the chain rule yields:

$$d\eta = \mathbf{dv}^T \nabla_{\mathbf{v}} \eta + \mathbf{dp}^T \nabla_{\mathbf{p}} \eta \; , \tag{5.31}$$

where $\nabla_{\mathbf{v}}\eta$ and $\nabla_{\mathbf{p}}\eta$ are the gradients of the scalar quantity η with respect to vectors $\mathbf{v}$ and $\mathbf{p}$, respectively, i.e. the vector of partial derivatives such that $[\nabla_{\mathbf{v}}\eta]_i = \dfrac{\partial \eta}{\partial v_i}$. Note that, if η does not depend explicitly on $\mathbf{p}$, $\nabla_{\mathbf{p}}\eta = 0$.

On the other hand differentiating (5.29) gives:

$$\boldsymbol{\varphi}_{\mathbf{v}} \mathbf{dv} + \boldsymbol{\varphi}_{\mathbf{p}} \mathbf{dp} = 0 \; ,$$

where $\boldsymbol{\varphi}_{\mathbf{v}}$ and $\boldsymbol{\varphi}_{\mathbf{p}}$ are the Jacobians of $\boldsymbol{\varphi}$ with respect to $\mathbf{v}$ and $\mathbf{p}$. Assuming that $\boldsymbol{\varphi}_{\mathbf{v}}$ is nonsingular we obtain:

$$\mathbf{dv} = -\boldsymbol{\varphi}_{\mathbf{v}}^{-1} \boldsymbol{\varphi}_{\mathbf{p}} \mathbf{dp} \; . \tag{5.32}$$

Introducing (5.32) into (5.31) yields:

$$\begin{aligned} d\eta &= -\mathbf{dp}^T \boldsymbol{\varphi}_{\mathbf{p}}^T \left(\boldsymbol{\varphi}_{\mathbf{v}}^T\right)^{-1} \nabla_{\mathbf{v}} \eta + \mathbf{dp}^T \nabla_{\mathbf{p}} \eta \\ &= \mathbf{dp}^T \left[\nabla_{\mathbf{p}} \eta - \boldsymbol{\varphi}_{\mathbf{p}}^T \left(\boldsymbol{\varphi}_{\mathbf{v}}^T\right)^{-1} \nabla_{\mathbf{v}} \eta \right] \end{aligned} \tag{5.33}$$

and hence the desired sensitivity vector is given by:

$$S_{\eta \mathbf{p}} = \nabla_{\mathbf{p}} \eta - \boldsymbol{\varphi}_{\mathbf{p}}^T \left(\boldsymbol{\varphi}_{\mathbf{v}}^T\right)^{-1} \nabla_{\mathbf{v}} \eta \; . \tag{5.34}$$

Note that $\boldsymbol{\varphi}_{\mathbf{v}}$ is usually a sparse Jacobian matrix. $\boldsymbol{\varphi}_{\mathbf{p}}$ is also very sparse in practice.

Derivation of branch current sensitivities with respect to controls

Let us assume a branch k connecting bus i to bus j, which can be a transmission line or a transformer. A general equivalent circuit of a branch is given in Fig. 5.5, where the shunt elements have been neglected for simplicity. Let r_k (resp. ϕ_k) be the transformer ratio (resp. phase angle). If the transformer is not a phase shifting one, ϕ_k = 0. If the circuit is used to represent a transmission line, r_k = 1 and ϕ_k = 0.

The primary and secondary currents are linked through:

$$I_2 = r_k \, I_1 = r_k \, Y_k \sqrt{V_i^2 + \left(r_k V_j\right)^2 - 2 r_k V_i V_j cos\left(\theta_i - \theta_j - \phi_k\right)} \; , \tag{5.35}$$

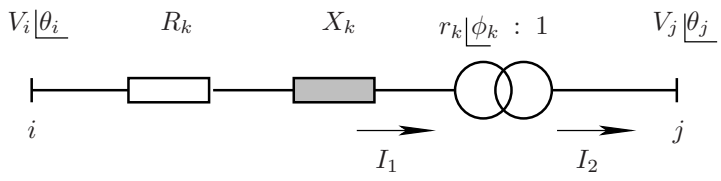

Figure 5.5: Simplified scheme of a line or transformer

where $Y_k = 1/\sqrt{R_k^2 + X_k^2}$, V_i (resp. θ_i) is the magnitude (resp. phase angle) of the voltage at bus i, and similarly for bus j.

In the context of QSS simulation, formally, the equations (5.29) are the long-term equilibrium equations of the model (2.1 - 2.4) and $\mathbf{v} = \left[\mathbf{x}^T, \mathbf{y}^T, \mathbf{z_c}^T, \mathbf{z_d}^T\right]^T$. If a simple load flow model is used, $\mathbf{v} = \mathbf{y}$, the vector of bus voltage magnitudes and phase angles. Setting $\eta = I_k$ (the current in a specific branch k) and $\mathbf{p} = \mathbf{u}$, the sensitivity formula (5.34) provides:

$$S_{I\mathbf{u}} = \nabla_{\mathbf{u}} I - \boldsymbol{\varphi}_{\mathbf{u}}^T \left(\boldsymbol{\varphi}_{\mathbf{y}}^T\right)^{-1} \nabla_{\mathbf{y}} I \ . \tag{5.36}$$

In our application, $\mathbf{u}$ relates to generator rescheduling, load shedding and phase shifter adjustment. The first two controls can be modeled as bus active and reactive power injections.

The term $\nabla_{\mathbf{u}} I$ is different from zero only if the branch of concern is a controlling phase shifting transformer; the only nonzero element correspond to the partial derivatives of I_k with respect to ϕ_k. Moreover, $\nabla_{\mathbf{y}} I$ contains only four nonzero elements, namely the partial derivatives of I_k with respect to V_i, V_j, θ_i and θ_j. All these derivatives are easily obtained from (5.35).

5.5 Illustrative examples on a simple system

5.5.1 Test system

In this section, illustrative examples are presented in detail, based on the academic system shown in Fig. 5.6[2], where in each bus a generator and a load are connected, all transmission lines have the same parameters and a phase shifter is placed in branch B5. Table 5.1 presents the base case conditions.

The system model used in the controller is linear and obtained from a DC approximation, thus replacing currents with active power flows. Hence, the optimization problem can be written as:

[2]Tests on a large-scale system are reported in Chapter 6.

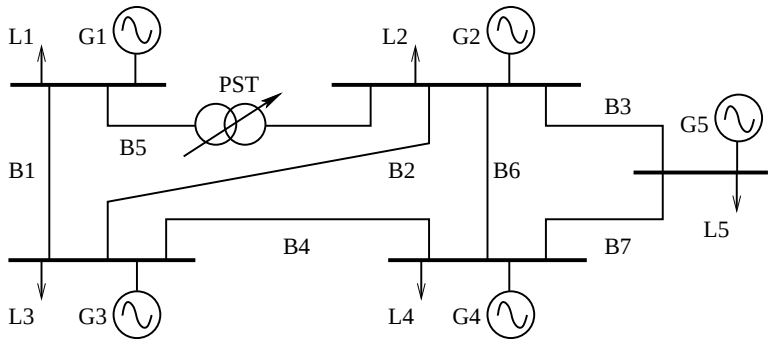

Figure 5.6: System used in illustrative example

Table 5.1: Base case generator production, load consumption and phase shifter position

Generator	P_g (pu)	Load	P_l (pu)	PST	Angle (deg.)
G1	10	L1	7	B5	0
G2	15	L2	8		
G3	15	L3	19		
G4	10	L4	16		
G5	6	L5	6		

$$\min_{\Delta\mathbf{u}^1,\Delta\mathbf{u}^2,\ldots,\Delta\mathbf{u}^J} \sum_{j=1}^{J}\sum_{i=1}^{n} d_i^j c_i |\Delta u_i^j| \tag{5.37}$$

subject to:

$$\mathbf{p}^j = \mathbf{p}^{j-1} + \mathbf{S}\,\Delta\mathbf{u}^j \qquad j = 1,\ldots,J \tag{5.38}$$

$$\Delta\mathbf{u}^{min} \le \Delta\mathbf{u}^j \le \Delta\mathbf{u}^{max} \qquad j = 1,\ldots,J \tag{5.39}$$

$$\mathbf{u}^j = \mathbf{u}^{j-1} + \Delta\mathbf{u}^j \qquad j = 1,\ldots,J \tag{5.40}$$

$$\mathbf{u}^{min} \le \mathbf{u}^j \le \mathbf{u}^{max} \qquad j = 1,\ldots,J \tag{5.41}$$

$$-\mathbf{p}_{no}^{max} \le \mathbf{p}_{no}^j \le \mathbf{p}_{no}^{max} \qquad j = 1,\ldots,J \tag{5.42}$$

$$-\mathbf{p}^{max} \le \mathbf{p}^J \le \mathbf{p}^{max} \tag{5.43}$$

where in the objective function (5.37), c_i is a cost associated with the i-th control change Δu_i, d_i^j is a *discount factor* used to weight the cost of this control at the j-th time step, and n is the total number of controls. The sensitivity matrix of branch power flows to controls $\mathbf{S}$ is easily derived from the DC load flow Jacobian and can be computed row-by-row or column-by-column from the sensitivity formula of Section 5.4.3.

We consider as disturbance the increase by 3 pu of load L4, supplied by generator G1, resulting in overloading lines B1 and B6. For the sake of illustration, we assume a fixed overload duration $T_{ol} = 60$ s and $\Delta t = 5$ s, which could be representative of a real implementation. Thus, the overload is first noticed by the controller at $t_0 = 5$ s (see Fig. 5.3). The settling delay M is set to $\Delta t = 5$ s. Hence the controller has to relieve the overloads in at most $J = (60-5-5)/5 = 10$ steps.

Note that this is a stringent test in which the control horizon is not receding. Thus, J decreases from 10 to 1 in the successive applications of the MPC algorithm. The number of constraints (5.38-5.42) decreases accordingly as time goes.

The available controls are the angle of the PST in branch B5, the production of generators G1 and G5 and the power of the interruptible load L3. Through the relative values of the costs c_i, priority is given to actions on the PST, then on the generators and finally on the load, for obvious reasons. Constraints are imposed on the changes in PST angle, power generations and load power that can take place in a single control step. The available controls, their costs and their bounds are given in Table 5.2.

Table 5.2: Available controls, costs, limits and bounds

control	c_i	Limits	Δu^{min}	Δu^{max}
PST	1	$\phi^{max} = \pm$ 25 deg.	- 1 deg.	1 deg.
gener. G1 and G5	10	P_g^{max} = 30 pu	- 2 pu	2 pu
load L3	100		0	2 pu

5.5.2 Simulations based on exact model

This subsection illustrates the behavior of the proposed controller when its model matches the system behavior exactly. To this purpose, the $\mathbf{S}$ matrix has been obtained by linearization around the current operating point. Then, this matrix has been used both to simulate the system response to the controller and in the controller itself. Under these ideal conditions, the behavior of various objective functions is compared.

We first consider the absolute-value objective (5.37). Figure 5.7 shows the time evolution of power flows and controls, respectively. All transmission lines have the same limit, $P^{max} =$ 3.5 pu, shown with the dash-dotted horizontal lines in the upper plot. For legibility reasons the control actions of generator G5 are not represented, but these can be easily computed as $\Delta u_{G5} = \Delta u_{L3} - \Delta u_{G1}$.

As can be seen, the initial two overloads are removed, while the other lines are kept within their limits. The controller uses the cheap PST to the greatest possible extent. Acting on the PST reduces the power flow in line B6 but increases the one in line B1. Therefore, the controller subsequently uses the more expensive generation rescheduling. This relieves the above two lines but increases the flow in line B7. Finally, load shedding is used because the problem cannot be solved with the sole help of PST and generators.

If more PST and/or generator controls are available, the overloads can be eliminated without resorting to load shedding. Two examples are given hereafter.

In the case of Fig. 5.8, it is assumed that a second PST is available in branch B6. The lower plot shows that in this case the problem can be solved using PSTs only.

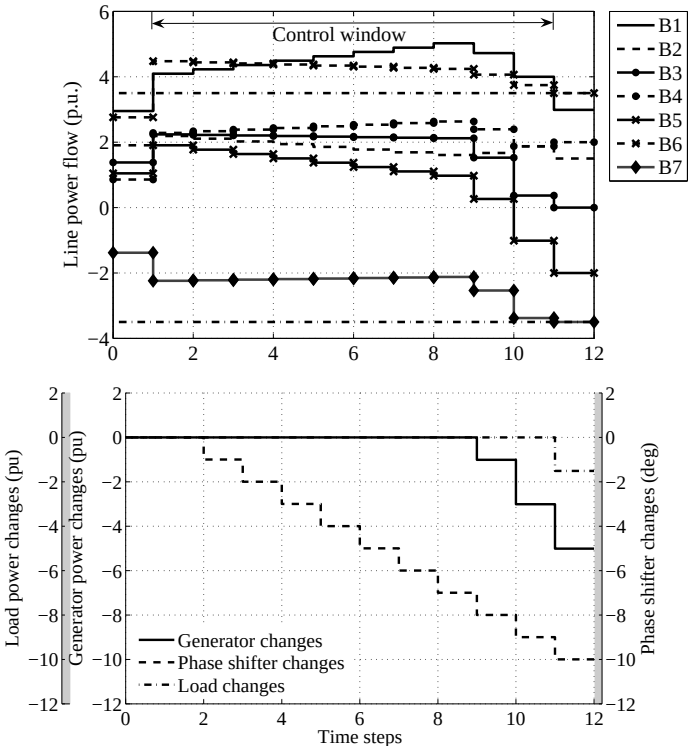

Figure 5.7: Line flows and control actions with absolute-value objective

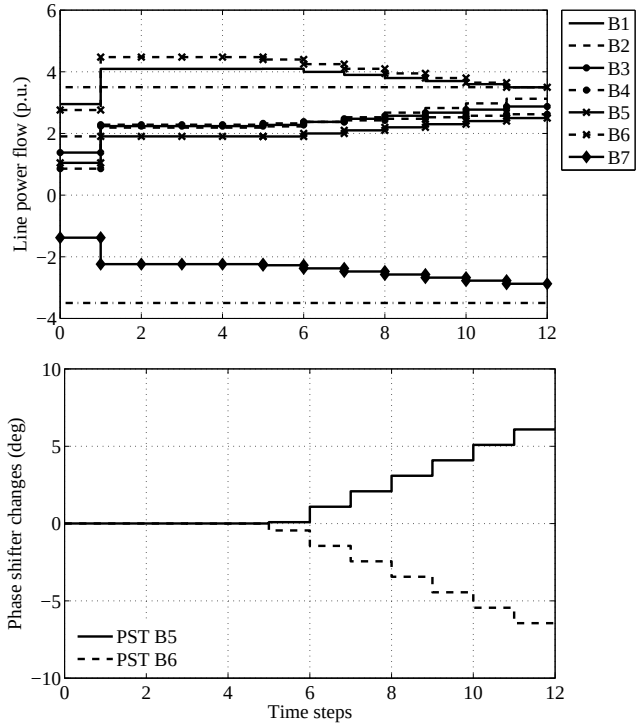

Figure 5.8: Same case as in Fig. 5.7 with an additional PST

In the case of Fig. 5.9, no PST is available but generator G4 can be rescheduled together with G1 and G5. As in the previous case, the overloads are eliminated without resorting to load shedding. In this case generator G5 is not represented as the problem is solved by rescheduling G1 and G4 only.

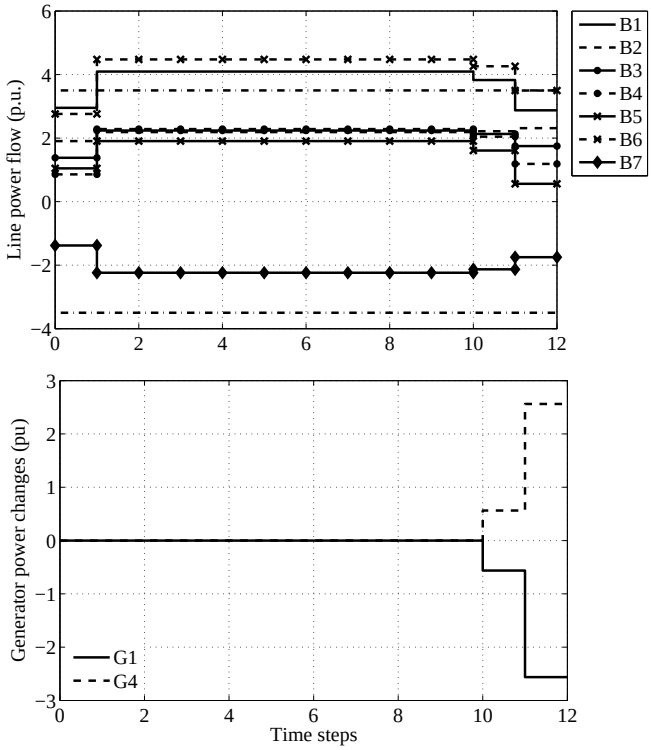

Figure 5.9: Same case as in Fig. 5.7 with an additional generator available for rescheduling

In the previous examples, the discount factors d_i^j were chosen to favor actions taken at the end of the control window, and the same factors were used for all types of controls, as indicated in Fig. 5.10.a. Alternatively, different control types can be assigned different discount factors in order, for instance, to favor early actions on generators and later actions on load shedding, see Fig. 5.10.b. Furthermore, the discount factors can be set so that overloads are corrected earlier in the control window. This choice is interesting because some time is left for the controller to apply additional corrections, not anticipated in the first control steps but required due to measurement noise or model inaccuracies, for instance.

An example is given in Fig. 5.11 where the discount factors favor PST and generators actions around the 2nd control step and load shedding around the 8th control step (as shown with dashed line in Fig. 5.10.b). A comparison with Fig. 5.7 shows that generation is indeed rescheduled earlier. However, this action is inhibited at the 4th time step by the fact that (the previously non overloaded) line B7 is approaching its limit. A second rescheduling takes place later on, at the same time as load shedding.

Note that the discount factors have to be chosen in order not to disturb the precedence that some controls must take over some others, as specified through the costs. For example, the

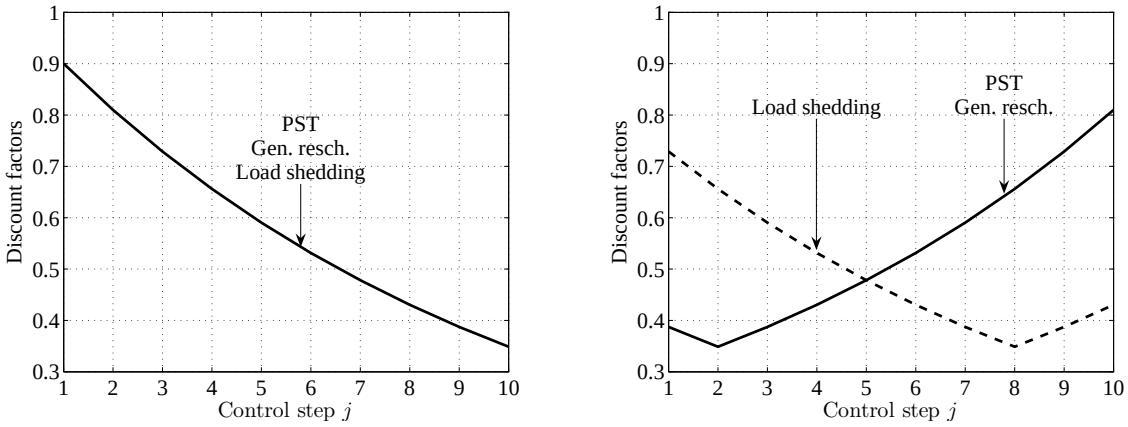

Figure 5.10: Discount factors

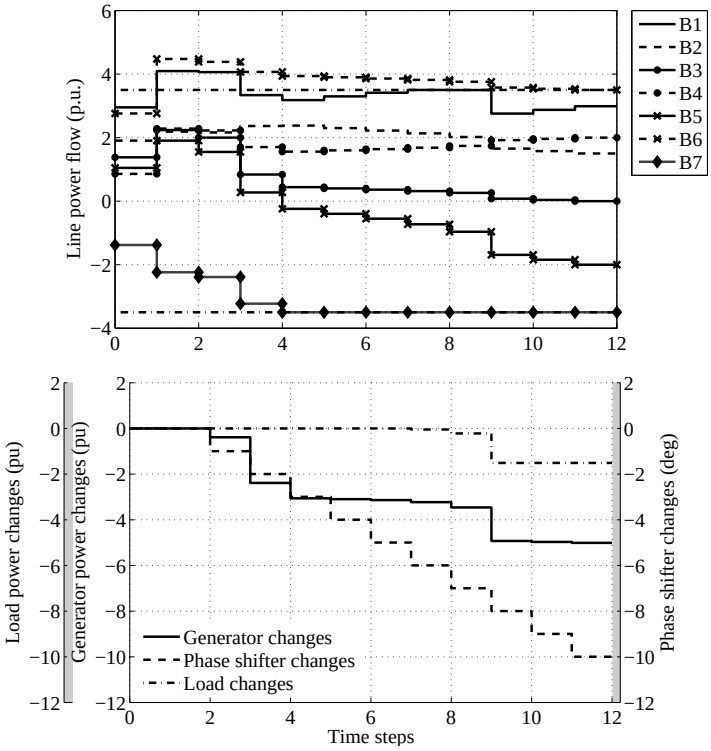

Figure 5.11: Same case as in Fig. 5.7 with different discount factors

cost of the most expensive control multiplied with the discount factor at a certain control step should not become smaller than the cost of a less expensive control, no matter the control step number.

As mentioned before, other objectives than (5.37) can be thought of, for instance the quadratic

one:

$$\min_{\Delta\mathbf{u}^1,\Delta\mathbf{u}^2,\ldots,\Delta\mathbf{u}^J} \sum_{j=1}^{J}\sum_{i=1}^{n} c_i \left(\Delta u_i^j\right)^2 \ , \tag{5.44}$$

where no discount factors are used. This objective tends to distribute the control changes more evenly over the time window. The control sequence obtained with the quadratic objective and the resulting line power flows evolution are shown in Fig. 5.12. As in the linear objective case, the initial two overloads are removed by the end of the control window, while the other lines are kept within limits.

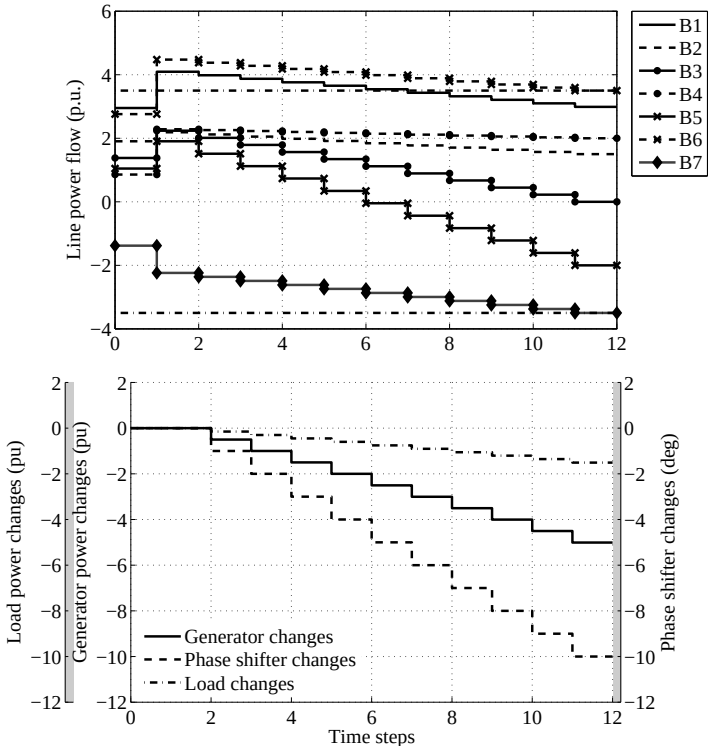

Figure 5.12: Line flows and control actions with quadratic objective

Comparing the final values of the load, generator and PST changes in Figs. 5.7 and 5.12, respectively, shows that both objectives in fact led to the same total changes, the control sequence differing by the time distribution of the variations. This appears to be linked to the following specific features of the considered example:

- we assume the system model exact;
- the number of PST changes (which is the "cheapest" control) is limited by the number of steps that can be taken in the fixed time window. Hence, the PST is used to the full extent whatever the objective;
- generation rescheduling is limited by the constraint (5.42) relative to line B7 (that gets more and more loaded);

- therefore, one may say that our problem had a single degree of freedom, the load shedding action.

In general the two objectives do not always yield the same total control changes.

Up to now we considered a fixed time overload duration T_{ol}. In order to illustrate the advantage of a receding control horizon we consider somewhat arbitrarily that T_{ol} is increasing with one third of Δt after each control step[3]. Thus, after three control steps another control step is available. In our case four more control steps are thus made available to alleviate the branch overloads. Figure 5.13 shows the time evolution of power flows and controls with the so receding control horizon. A comparison with Fig. 5.12 shows that part of the more expensive generator rescheduling and load shedding actions were replaced by less expensive PST actions. Another aspect that should be mentioned is the fact that the magnitude of control actions is decreasing towards the end as more time is given to the controller to solve the problem.

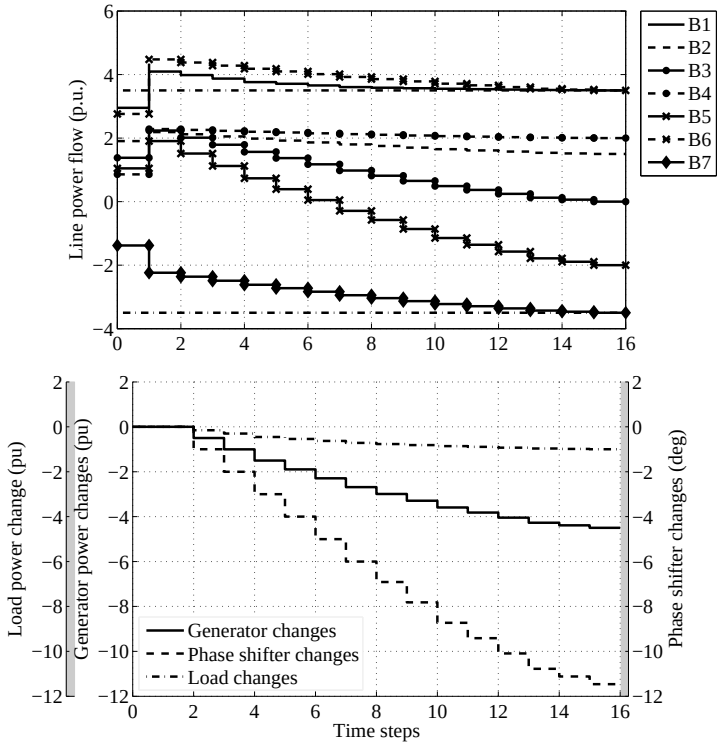

Figure 5.13: Line flows and control actions with quadratic objective and receding horizon

5.5.3 Comparison with OPF

The results for the static OPF problem described by Eqs. (5.1-5.4) were obtained using the Interior Point Method and the software referred to in [CGE07]. The method is appealing mainly

[3]In practice the update of control horizon should rely on curves of the type shown in Fig. 2.15.

due to its speed of convergence, the ease in handling inequality constraints and the fact that the initial point need not be strictly feasible [IWT97, TQ98, CGE07].

As in the MPC approach, the objective of the OPF problem was to minimize the total cost of control actions required to alleviate the overload. The OPF considered a complete system model. Thus, the equality constraints involved nodal active and reactive power balance equations and the inequality constraints involved operating limits, such as limits on branch currents.

Table 5.3 presents the comparison between the OPF and the proposed MPC algorithm in terms of total control actions and *final* active power flows. Where the OPF Case 1 considers operation limits on branch currents, while Case 2 considers limits on branches active power flows as in the MPC approach.

Control actions			
	OPF		MPC
	Case 1	Case 2	
PST (deg)	10	10	10
G1 (pu)	-6.2	-6	-5
G5 (pu)	2.85	2.87	3.49
L3 (pu)	-3.15	-2.92	-1.51

Line active power flow (pu)			
	OPF		MPC
	Case 1	Case 2	
B1	2.11	2.25	2.99
B2	1.12	1.18	1.5
B3	0	0	0
B4	2.34	2.3	2
B5	2.39	2.31	2
B6	3.48	3.5	3.5
B7	3.48	3.5	3.5

Table 5.3: Final branch power flows and total control actions comparison OPF vs. MPC

Note that the considered OPF problem takes into account line losses and reactive power flows. This explains part of the differences between OPF Case 2 and the MPC results in terms of total generator and load control actions and final active power flows. It can be seen that even more control actions are required when the branch currents are monitored, but resulting in smaller active power flows.

Given the small system size a comparison between the computing times of the two algorithms is not relevant.

A more detailed model of the type used in the OPF could be used in the MPC algorithm as well. Anyway, in spite of these possible improvements, the fact remains that the closed-loop MPC approach offers the possibility to correct modeling errors and measurement noise effects.

5.5.4 Simulations with approximate controller model

A realistic test of the proposed method requires to consider the effect of model inaccuracies and measurement noises.

To deal with the first aspect, the system response was simulated with the reference matrix $\mathbf{S}$ while random errors were introduced on the reactances of (overloaded) lines B1 and B6 before building the $\mathbf{S}$ matrix used by the controller. The random error was uniformly distributed in the interval $[-0.2X \;\; 0.2X]$ where X is the reactance of the line of concern.

Under the effect of these random errors, one may expect the model used by the controller to be either "pessimistic" or "optimistic" with respect to the real system behavior. These two situations are illustrated in Figs. 5.14 and 5.15, respectively, where the quadratic objective was employed. Thus, both should be compared with the line power flows and control sequence shown in Fig. 5.12 which were obtained using the exact model in the controller.

In the case of Fig. 5.14, it can be seen that generator rescheduling and load shedding decrease with time because the controller senses that the situation is improving faster than initially expected. While the PST total action is identical, the generator rescheduling and load shedding actions are slightly changed.

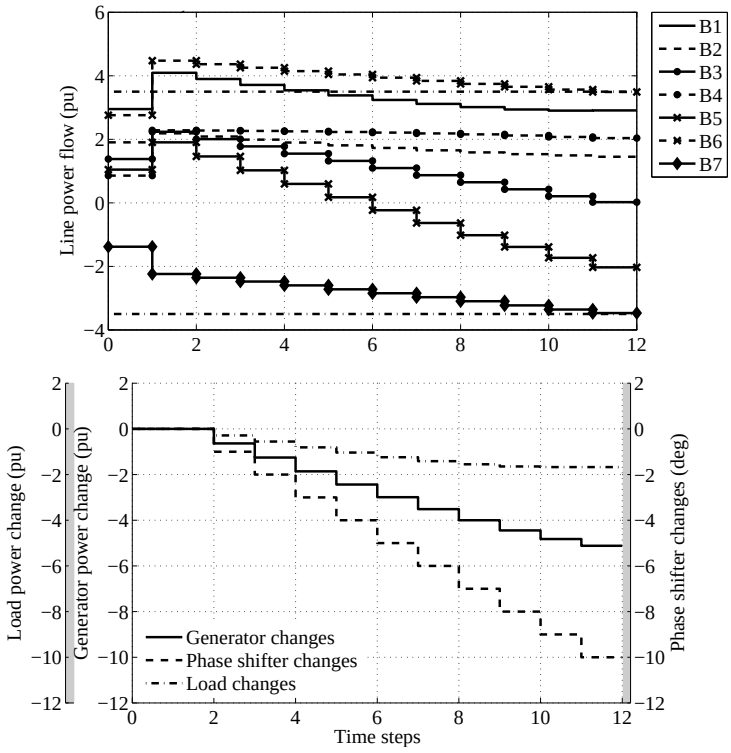

Figure 5.14: Line flows and control actions; model used by controller is pessimistic

Figure 5.15, on the other hand, shows a case where the model available to the controller is optimistic. This leads to control actions increasing with time, as the situation is not improving as anticipated. In this case, the controller succeeds maintaining the power flows in all branches close to their limits. Nevertheless, at the end of the control window the initial overload of branch B6 is not alleviated, while branch B7 gets overloaded as a result of the control actions. As the initial overloaded branch will be tripped by its protection system after the corresponding maximum overload duration, this case should be considered as a failure.

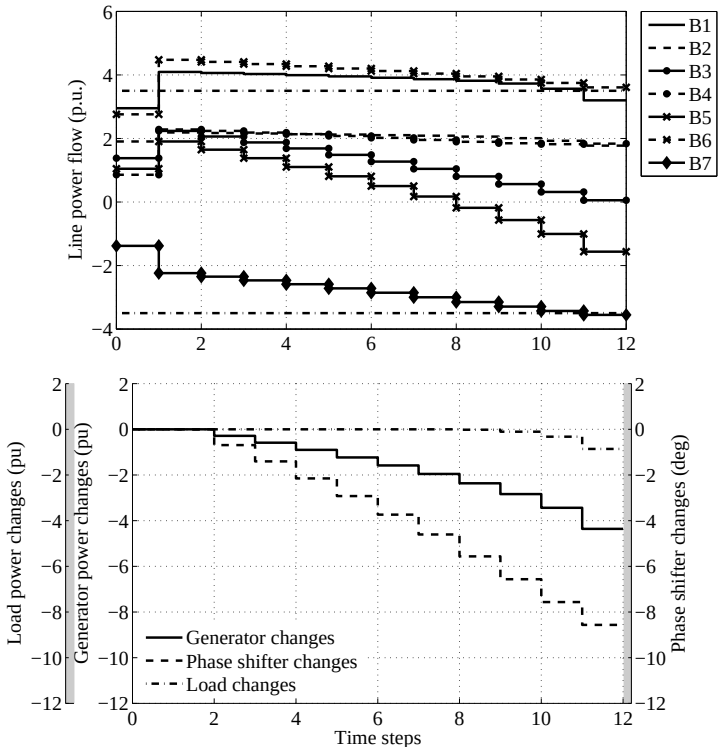

Figure 5.15: Line flows and control actions; model used by controller is optimistic

In order to estimate the failure rate of the controller, 5000 Monte-Carlo simulations were run, involving the above mentioned random errors. The statistical distributions of power flows in branches B1 and B6 at the end of the control window are shown in Fig. 5.16, where the dash-dotted vertical line represents the thermal limit. One can see that the algorithm failed to eliminate the overload in line B6 in more than half of the cases. This means that the controller could not prevent line B6 from being tripped.

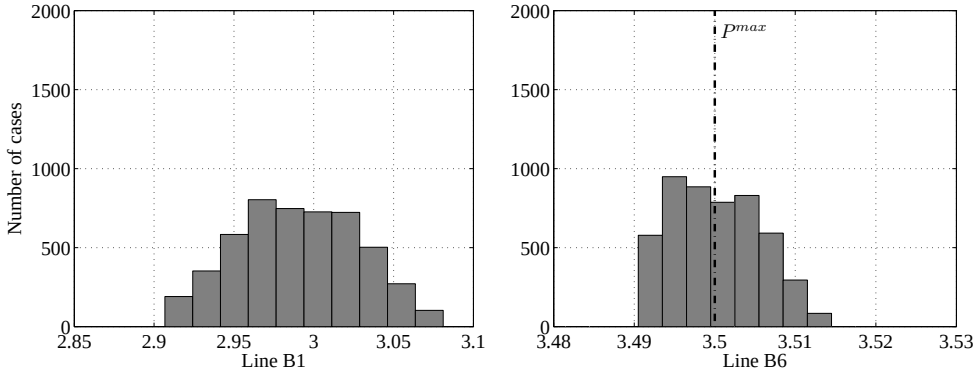

Figure 5.16: Distribution of final power flows in presence of random model errors

In conclusion, in the presence of modeling errors, it takes more time to the MPC scheme to reach its objective. With a control window updated with time, i.e. extended in response to the

observed decrease in line currents, and with a specific correction method, the controller would be given more chances to meet its target.

5.5.5 Simulations incorporating noisy measurements

An other source of inaccuracy is the noise affecting the power flow measurements gathered at each control step.

In the case of Fig. 5.17, an identical error was added to each component of the successive $\mathbf{p}^j$ vectors. In the case of Fig. 5.18, the noise was a random variable uniformly distributed in the interval $[-0.3 \;\; 0.3]$ pu. In both cases the line flows shown in the figures are the real ones. As can be seen, the MPC algorithm adjusts its control sequence and succeeds removing the line overloads.

Although the controller acted successfully in both cases, there is a risk of failure especially if the measurement noise becomes too high. To face this case as well as the situations with modeling inaccuracies, the techniques discussed in the next section might prove useful.

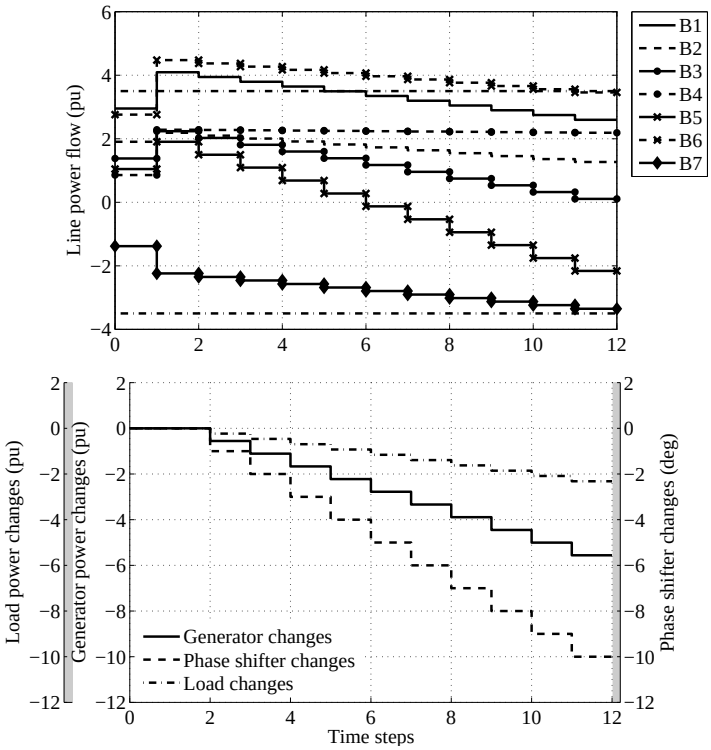

Figure 5.17: Line flows and control actions; constant measurement error on power flows

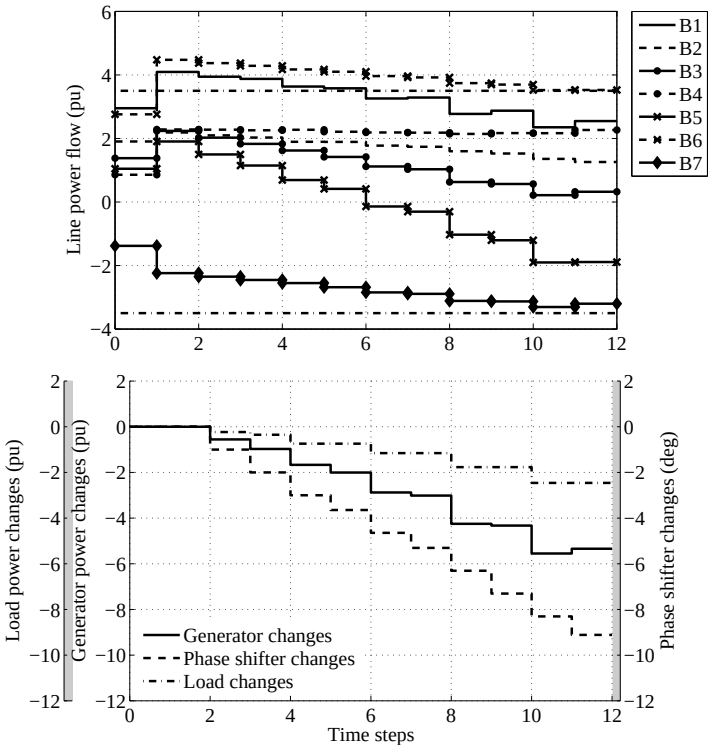

Figure 5.18: Line flows and control actions; random measurement errors on power flows

5.5.6 Correction of errors in the MPC scheme

As already mentioned, the MPC algorithm may fail reaching its target due to modeling errors or measurement noise, causing the overloads to be alleviated too late, *especially in the case of a fixed overload duration* T_{ol}. The problem is likely to be less severe if more controls (i.e. more degrees of freedom) are available to relieve the line overloads.

One way of counteracting this problem consists of setting the limit P^{max} of the initially overloaded lines to a smaller value, say $P^{max} - \varepsilon$, in order to cause the MPC algorithm to act more, and hence the line power flows to come back faster below their limits. Thus, (5.28) is replaced by:

$$-(\mathbf{p}^{max} - \varepsilon) \leq \mathbf{p}^J \leq (\mathbf{p}^{max} - \varepsilon) \ , \tag{5.45}$$

where ε is a positive constant to be adjusted.

The limits $\mathbf{p}_{no}^{max}$ in (5.42) relative to the initially non overloaded lines are left unchanged. This means that, at a given time step, if the measured power flow in an initially overloaded line becomes smaller than P^{max}, the line is moved to the non-overloaded category, even if its power flow remains larger than $P^{max} - \varepsilon$. Thus the final value could be in between the real and the decreased limits. This is equivalent to specifying as a target the interval $[P^{max} - \varepsilon, P^{max}]$ instead of a single value P^{max}[4] (this is one of the methods meant to ensure the stability of the

[4]The MPC optimization objective being to minimize the costs of control actions needed to remove the overload, the method tends to bring the power (or current) a little below P^{max}, as seen from all examples.

MPC algorithm mentioned in Section 5.3).

The above correction makes the controller operate a bit conservatively, but this is fully acceptable for a system protection scheme aimed at acting in rare emergency conditions. Due to the closed-loop nature of MPC, even if the controller starts with large control actions, it will subsequently adjust them with respect to received measurements, and stop acting as soon as the line overloads are alleviated.

In order to illustrate the behavior of the proposed correction we have considered the failure case presented in Fig. 5.15 and ε = 0.05 pu, thus the enforced line limit is $P^{max} - \varepsilon$ = 3.45 pu. The results are shown in Fig. 5.19. As expected, the control actions are more important in the beginning as the imposed limit is more constraining, but they are decreasing in magnitude towards the end. This is opposite to the behavior observed in Fig. 5.15 with the original limits. Comparing the control actions with the ones obtained when using the exact model (see Fig. 5.12), it can be seen that there is a slight increase in the amount of power rescheduled and shed. Nevertheless, this is acceptable since at the end of the control horizon all line flows are between limits.

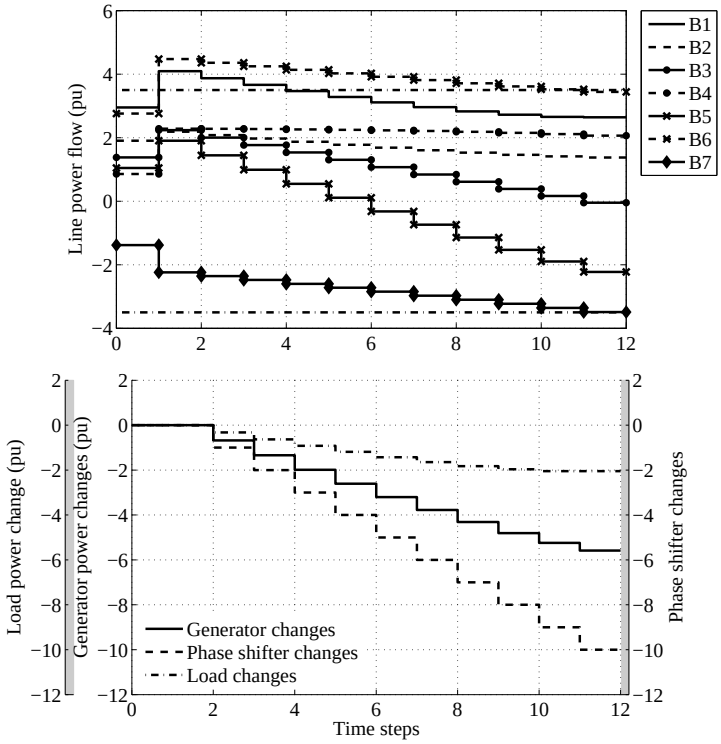

Figure 5.19: Line flows and control actions; with correction of line limit

Monte-Carlo analysis can be used to choose ε. For instance, Figure 5.20 shows the statistical distribution of final power flows over the set of 5000 cases previously considered in Fig. 5.16, when setting the overloaded line limit to $P^{max} - \varepsilon = 0.48$ pu, which represents only a small decrease (ε = 0.02 pu) with respect to the real limit. As shown by the histogram, this was enough for the controller to operate successfully in all 5000 cases.

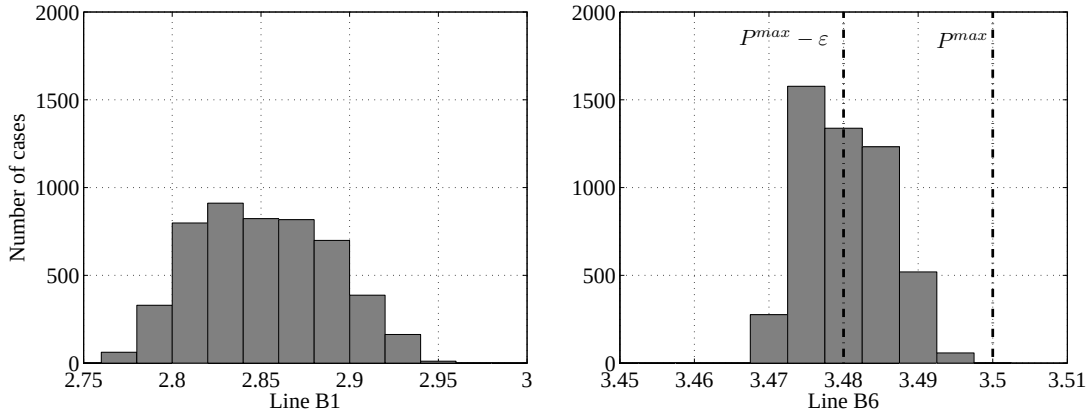

Figure 5.20: Distribution of final power flows; same cases as in Fig. 5.16 using P^{lim} as line limit in the optimization

As an alternative, to setting ε to a single value that should satisfy all possible disturbances and system conditions, ε could be adjusted dynamically when the overload reduction is smaller than expected. For instance, at each time step one may subtract from P^{max} the difference between the measured and predicted line power flows, divided by the number r of remaining steps in the control window:

$$\varepsilon = \frac{P_{meas} - P_{pred}}{r} \ . \tag{5.46}$$

As in the previous method, the controller is forced to act more strongly in order to compensate for the discrepancy. If at one time step ε becomes negative, the respective value is not added to P^{max} since the system behavior is more satisfactory than expected.

Figure 5.21 shows the statistical distribution of final power flows over the same set of 5000 cases using the above dynamic adjustment of P^{max}.

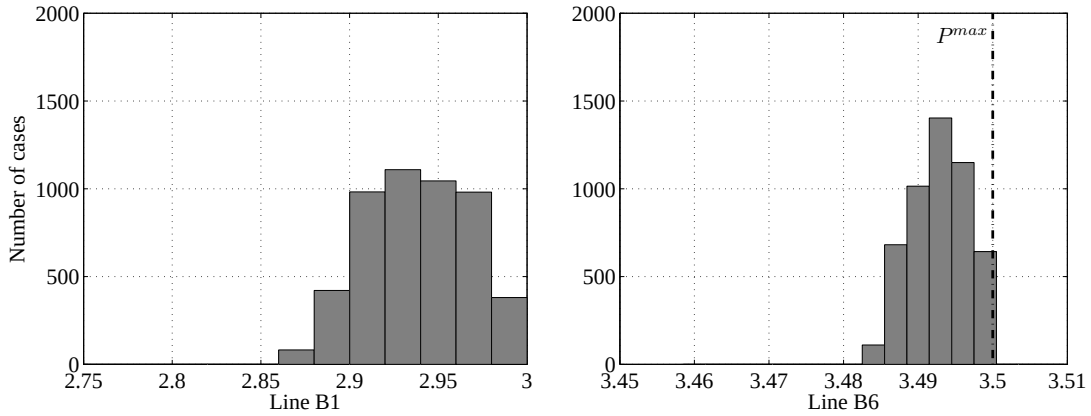

Figure 5.21: Distribution of final power flows; same cases as in Fig. 5.16 using dynamic adjustment of P^{max}

As in the previous test, the controller operated successfully in all the cases. Nevertheless, comparing the results with the ones in Fig. 5.20 one may guess that with the dynamic adjustment of branch limits the overall control effort is smaller on the average. This is explained by the fact that in some cases setting ε to 0.02 pu forces the controller to act more than needed.

Both corrective methods have been found to work satisfactorily on the test system, but have to be tuned and tested more carefully with a more realistic model taking into account the presence of other controls acting in the power system. This is the purpose of the next chapter.

5.6 Concluding remarks

The proposed centralized emergency control scheme acts to bring line currents below their limits before they are tripped. It is inspired of MPC, and operates in closed-loop in the sense that, at each time step new measurements are used to update a multi-step optimization problem, and hence cope with the new prevailing conditions. Various control actions can be included in the objective function with different priorities, and various objective functions can be considered.

Another feature of the proposed scheme is the capability to update the control horizon in the course of applying the actions. Thus, as transmission lines get alleviated, more time is left to act, i.e. more control steps become available.

The closed-loop nature of the control guarantees some robustness with respect to modelling errors and measurement noises. However, they may lead the controller to take more time to remove the overload. This may be critical in the case where the overload duration is fixed (i.e. not updated with the improving conditions) and when a limited number of controls are available. This can be compensated by reducing, statically or dynamically, the limits assigned to overloaded transmission lines in the optimization problem.

Chapter 6

Simulation of the voltage and thermal protection schemes on a real-life system

In the previous chapters we presented and tested with satisfactory results two system protection schemes aimed to deal with different, but interacting problems: voltage instability and thermal overload.

The results reported in this chapter relate to the tests performed on the model of a real-life system experiencing voltage and/or thermal problems. These tests allowed us to further analyze the behavior of the proposed system protection schemes and to study some other features that could not be addressed on the small systems used for preliminary tests. For example, the ability to adjust the control actions to the disturbance location and the coordination with other controllers (not having the same goals) acting in the system.

The results will not only confirm that each category of problems can be dealt with appropriately, but also that the wide-area and the local controllers cooperate satisfactorily for problems that are beyond their individual capabilities.

6.1 Simulated system

The tests have been performed on the real-life system presented in Section 6.1. For easiness we reproduce the one-line diagram in Fig. 6.1.

The responses of the real-life system have been obtained using QSS simulation, with a time step of 1 second and a simulation interval of 1000 seconds. Hence, electromechanical transients are not simulated; this is acceptable considering that the fastest protection is the undervoltage load shedding which is not going to act in less than 3 seconds (the value assigned to τ_{min}). Obviously, detailed time simulation can be used instead of the QSS approximation; it is even recommended for final verification of the protection behavior.

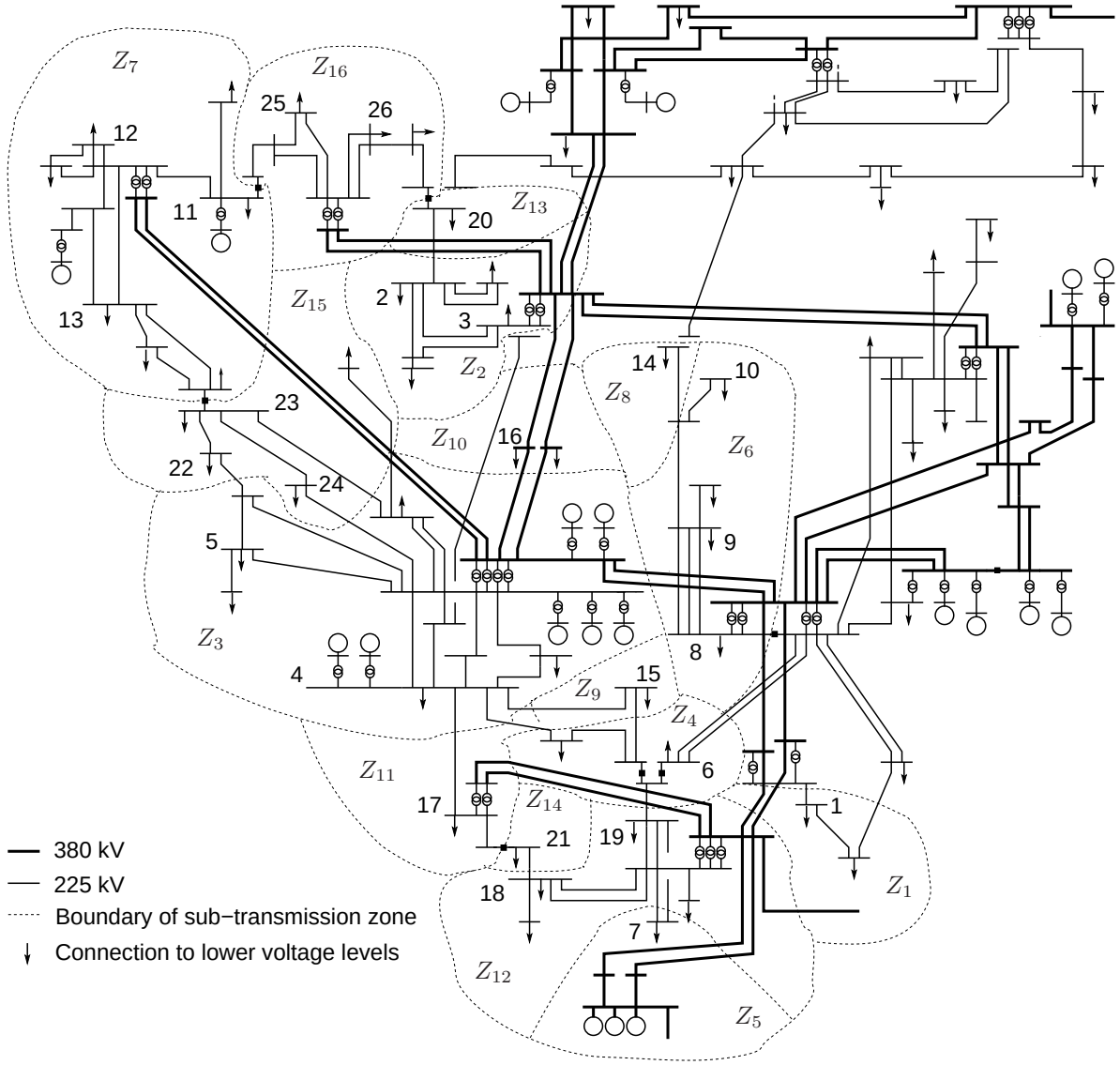

Figure 6.1: One-line diagram of the studied region within RTE system

The criterion to accept a post-disturbance evolution was that all transmission voltages remain above V^{crt} = 0.8 pu. It may happen that voltages recover after reaching this low value, thanks to secondary voltage control, but this was not accepted considering the nuisance for customers and the lack of reliability of the load model.

The examples provided in this section involve the disturbances determined in Section 3.5:

D1: loss of a transmission line inside zone Z_7 followed by the trip of a transmission line connecting Z_7 to Z_3 (see Fig. 6.1);

D2: loss of a transmission line inside zone Z_3 followed immediately by the trip of a transmission line connecting Z_{15} to Z_3;

D3: loss of two transmission lines connecting Z_7 to Z_3 with automatic reclosure of a switch between Z_7 and Z_{15};

D4: loss of two transmission lines connecting load zone Z_{15} to Z_3;

D5: loss of two transmission lines, feeding zone Z_{15};

D6: loss of two transmission lines in zone Z_{12};

D7: loss of two transmission lines connecting Z_{16} to Z_2.

6.2 Distributed undervoltage load shedding SPS

6.2.1 Choosing the load shedding controller location

No attempt was made to optimize the location of the controllers. Instead, the previously mentioned geographical zones Z_1 to Z_{16} were re-used, all of them being provided with at least one controller. Some zones with a large load power received several controllers, each taking care of a cluster of loads based on topology.

By so doing, a total of 26 controllers were considered, which are denoted C_i $(i = 1, \ldots, 26)$ in the sequel. They are identified in Fig. 6.1 by their numbers i $(i = 1, \ldots, 26)$ displayed next to the transmission bus they monitor. For instance, the figure shows that zone Z_7 received the controllers C_{11}, C_{12} and C_{13}, respectively. As individual loads at distribution level were not known from the available data, power was shed homothetically in each cluster, with a lower limit of $\min_k P_k$ = 10 MW.

6.2.2 Choosing V^{th}

As already illustrated in the Nordic 32 test system, the voltage threshold V^{th} should be set high enough to avoid delaying the controller actions. This is best seen from Figs. 6.2.a and b, similar to those presented in Section 4.4.4, and related to disturbances D1 and D3, respectively. In this figure, the dots indicate protection failures, i.e. cases where the 0.80 pu voltage criterion was *temporarily* or *permanently* reached at one or several transmission buses. For clarity, the figures do not show results for $V^{th} > 0.90$ pu, which correspond to all stars.

These results confirm that V^{th} should be taken as high as possible in order the protection to operate reliably. However, above 0.90 pu, the gain in reliability becomes marginal.

On the other hand, according to standard operating rules, V^{th} should be chosen low enough so that no load is shed for any single contingency with acceptable system post-disturbance response. Hence, all single outages were simulated, and the lowest voltage reached in the post-disturbance period was recorded at each bus monitored by a load shedding controller.

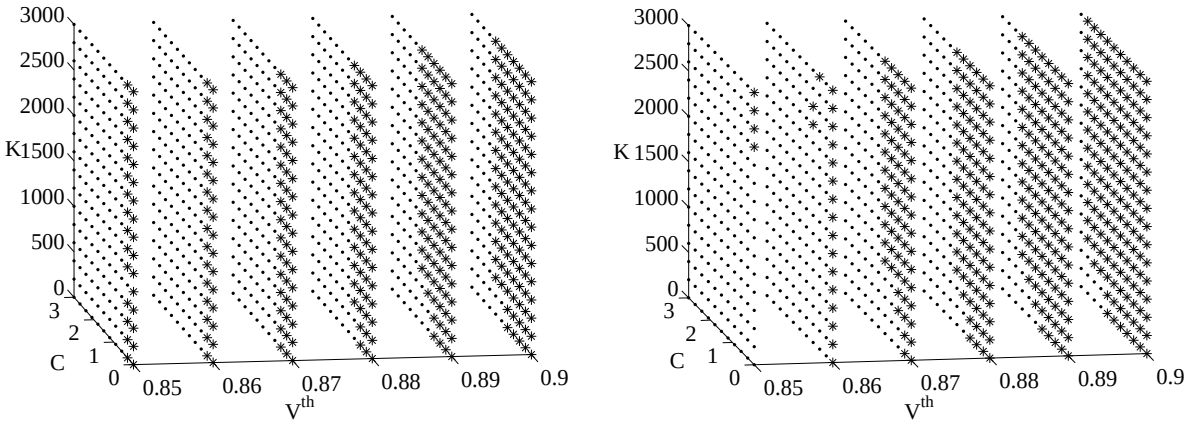

Figure 6.2: Performance of load shedding scheme for different C, K and V^{th} settings (disturbances D1 and D3)

Table 6.1 gives the minimum over all disturbances, for each controller. As can be seen, setting $V^{th} = 0.92$ pu for all controllers would be acceptable.

Table 6.1: Minimum voltage reached after acceptable disturbances

zone	controller	min. volt. (pu)	zone	controller	min. volt. (pu)
Z_1	C_1	1.02	Z_8	C_{14}	0.94
Z_2	C_2	0.97	Z_9	C_{15}	1.00
	C_3	0.98	Z_{10}	C_{16}	1.01
Z_3	C_4	1.00	Z_{11}	C_{17}	1.02
	C_5	1.00	Z_{12}	C_{18}	0.98
Z_4	C_6	0.94		C_{19}	**0.93**
Z_5	C_7	**0.93**	Z_{13}	C_{20}	0.99
Z_6	C_8	1.00	Z_{14}	C_{21}	1.01
	C_9	0.96	Z_{15}	C_{22}	**0.93**
	C_{10}	0.95		C_{23}	0.95
Z_7	C_{11}	0.99		C_{24}	0.95
	C_{12}	0.98	Z_{16}	C_{25}	1.00
	C_{13}	0.94		C_{26}	1.00

In addition, N-2 or more severe disturbances *with acceptable system responses* could be also involved in the choice of V^{th}. This is a matter of design criterion. Such a case, corresponding to the outage of two transmission lines in zone Z_{16}, is illustrated in Fig. 6.3. If it is not allowed to shed load (considering that the system response is acceptable), then V^{th} has to be decreased in order to cope with the lower voltages reached after these more severe disturbances. In this case it would be more appropriate to select non uniform values of V^{th} ranging from 0.86 to 0.90 pu.

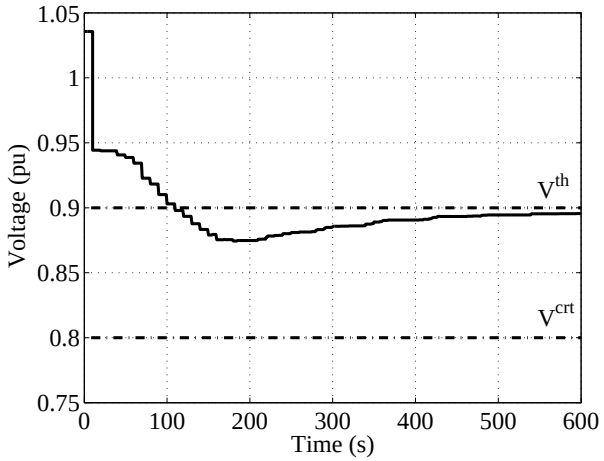

Figure 6.3: Post-disturbance acceptable voltage evolution

As a compromise between protection security and selectivity, V^{th} was set to 0.90 pu. This leaves some margin with respect to the 0.93 pu ceiling corresponding to N-1 contingencies without affecting the protection performance. By so doing, we accept to shed load after *some* N-2 or more severe contingencies which do not cause unacceptable voltages. The same value V^{th} is used for all controllers for the sake of simplicity.

Finally, note that in highly compensated (or capacitive) systems, the same procedure will naturally lead to higher V^{th} values, since after acceptable disturbances voltages will settle to higher values. Critical voltages will be also higher and hence V^{th} will remain close to the latter, thereby avoiding undue delays that would lead to shedding more load. A similar procedure led to values of V^{th} in the range $[0.9 \;\; 0.95]$ pu when devising the undervoltage load shedding scheme of the 735-kV system detailed in [LMC03].

6.2.3 Choosing C and K

With the voltage threshold V^{th} set to 0.90 pu, (C,K) diagrams were determined in order to identify the best (C,K) combination. Figures. 6.4.a to d show the total amount of power shed for disturbances D1, D3, D4 and D5, respectively.

As in the Nordic32 system case, the zones of equal shedding are not limited by smooth boundaries. Furthermore, setting parameter C to 0 does not necessarily yield the smallest load shedding amount. This observation comes to support the recommendation made in Section 4.4.6, to choose a larger C value.

Taking into account these recommendations, the settings in Table 6.2 have been adopted for all controllers. These settings mean that the shortest shedding delay is 4 seconds, and corresponds to a case where, right after the disturbance, the voltage settles a little above 0.80 pu (the lowest accepted value).

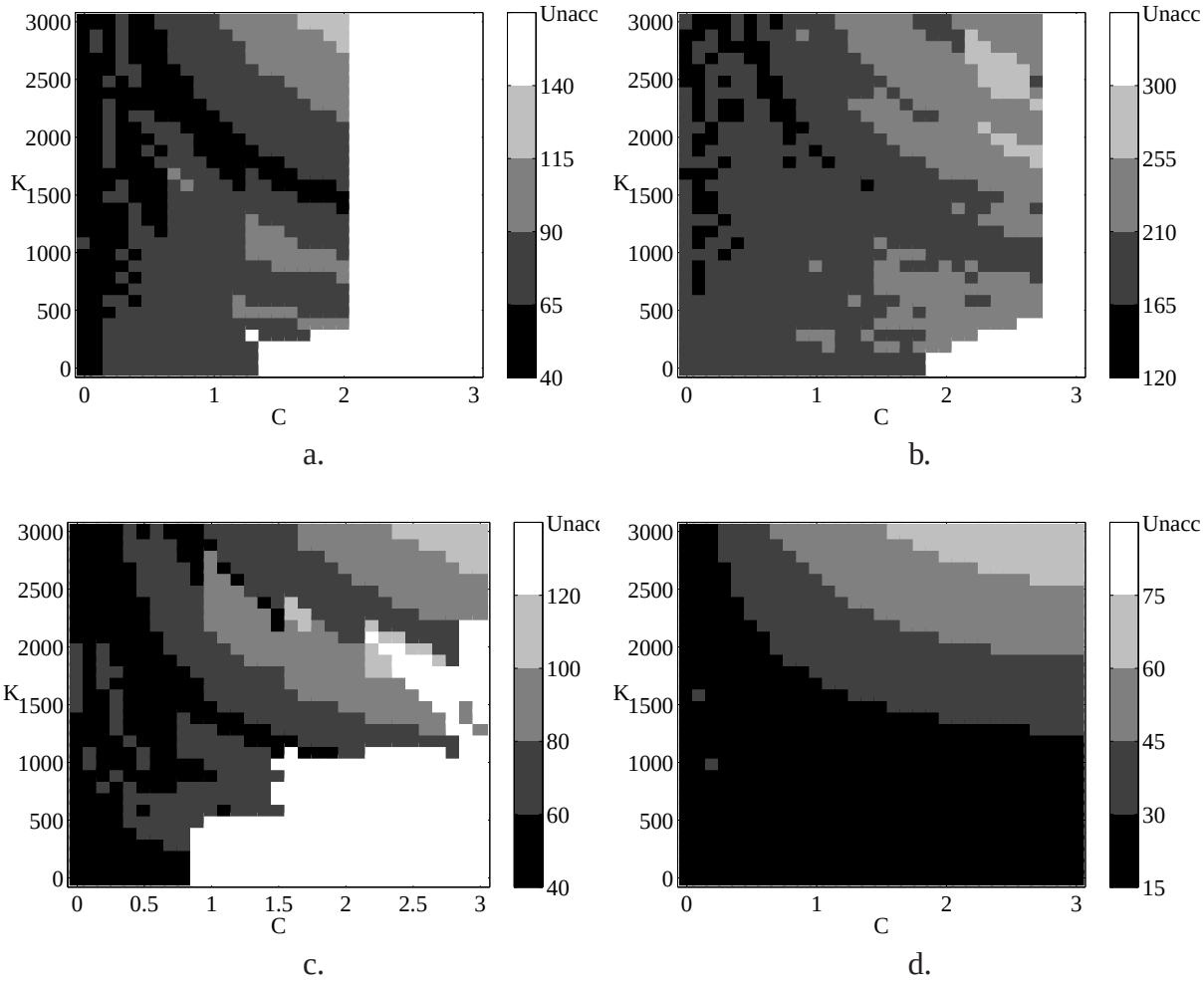

Figure 6.4: Total power shed (MW) for various (C, K) values, with $V^{th} = 0.9$ pu (disturbances D1, D3, D4 and D5)

Table 6.2: Controller settings

V^{th}	C	K	τ_{min}	$\min_k P_k$	ΔP_{tr}^{sh}
0.9 pu	0.4 pu·s	2000 MW/pu	3 s	10 MW	250 MW

In a real application it is recommended to determine the controller parameters settings from a large combination of disturbances, system loadings and network configurations. For example, the best value for the (C, K) combination could be determined as the one minimizing the total load shedding over all considered scenarios:

$$P_{min}^{sh} = \sum_{s=1}^{S} P^{sh}\left(s, C, K\right) \ , \tag{6.1}$$

where $P^{sh}\left(s, C, K\right)$ denotes the power shed in the s-th scenario (s = 1,...,S) with the protection parameters set to (C, K).

6.2.4 SPS Selectivity in terms of location

This section illustrates one aspect of SPS selectivity, i.e. the ability of the distributed protection to adjust the shedding location to the disturbance it faces. This relates to the fact that the area experiencing the largest voltage drops changes with the disturbance, and different controllers are activated.

For the disturbances involving voltage problems, resulting in load shedding controller activation, Table 6.3 provides the most affected zones, the controllers that were activated, and the blocks of power that were sequentially shed, for the V^{th}, C and K settings chosen in the previous sections. Let us recall that different settings may lead to different combinations of controller actions. A zero value in the table indicates that the corresponding controller was temporarily started but switched back to idle state before acting (see Fig. 4.2).

As can be seen, the affected zones and the activated controllers change significantly from one disturbance to another.

Table 6.3: Controllers activated by the four disturbances

disturb.	zone	controller	ΔP^{sh} (MW)
D1	Z_7	C_{13}	35 + 25
	Z_7	C_{12}	0
D3	Z_7	C_{13}	26 + 37
	Z_{15}	C_{23}	22 + 24
	Z_7	C_{12}	27
	Z_{15}	C_{22}	20 + 17
	Z_7	C_{11}	0
D4	Z_{15}	C_{24}	36
	Z_{15}	C_{22}	20
	Z_{15}	C_{23}	0
D5	Z_{15}	C_{24}	24
	Z_{15}	C_{22}	0
	Z_{15}	C_{23}	0
D6	Z_{14}	C_{21}	73
D7	Z_{13}	C_{20}	32
	Z_{16}	C_{26}	48
	Z_7	C_{13}	20
	Z_{16}	C_{25}	0
	Z_7	C_{11}	0
	Z_7	C_{12}	0

6.2.5 SPS selectivity in terms of total power cut

Another aspect of selectivity is the ability to adjust the load shedding amount to the severity of the disturbance.

Let us stress that the proposed distributed controller scheme is not claimed to yield minimum load shedding, although the controllers settings have been chosen so as to meet this objective *globally* (i.e. over the whole set of disturbances). Tests have thus been performed to assess the degree of sub-optimality in terms of amount of power cut.

As a benchmark, a method inspired of [MC99] has been used to compute the minimal power that should be shed *in a single step* to save the system.

First, loads are ranked with respect to their efficiency in restoring voltages. Two criteria have been used. The first one is based on the sensitivities detailed in [CVC05]. In the second one, loads are ranked by increasing order of post-disturbance transmission voltages; a snapshot of voltages is taken when one of them reaches 0.8 pu. The voltage ranking has some similarity with what the distributed controllers do, *except that here load is shed in a single step*, which results in shedding less [LMC03]. Then, for a given shedding time, a binary search is used to find the minimum total power to cut. For a given value of power, shedding is distributed over the loads by decreasing order of the ranking. Finally, the procedure is repeated for various shedding delays.

Figures 6.5.a and b show the so obtained minimum shedding as a function of shedding time, for disturbances D1 and D3, respectively. The curves confirm that beyond some delay, shedding later requires to shed more [VCV98]. Also, as expected, sensitivity-based ranking yields lower load shedding. Thus, the minimum shedding (unfortunately not known when facing the disturbance!) is 18 MW for disturbance D1 and 95 MW for disturbance D3.

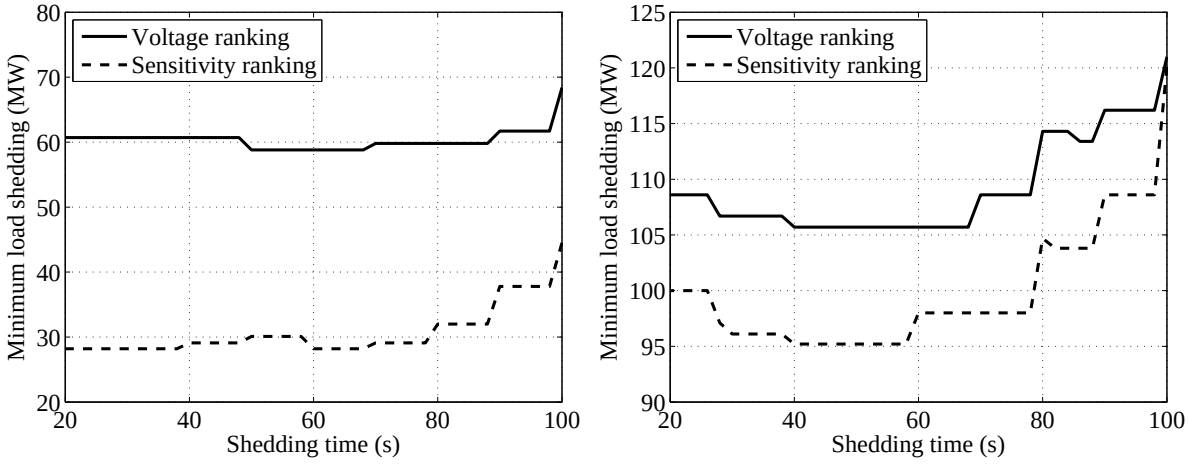

Figure 6.5: Minimum (single-step) shedding vs. time (disturbances D1 and D3)

These amounts are to be compared to those shed by the distributed controllers. Figures 6.4.a and b show that they can shed as few as 40 MW for disturbance D1 and 120 MW for disturbance D3. These values are not far from the benchmark values, if one considers that each shedding is lower limited to 10 MW. When the settings of Table 6.2 are used, the distributed controllers shed 60 MW (respectively 173 MW) after disturbance D1 (respectively D3), as can be checked from the last column of Table 6.3. These values are less close to the optimum. The reason is that the settings of Table 6.2 were not optimized for D1 and D3 but are a compromise over a larger set of disturbances.

6.2.6 SPS robustness with respect to load model uncertainty

As already mentioned, the closed-loop nature of each controller compensates for uncertainties in dynamic system behavior. This section aims at illustrating the robustness of the proposed scheme with respect to load modeling inaccuracies.

The controllers' ability to adapt to unforeseen load characteristics is illustrated by Fig. 6.6, showing the evolution of the lowest transmission voltage for different load exponents α and β, after disturbance D1 and D3. Although the controllers were tuned from simulations performed with $(\alpha = 1.4, \beta = 2)$, they respond very satisfactorily (if not better) when facing different load characteristics.

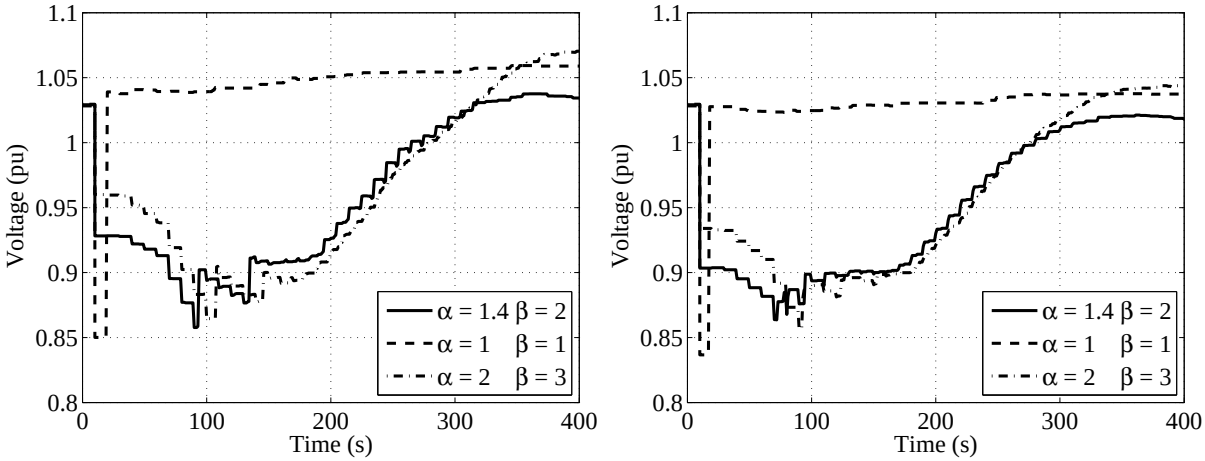

Figure 6.6: System response with load shedding, for various load behaviors (disturbances D1 and D3)

One can also see that the smaller α and/or β, the faster and the deeper the voltage drop below $V^{th} = 0.90$ pu, and hence the faster the shedding and the voltage restoration.

Different load characteristics lead to different shedding amounts. Figure 6.7 shows the *difference* in power cut, for disturbance D3, when the load exponents change from $(\alpha = 1.4, \beta = 2.0)$ to $(\alpha = 1.0, \beta = 1.0)$. Positive values correspond to cases where less load is shed with $(\alpha = 1.0, \beta = 1.0)$; this tends to occur for small values of C or K. The white region of the diagram corresponds to (C, K) settings for which the protection failed for at least one of the two load characteristics. In fact, a comparison with the diagram in Fig. 6.4.b shows that the region of successful operation of the protection remains almost the same in spite of the large difference in load behaviors.

Other tests were made assuming a smaller or even no reactive power counterpart when dropping active power. An example is provided in Figs. 6.8.a and b, relative to disturbance D1 and D3. In the simulation shown with heavy line, the load power power factor was left unchanged after shedding. In the other two cases, 50 % and 0 % of the reactive power were cut, respectively.

As can be seen, although the C and K parameters were tuned under the assumption of constant

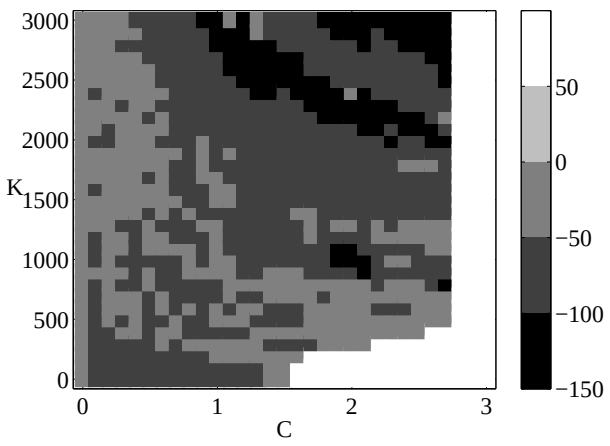

Figure 6.7: Difference in power shed (MW) when load exponents change from $(\alpha = 1.4,\ \beta = 2.0)$ to $(\alpha = 1.0, \beta = 1.0)$ (disturbance D3)

power factor, the controllers adjust to the changing conditions by shedding more active power (see captions in Fig. 6.8). Nevertheless, the voltage evolution is hardly affected.

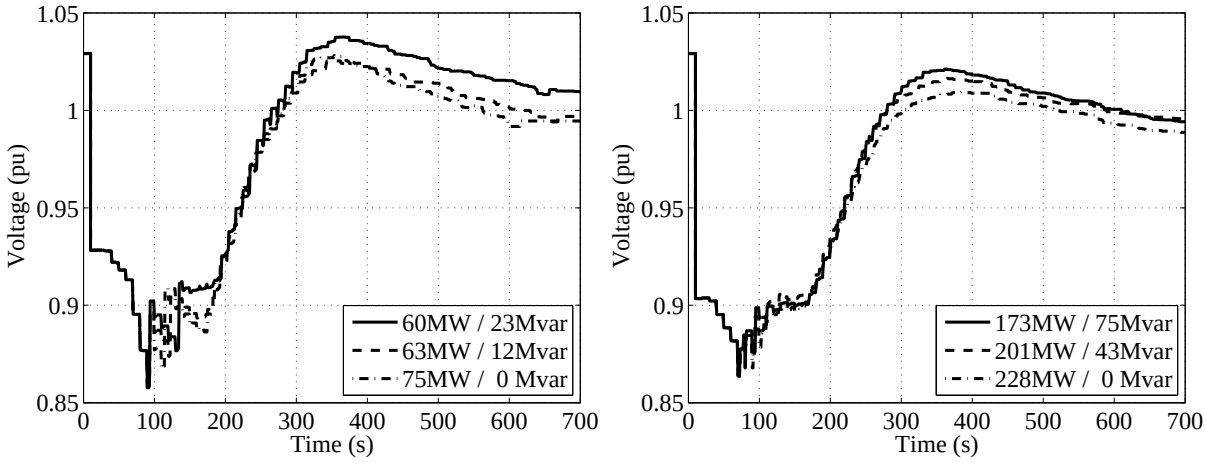

a. b.

Figure 6.8: Effect of shedding under unexpected load power factors (disturbances D1 and D3)

6.2.7 SPS robustness with respect to component failure

Another aspect of robustness has to do with the possible failure of some controllers. This section aims at demonstrating the performance of the proposed scheme in this respect.

Table 6.4 shows the power shed by each controller in response to disturbance D4, in various scenarios. Case 1 corresponds to the base case simulation, where all controllers are acting normally, while the other cases correspond to failures, as detailed hereafter.

In Case 2 the voltage measurement used by controller C_{24} was assumed to be systematically

Table 6.4: Load shedding amounts (MW) in various scenarios

	Case					
controller	1	2	3	4	5	6
C_{22}	20	15	62	-	62	-
C_{23}	0	0	21	0	-	58
C_{24}	36	44	-	54	-	-
Total	56	59	83	54	62	58

0.01 pu smaller than the correct value, causing this controller to act faster and shed more power. This is compensated by a smaller action of C_{22}.

Case 3 simulates a full failure of C_{24} (identified with a "-" in the table); this is covered by a stronger action of C_{22}, while C_{23} comes into play. Similarly, Case 4 corresponds to failure of C_{22}; it causes C_{24} to take a stronger action, but the help of C_{23} is not needed.

Cases 5 and 6 correspond to the failure of two controllers at the same time. In both cases, the remaining controllers succeed stabilizing the system with a little more effort than in Case 1.

As in the Nordic 32 system case, we can conclude that the redundancy among controllers makes the protection scheme very reliable. Furthermore, substituting one controller with another does not significantly increase the amount of power shed. It may even decrease a little bit. Case 3 appears as an exception and is discussed in the next section.

6.2.8 Extensions and variants

Centralized variant of SPS

The proposed scheme is meant to operate in a fully distributed way, each controller using local information and taking local actions, as underfrequency load shedding controllers do [JLT02]. Nevertheless, comparing Case 3 with Case 5 in Table 6.4, shows that C_{22} alone could have saved the system, without the intervention of C_{23}. In Case 3 more load has been shed because both controllers acted at the same time, not knowing about their respective actions. This is the price to pay for not having communication between controllers, other than through network voltages.

Based on these results, one may also think of implementing the scheme in a centralized way, by collecting all voltage measurements at a central point, running the computations involved in Eqs. (4.2-4.7) in a single processor, and sending back load shedding orders (with some communication delays to be taken into account). In this case, additional information exchanges and interactions between controllers may be envisaged without further penalizing the scheme. For example, signals could be sent which may accelerate, inhibit or even reset the actions of other controllers affected by the same disturbance.

In order to make a comparison, a variant with communicating controllers was considered in which: (i) all controllers are reset when one is acting, and (ii) if the integrals (4.2) of two controllers reach the C value at the same time, only the one observing the greater voltage drop is acting.

Figure 6.9 shows the results obtained with the above variant in the case of disturbance D4. The comparison with the corresponding decentralized SPS diagram in Fig. 6.4.c, in terms of difference in power cut, is presented in Fig. 6.10. Positive values correspond to cases where less load is shed with the centralized configuration and white region of the diagram corresponds to (C, K) settings for which the protection failed for at least one of the SPS configuration.

It can be seen that some load shedding can be avoided, for some combinations of C and K. Nevertheless, there is no systematic decrease. Also, for some other disturbances it has been observed that the region of successful operation of the protection shrinks significantly; this is attributable to the delays introduced by the resets.

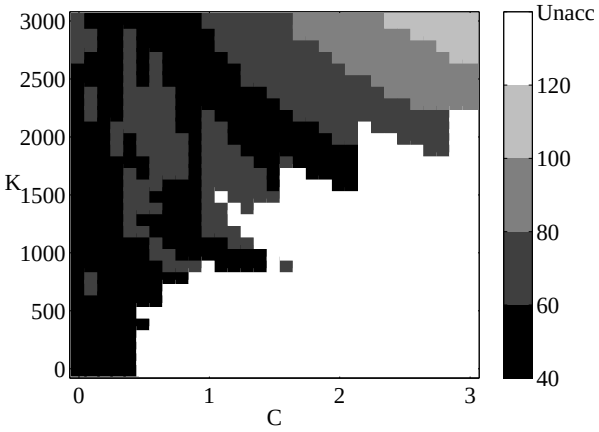

Figure 6.9: Total power shed (MW) for various (C, K) values with centralized configuration

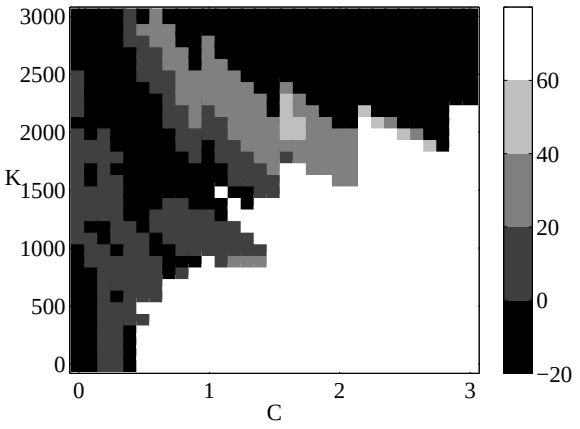

Figure 6.10: Difference in power shed (MW) between centralized and decentralized configuration

Although communication between controllers could bring some improvements, a scheme re-

mains to be found in order to obtain substantial benefits that would compensate for the increased complexity.

Redundant measurements

In order to protect the SPS against erroneous measurements, it is desirable for each controller to rely on several voltage measurements, taken at closely located buses. Some filtering can remove outliers from the measurements, and the average value of the valid ones can be used as V in Eqs. (4.2, 4.5). If all data are dubious, the controller should not be started; other controllers will take over, as illustrated in Section 6.2.7.

Average voltage drop

One reason for averaging the voltage drop over time in Eq. (4.5) is the necessity to filter out transients and measurement noise. However, the average need not be computed over the τ seconds elapsed since the last shedding. Instead, a shorter time window may be considered:

$$\Delta V^{av} = \frac{1}{\tau'} \int_{t_0+\tau-\tau'}^{t_0+\tau} \left(V^{th} - V(t)\right) dt \ , \tag{6.2}$$

with $\tau_{min} < \tau^{'} < \tau$, so that ΔP^{sh} relies on more recent voltage values. This might lead to shed less power in some cases.

As illustrated in Fig. 6.11.a, if the monitored voltage is decreasing, more load will be shed since the average voltage drop computed over the last τ' seconds is larger. Therefore, in the first instants of a voltage unstable evolution, when the voltage is decreasing, the large sheddings will faster arrest the voltage drop. At the same time, it is known that shedding faster may result in shedding less.

On the contrary, if the voltage profile is improving, computing the voltage average over the last τ' seconds leads to a smaller amount of load shed, see Fig. 6.11.b. Hence, using (6.2) further adjusts the controller actions to the prevailing conditions.

Figures 6.12.a and b show the difference in power cut, for disturbances D1 and D3, respectively, when the voltage average is computed over τ seconds and over the last τ' = 3 s. Positive values correspond to cases where less load is shed when using τ' and the white region of the diagram corresponds to (C, K) settings for which the protection failed for at least one of the two configurations or if the amount of load shed was identical. The white strips observed for small values of C or small values of K are easily explained. When C = 0, τ is limited to 3 s and it does not make a difference to use τ or τ'. When K is small, ΔP^{sh} is lower limited to 10 MW, whatever the way the average voltage drop is computed.

Analyzing the results, it has been observed that for "mild" disturbances, as the one illustrated in Fig. 6.12.a corresponding to D1, computing the voltage average over the last τ' seconds

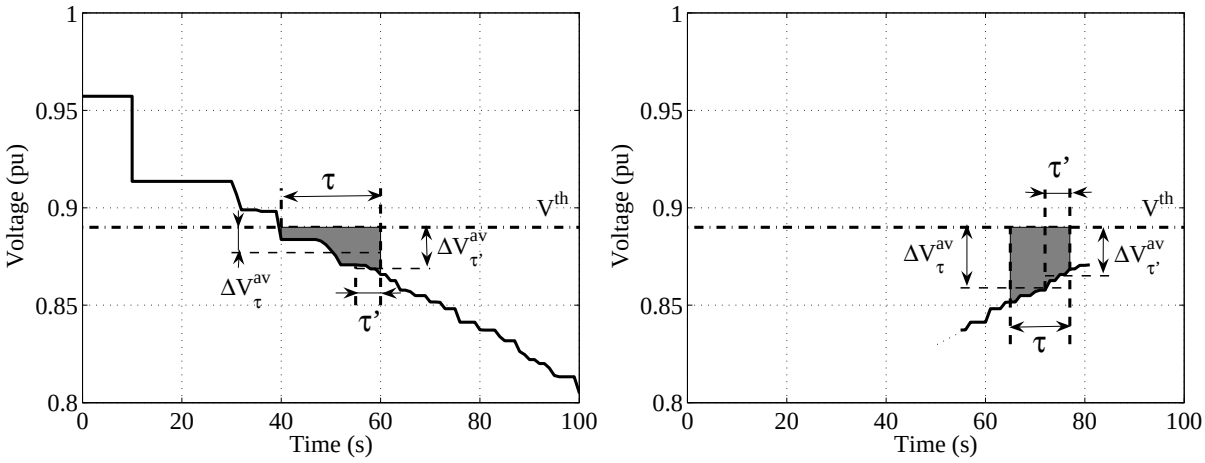

Figure 6.11: Illustration of influence of time interval on the computed average voltage drop

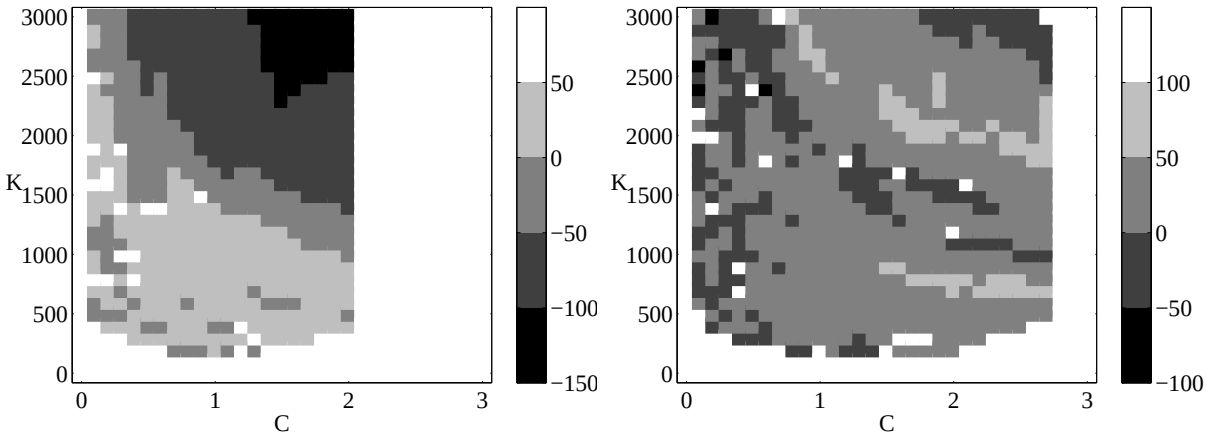

Figure 6.12: Difference in power shed (MW) with ΔV^{av} computed over τ and τ'

leads to smaller load shed for small values of C or K and greater load shed with the increase of C or K. This is explained by the fact that for large values of C or K one load shed step is enough to solve the voltage problem. As the voltage has a decreasing trend results that the voltage average is larger, thus the resulting load shed amount is greater (see Fig. 6.11.a).

On the contrary, for "severe" disturbances, as the one illustrated in Fig. 6.12.b corresponding to D3, for a major part of (C,K) combinations the SPS behavior is improving.

Thus, if this variant of the main distributed undervoltage SPS is to be implemented, the parameters C and K have to be readjusted in order to ensure the minimum over all considered disturbances.

6.2.9 Behavior in the presence of combined voltage and thermal problems

As illustrated in Fig. 6.4.d, corresponding to disturbance D5, no matter the (C,K) combination, the undervoltage load shedding SPS succeeds solving both voltage and thermal problems after that disturbance. Indeed shedding load to stabilize voltages also reduces the current in the (slightly) overloaded line and prevents the latter from being tripped.

The outcome is not so successful for disturbances D6 and D7. Eventhough, for the considered parameter settings, the undervoltage SPS succeeds solving the voltage problems, it cannot prevent the trip of the overloaded line, see Figs. 6.13.a and b. As can be seen, the line current is decreasing under the effect of load shedding, but increases again due to load restoration by LTCs.

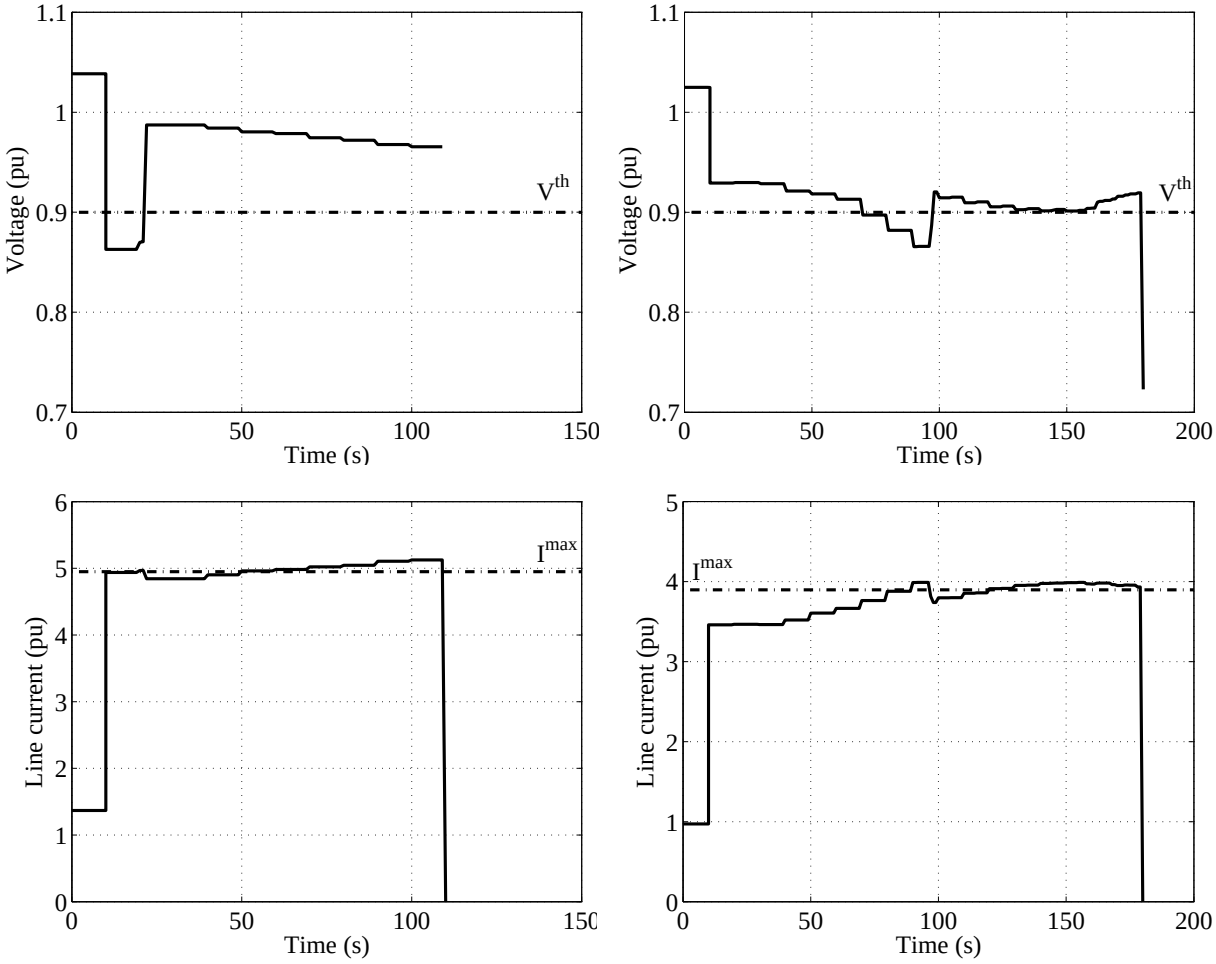

Figure 6.13: Evolution of lowest monitored voltage and line current with undervoltage SPS acting alone (disturbances D6 and D7)

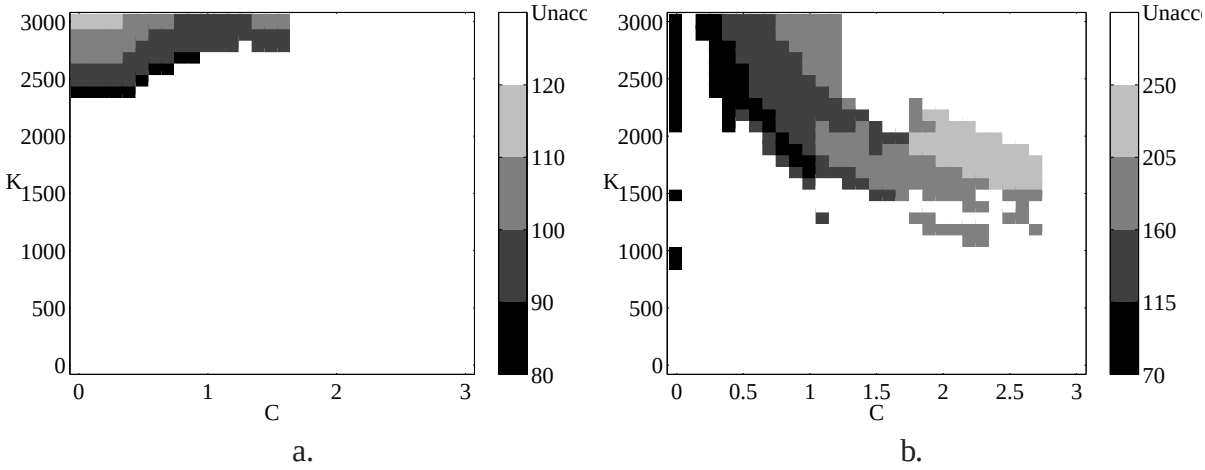

Figure 6.14: Total power shed (MW) for various (C, K) values (disturbances D6 and D7)

Testing the entire set of (C,K) combinations revealed that there are some values for which the undervoltage SPS solves both problems, see Figs. 6.14.a and b. At first glance, one could think of adopting one of these successful settings and rely on undervoltage to tackle both voltage and thermal overload problems. However, this is not recommended at all since it would: (i) lead to shedding prohibitive amounts of load in other (less severe, pure voltage instability) cases, and (ii) leave little margin in the (C, K) space with respect to protection failure.

6.2.10 Concluding remarks

As observed in the Nordic32 test system, the closed-loop design of the undervoltage load shedding controllers helps them to adjust their emergency action to the severity of the faced disturbance. Furthermore, it was shown that the distributed structure allows to adjust to the disturbance location.

The redundancy among controllers guarantees robustness with respect to unexpected load behaviors or controller failures. It is even recommended not to start the load shedding action if the received voltage measurements are doubtful, as other controllers will take over.

Finally, it was shown that undervoltage load shedding could also act successfully for disturbances resulting in both voltage and thermal problems. However, in some cases, even though the thermal overload was initially alleviated when dealing with the voltage problem, the undervoltage SPS could not prevent the line from being overloaded, then tripped due to load power restoration. For these disturbances few (C,K) combinations are available when setting the controller parameters.

Therefore, it is recommended to resort to a line overload alleviation SPS in order to prevent the line trip. The MPC-based scheme described in Chapter 5 has been used to this purpose and the results are reported in the remaining of this chapter.

6.3 Centralized thermal overload alleviation SPS

6.3.1 Choosing the main parameters

As shown in Chapter 3, thermal overload problem may aggravate an already unstable system or lead to cascading effects on the remaining equipments, which could result in system islanding. In such emergency cases, corrective measures have to be taken to quickly prevent some of the overloaded lines from being tripped.

In the Western region of the RTE system, 114 transmission lines are equipped with an overcurrent protection, allowing a 140 $\%$ overload to last for at most 60 seconds[1].

In Chapter 5 we mentioned emergency actions against thermal overload such as phase shifting transformer angle changing, generation rescheduling, load shedding, line and bus-bar switching and FACTS devices. In our tests of the RTE system, we concentrated on load shedding only. One reason is that the very structure of the Western region does not make generation rescheduling possible, and no phase shifting or FACTS device is available. The second reason is that we wanted both the undervoltage and overcurrent load shedding schemes to coexist (and possibly compete?) in our tests.

As the loads were already grouped into topology-based clusters for the distributed undervoltage load shedding scheme, we have reused the same groups for the centralized overload alleviation protection scheme. Thus, we assume that the centralized overload alleviation protection scheme sends orders to the 26 shedding controllers. Furthermore, we consider the same limits for both types of load shedding:

$$\min_k P_k = 10 \text{ MW}$$

and

$$\Delta P_{tr}^{sh} = 250 \text{ MW} \ .$$

Nevertheless, we have considered that any control action smaller than 1 MW is discarded, as in some other location the load shedding amount will be rounded to the minimum value. Moreover, this will be compensated in future control steps, due to the close-loop nature of the MPC-based scheme.

As for voltage instability, the location and the amount of load shedding matters a lot when dealing with transmission lines thermal overload. Shedding at a less appropriate place requires shedding more. The best location for load shedding may vary significantly with the overloaded line, system loading and topology. Even if the best shedding location is identified, tripping less load than necessary will obviously not be effective in alleviating the line overload.

The sequence of controls is obtained as the solution of an optimization problem of the type

[1]The same protections also act at two lower overload levels, with obviously longer delays. These delays, however, are long enough to allow an operator intervention and are therefore not considered in the tests.

(5.22 - 5.28) using the quadratic objective (5.44). The system representation at the heart of the MPC-based controller is a sensitivity model of the type (5.23). This is a very simplified model that does not take into account dynamic components such as load tap changers, secondary voltage controllers and undervoltage load shedding. This choice was made on purpose: (i) to test the ability of the MPC-based scheme to compensate such modeling simplifications and (ii) to keep a tractable multi-step optimization problem, compatible with real-time applications. As loads are grouped into clusters, one element of the sensitivity matrix $\mathbf{S}$ in (5.23) represents the sensitivity of a branch current with respect to the total load of a specific cluster, and is obtained as:

$$S_{Ic} = \frac{\sum_{l=1}^{L} \frac{P_l}{P_{lc}} S_{Il}}{L} , \tag{6.3}$$

where L is the number of loads in the cluster of concern, P_l represents the interruptible power of load l, $P_{lc} = \sum_{l=1}^{L} P_l$ is the total interruptible power in the cluster, and S_{Il} is the sensitivity of the branch current with respect to load l, computed with formula (5.36), where the first term is zero.

The sampling time Δt has to take into account the transmission delays to send the measurements to the controller, the measurement filtering process, the time to solve the optimization problem, and the transmission delay to send back the control actions. Therefore, we consider that a time step of $\Delta t = 10$ s is a realistic choice. The settling delay M being left to 5 seconds, formula (5.18) indicates that the controller has at most 5 steps to remove the overloads.

We first present the results obtained with the thermal overload load shedding scheme acting alone. Then, we demonstrate the performance of both load shedding schemes acting concurrently.

6.3.2 Detailed analysis of performance

In order to analyze the behavior of the centralized overload alleviation controller, we first consider the pure thermal problem resulting from disturbance D2, see Section 3.5.

Figure 6.15 reproduces the evolution of an overloaded line current and the lowest bus voltage after the disturbance in the absence of load shedding. As can be seen, right after the disturbance, the line which is part of the transmission path feeding the load area, gets directly overloaded and after the maximum overload duration T_{ol} = 60 s, is tripped by its protection (Fig. 6.15.a). The voltages in the affected area remain acceptable after the initial disturbance, but drop to very low values just after the tripping of the overloaded line (Fig. 6.15.b).

The line current evolution in the presence of the proposed controller is shown in Fig. 6.16. In order to alleviate the overload, some 120 MW were shed in three steps and in four different locations, namely in the zones controlled by the undervoltage load shedding controllers C_5, C_{22},

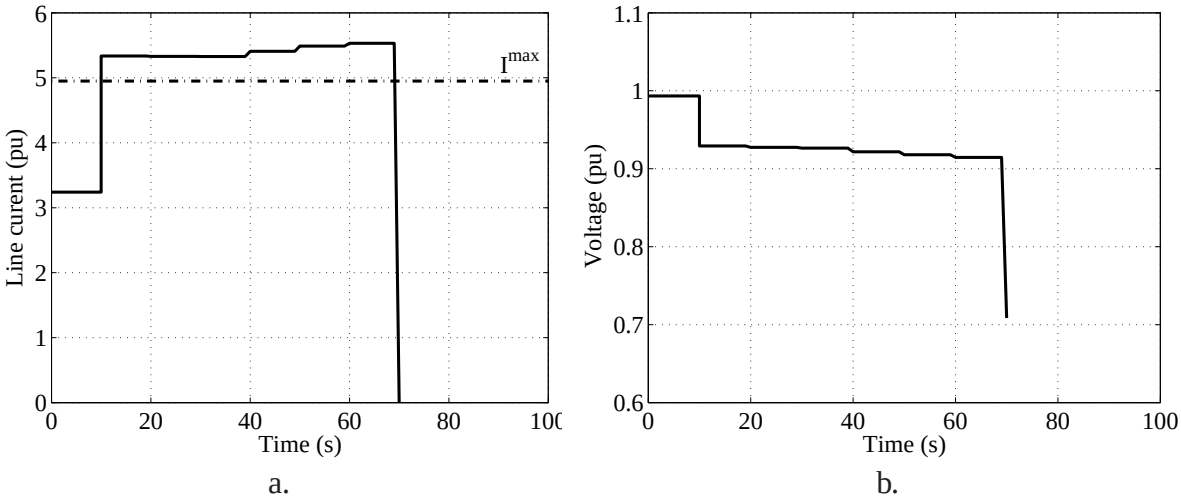

Figure 6.15: Evolution of line current and lowest transmission voltage without load shedding (disturbance D2)

C_{23}, C_{24} (not acting, however, as already mentioned). The loads in these zones are responsible for the line overload in the post-contingency configuration.

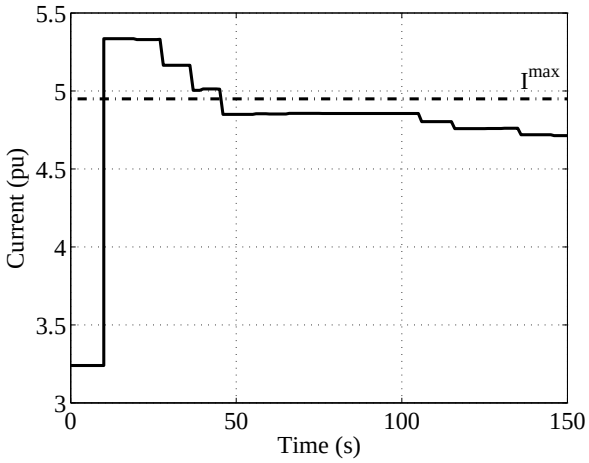

Figure 6.16: Line current evolution with load shedding (disturbance D2)

According to the first control sequence determined by the MPC algorithm with quadratic objective, there was a need to shed a total of 90 MW in 5 steps over 4 zones. This would lead to shedding less than 10 MW in each zone, which is the imposed lower limit. Therefore at the first control step, 4×10 = 40 MW are shed effectively, which is more than the computed value. This larger than expected action is felt by the controller at the next control sequence. As a result, the scheme operates in only 3 steps instead of the 5 initially scheduled. This is a direct outcome of the closed-loop nature of MPC.

In this particular scenario, the larger load shedding step effectively applied worked in favor of the scheme, leaving 2 control steps for additional corrections, if needed.

We consider now disturbance D5. In the first instants the system is not subject to voltage or overload problems. But, under the effect of load power restoration by LTCs, transmission voltages are decreasing and the currents in the lines through which the power was redirected are increasing, see Fig. 6.17[2]. This process is slow and, hence, the overload in the first instants is not important. As a result, the computed control actions are not significant. In fact, as in the previous case, they are smaller than the minimum shedding amounts; hence, the first control action involving 20 MW of load is enough to solve the overload problem.

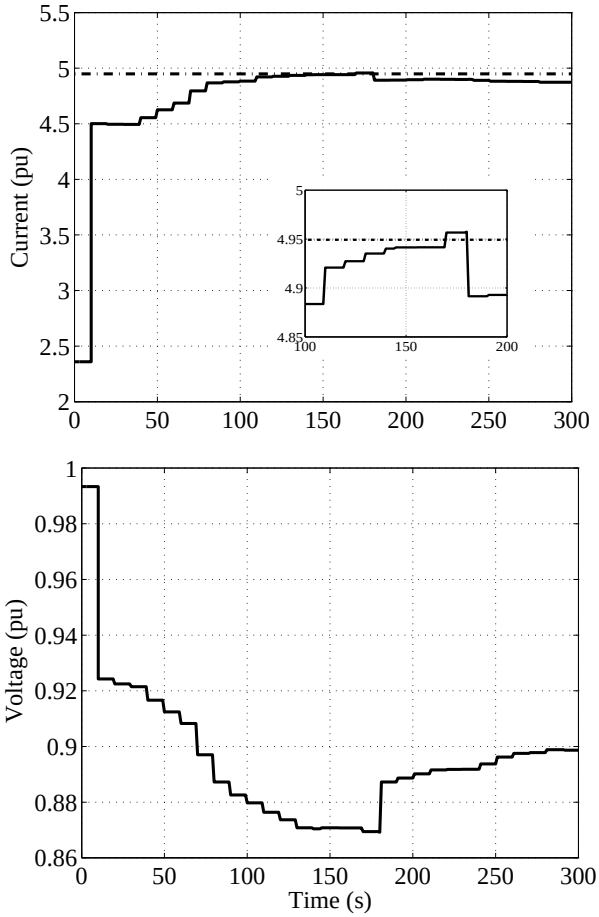

Figure 6.17: Evolution of line current and lowest transmission voltage with load shedding (disturbance D5)

D5 is definitely a "mild" disturbance. The same conclusion was drawn from the results obtained with distributed undervoltage load shedding, see Fig. 6.4.d. Comparing the load shed by the two protection schemes one can say that the actions are equivalent; the only difference lies in the fact that the centralized protection acted in two zones, controlled by C_{23} and C_{24}, while the distributed protection acted only in the zone controlled by C_{24}.

Next we report on the response to disturbance D6. In Section 6.2.9 it was shown that distributed undervoltage load shedding was unable to prevent the line tripping, the reason being that this

[2]The inner window in the upper diagram represents a zoom over the interval of interest.

protection scheme was not designed to solve that sort of problems. In Fig. 6.18, we present the overloaded line current and lowest voltage evolutions obtained with the thermal overload alleviation scheme in operation.

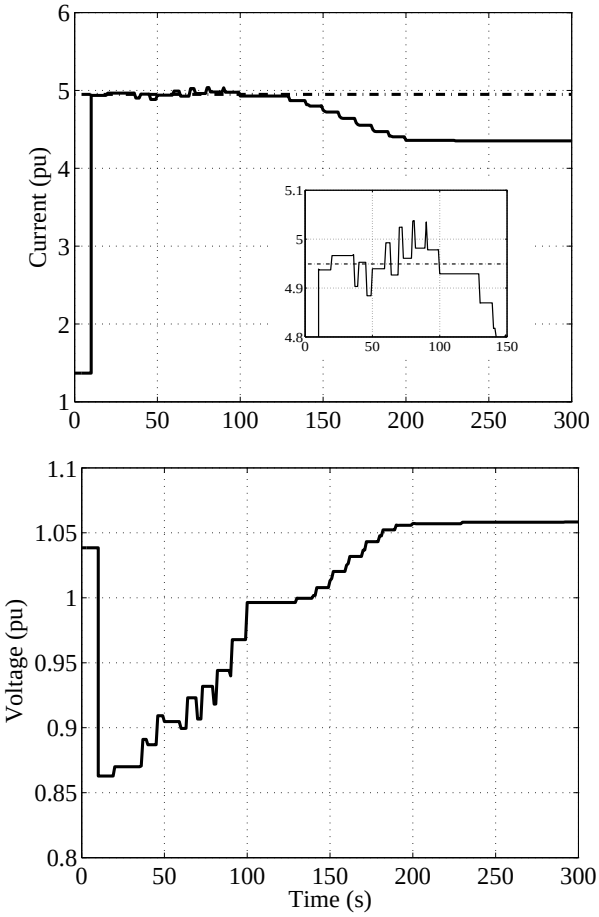

Figure 6.18: Evolution of line current and lowest transmission voltage with load shedding (disturbance D6)

It is easily seen that the proposed protection system succeeds saving the system. For this, a total of 140 MW was shed in seven control steps. Expectedly, the load shedding location has changed, as the disturbance is located in another area with respect to the previous disturbances. It takes place in the zones controlled by C_{18} and C_{21}.

As already mentioned, given the values of T_{ol}, Δt and M, the maximum number of control steps is five. The higher number of control actions (seven) is explained by the fact that after the first two control steps the line current becomes smaller than its limit and remains so for a short period of time. Therefore, when the current increases again above the limit (see Fig. 6.18) the reference time t_0 is reset and another 60 seconds are available to solve the problem. The so obtained control steps are used to their full extent as during the second control interval the load recovery process is more pronounced. This is explained by the fact that more LTC transformers start their action after the initial time delay (20 or 50 seconds depending on the transformer

level). It can be seen that the load shedding action is almost immediately counteracted by load restoration process.

The load shedding actions succeed to also restore the voltages. At the end of the load shedding sequence the voltages increase thanks to the secondary voltage controllers raising generator voltages.

We finally consider disturbance D7. As shown in Fig. 6.19.a (left plots), despite a significant load shedding, 270 MW, spread over 6 different locations, the controller was unable to prevent the overloaded line from tripping. This is due to the pronounced effects of load restoration by LTCs.

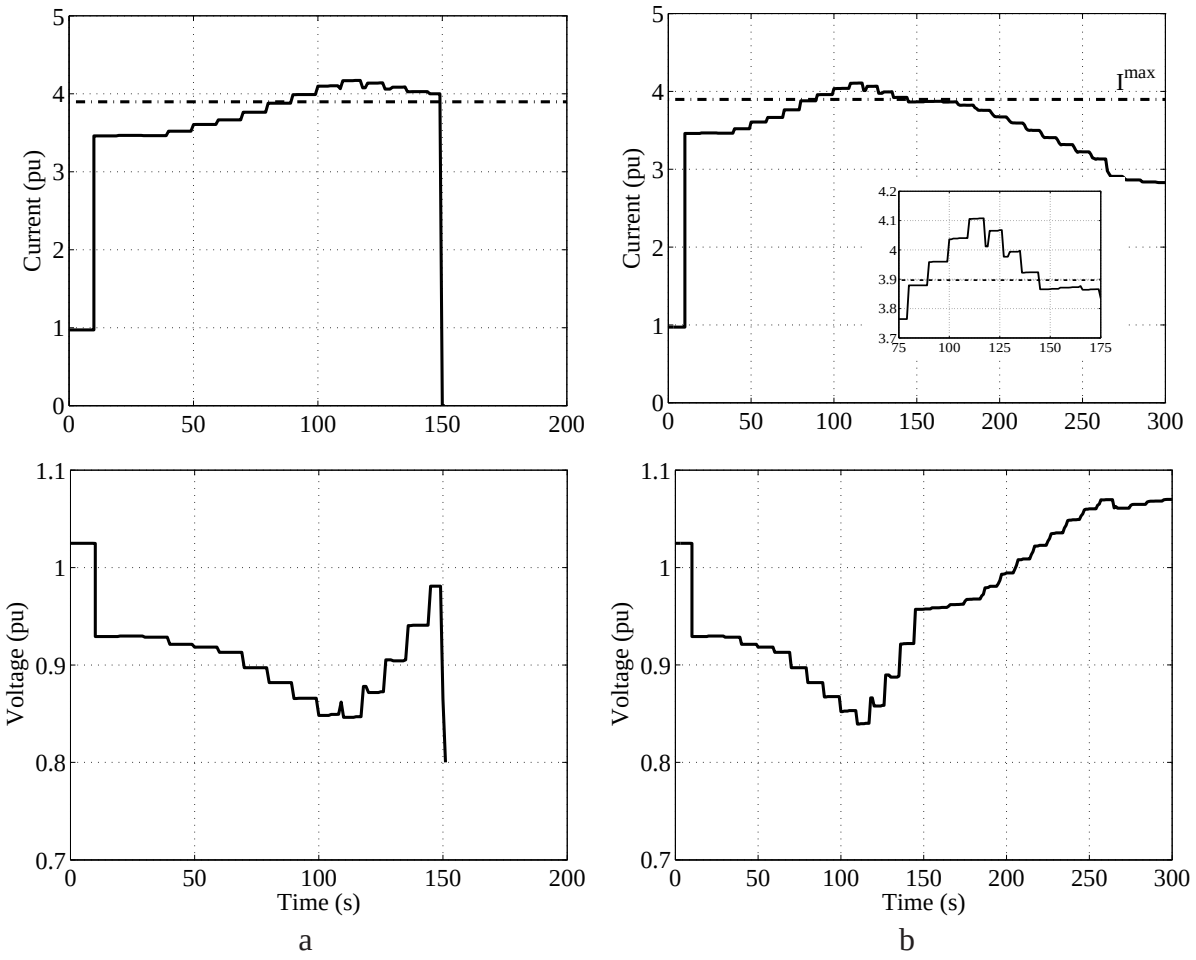

Figure 6.19: Evolution of line current and lowest transmission voltage with load shedding (disturbance D7). Left plots without LTC blocking; right plots with LTC blocking

In order to support this claim we present in Fig. 6.19.b (right plots) the system evolution when resorting to an *LTC blocking scheme*. The latter has been implemented in a distributed manner, similarly to undervoltage load shedding[3]. Furthermore, it relies on the same zones and the same

[3]This is not the case of the LTC blocking scheme presently used by RTE. Our objective was not to simulate the latter but rather to validate our controller, as well as test a possible extension of our distributed SPS.

monitored 225-kV buses. The logic is as follows. If the voltage at the monitored transmission bus stays below some threshold for a specified period of time, all tap changers within the zone are blocked on their current positions. If the monitored voltage recovers above a reset value, the tap changers are released and left to act normally. We chose a blocking threshold of 0.89 pu and a reset value of 0.92 pu, respectively.

As can be seen from the plots, by blocking the LTCs, the load shedding actions taken to alleviate the line overload are more effective. Furthermore, the load shedding effort is smaller: only 230 MW, distributed over four control steps, suffice to solve the problem. There is no load shedding in the first control step as the corresponding control actions were smaller than 1 MW and, hence, were discarded.

6.3.3 Summary and discussion

Experimental evidence has been provided that the proposed MPC-based protection scheme acts properly when the system is subject to line overloads only, see for instance Fig. 6.16. Line tripping is avoided as intended.

When dealing with disturbances that result in both voltage and thermal problems, the action of the proposed scheme is successful:

- if the load restoration process is not too pronounced, see Fig. 6.17 relative to D5, or
- if the actions are taken fast enough after the disturbance, i.e. before the load restoration process driven by LTCs starts acting. This can be seen in Fig. 6.18 relative to D6, where the protection scheme succeeds to clear the overload problem before LTCs act. Later on, when the line gets overloaded again, all control steps are necessary to counteract the load restoration process and to alleviate the line overload.

In all cases the closed-loop feature of MPC helped the controller to adjust or even stop its actions. Furthermore, let us recall that all tests were performed in the presence of fixed-delay protections, leaving the controller no more than 5 steps to perform its task. Hence, there was no chance to take benefit from an increasing overload duration when the current decreases. The benefit of such a situation, however, can be foreseen in the case of disturbance D6, where the tolerated overload duration is prolonged after the line current is temporarily brought below its limit by the initial control actions.

In order to ensure dependability of the proposed SPS, the load restoration process should be taken into account. There are at least two methods to do this.

The first method would consists of accounting for the load restoration mechanism into the system model used by the MPC algorithm. For example, LTC actions could be modeled through equations of the type (5.23) involving transformer ratios. This better anticipation capability would hopefully lead to reinforcing control actions. The main drawback of this approach,

however, is a significant increase in size of the optimization problem, which may result in prohibitive computing times.

Since load power restoration is the most typical mechanism leading to voltage instability, a second approach consists in combining the action of the overload alleviation controller with a another protection scheme dealing with voltage instability. The latter method was already used when resorting to tap changer blocking, see Fig. 6.19.b relative to D7. The technique is considered in more detail in the next section, where distributed undervoltage load shedding scheme is combined.

Last but not least, the simple methods presented in Section 5.5.6 to compensate for modelling inaccuracies could be also used. In the present case, the non modeled components such as LTCs and secondary voltage control can be considered as inaccuracies of the model used by the MPC algorithm, causing a difference between measured and predicted values of the line current. The correction proposed in Section 5.5.6 can be used to compensate for such discrepancies. This technique being rather simple, we preferred to concentrate on the tests reported in the next section.

6.4 Distributed undervoltage and centralized thermal overload protections acting together

The response of the two proposed SPS acting together was tested following disturbances D6 and D7, which were not properly dealt with by any of the two SPS acting individually. Let us recall that the distributed undervoltage load shedding scheme succeeds solving the voltage problem in both cases (see Fig. 6.13) but does not properly deal with the line tripping in the sense that unacceptable (C,K) combinations have to be chosen to save the system (see Fig. 6.14). On the other hand, the centralized overload protection scheme correctly addresses the line overload problem but its actions are counteracted by the load restoration mechanism from which the voltage problem originates.

Figure 6.20 relates to disturbance D6 and presents the time evolution of the overloaded line current and the lowest monitored bus voltage. The actions of the distributed undervoltage and the centralized overload load shedding schemes are depicted by a circle and squares, respectively. For both SPS the settings determined and/or chosen in the previous tests have been reused.

As can be seen, just after the disturbance, the voltage sharply drops below the V^{th} threshold and shortly after, the line current also exceeds its limits. However, the line overload does not have time to be acknowledged by the centralized controller since at t = 21 s the undervoltage SPS time integral (4.2) reaches the C value, which triggers the shedding of 73 MW. This results in both voltage recovery and line relief.

Nevertheless, some 50 s later, the line current oversteps its limit again. This time, the overload is detected by the centralized protection which manages to alleviate the overload in two control

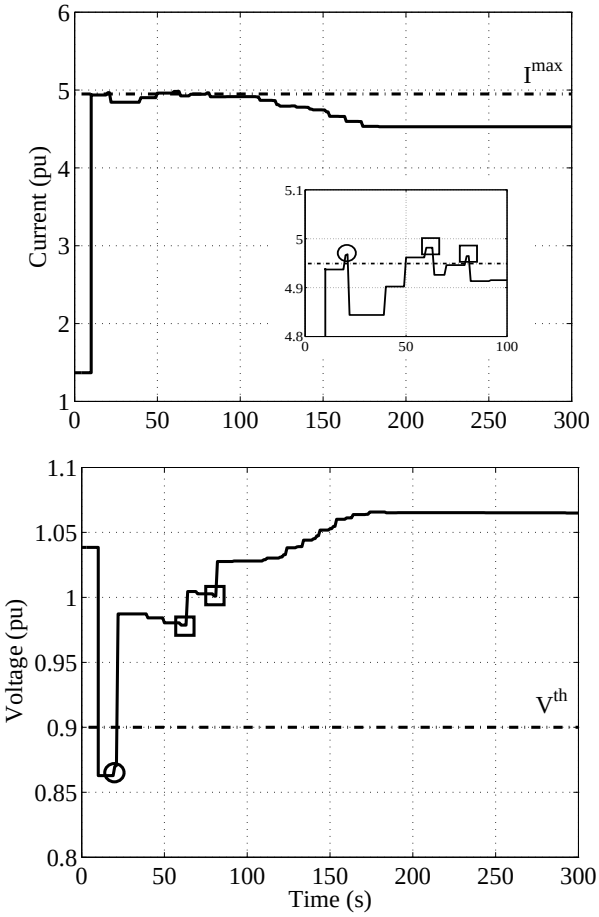

Figure 6.20: Evolution of line current and lowest transmission voltage, with both protection schemes in operation (disturbance D6)

steps, each involving 20 MW shedding. When the centralized protection was acting alone, its actions were almost immediately counteracted by the load restoration (see Fig. 6.18). This effect is much less pronounced in the present simulation; most likely this is attributable to the initial load shedding action, which has somewhat attenuated the effects of the subsequent load restoration.

After the first load shedding aimed at alleviating the line overload, the current shortly comes back below its limit, but the controller is not reset since at the next sampling time, the newly collected measurement reveals that the line is again overloaded.

The combined action of the two SPS not only succeeds saving the system, but also leads to a smaller load shedding: 73+20+20 = 113 MW to be compared with the 140 MW shed by the centralized thermal overload protection acting alone (see Section 6.3.2).

We finally consider the case of disturbance D7, with the system evolution shown in Fig. 6.21. The voltage does not drop below V^{th} under the effect of the disturbance (as in the previous case) but under the more progressive effect of load restoration. Soon after, the line current exceeds its limits, which is detected by the centralized controller at t = 90 s. However, the

response time of some undervoltage load shedding controllers being smaller than the sampling time of the overload alleviation controller, the former act in the first place. This allows the voltage to recover above V^{th} and the line current to fall below its limit. As for disturbance D6, the load shedding action slows down the subsequent load restoration process.

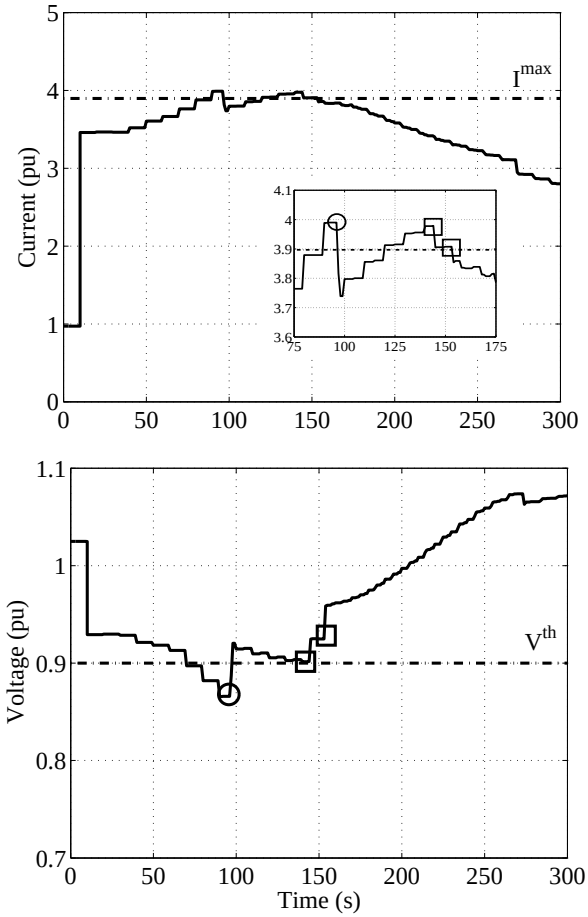

Figure 6.21: Evolution of line current and lowest transmission voltage, with both protection schemes in operation (disturbance D7)

Nevertheless, the line current is slowly increasing and again exceeds its limits. At this time the voltage is above V^{th}. The overload alleviation controller initiates its sequence of actions and succeeds to reduce the current in three control steps. In fact, the first control action was smaller than 1 MW and hence was discarded. The next two actions, noticeable in the figure, are sufficient to solve the problem well before the T_{ol} delay is elapsed.

Once again, less load is interrupted when the two SPS act together: 170 MW to be compared to the 230 MW shed without success by the overload alleviation controller acting alone.

These results indicate that the combination of the two SPS make up a dependable protection properly addressing both voltage and thermal overload problems.

Chapter 7

Conclusion

7.1 Main contributions of the thesis

System Protection Schemes (SPS) offer a cost effective way of protecting a power system against disturbances for which preventive actions are too expensive, especially under the pressure of the electricity market. They are also needed to face unpredictable disturbances whose severity goes beyond what is usually considered in planning. SPS are likely to play a larger and larger role in making power system operation more reliable. Hence, there is a need to improve the existing SPS logic and/or design new schemes.

In spite of technological advances in wide-area measurements, communication and computation means, distributed SPS are likely to remain the preferred choice of planners, due to their higher simplicity and hence reliability. However, for some problems a system-wide view is essential in order to take the most suitable actions.

The work reported in this thesis goes along these two directions. On one hand, we show that voltage instability can be counteracted in a very distributed manner. On the other hand, for thermal overload alleviation, we propose a centralized controller relying on a real-time model of the system.

In order to tune and validate an SPS, there is a need to envisage wide sets of situations that it could face. Instead of considering arbitrary combinations of events, for which there is in any case a combinatorial explosion of possible scenarios, it is desirable to identify plausible sequences of cascading outages. In this respect, we devised a practical event-tree based algorithm which takes into account protection hidden failures as well as the system response to the initial fault and subsequent failures. For instance, we handle as deterministic events the automatic trip of overloaded lines and limited generators experiencing low voltages. On the other hand, we handle as low-probability hidden failures the trip of lines approaching their thermal ratings as well as generators approaching or reaching their field current limits. To reproduce the time sequence of events, we use Quasi Steady-State time simulation. Furthermore, in order

to discard harmless sequences, we use a fast linear approximation based filtering method.

The algorithm was tested on a detailed model of the Western region of the RTE system. The identified cascading events show different failure modes: purely voltage unstable, purely thermal cascading and interesting combinations of both. These scenarios were used to test and validate the proposed SPS.

To deal with long-term voltage instability we have proposed an undervoltage load shedding scheme having the following characteristics:

- *distributed structure*. Load shedding controllers are installed in areas where voltage instability effects are felt most strongly. The shedding decision is taken locally, each controller monitoring one (or several) transmission voltages and controlling a group of loads;
- *response-based*. The load shedding action relies on voltage measurements which reflect the disturbance impact and the actions taken so far by the SPS and by other controllers acting on the system;
- *rule-based*. Each controller acts when its monitored voltage falls below some threshold for some time. A simple integral-based rule adjusts the delay between successive sheddings and the amount of power cut according the voltage evolution;
- *closed-loop operation*. The controller is able to activate a load shedding rule several times, based on the measured result of the previous activations.

Our tests on the small Nordic32 test system as well as on the real-life system have clearly demonstrated that the above features yield the following advantages:

- the response-based and closed-loop operation allow to adjust to the severity of the situation, even if the latter was not considered in the design phase;
- the distributed structure allows to adjust to the disturbance location;
- it also provides higher reliability: the failure of one controller will not directly or detrimentally affect the operation of the whole protection scheme;
- the closed-loop operation also makes the SPS robust with respect to unexpected load behaviors or controller failures.

These properties are obtained without information exchange between controllers, the latter being implicitly coordinated through network voltages. The fact that there is no need for dedicated communication between controllers and that no system model is required by the controllers make the protection scheme definitely simpler and hence more reliable. As mentioned before, another source of power system failure is cascade tripping of overloaded transmission lines. To stop these cascading effects, we have proposed a centralized overload alleviation

SPS. This protection scheme acts to reduce the currents below their admissible values before the overloaded lines are tripped. The algorithm is inspired by Model Predictive Control (MPC). It also operates in closed loop in the sense that, at each time step new measurements are used to update a multi-step optimization problem, and hence cope with the new prevailing conditions. This closed-loop nature of MPC guarantees some robustness with respect to modeling errors and measurement noises.

The proposed scheme has been extensively tested on a small 5-bus academic system where various control actions were included in the objective function with different priorities, and various objectives were considered. The proposed scheme was also tested on the above mentioned real-life system; a quadratic control objective was considered and control actions focused again on load shedding.

Our tests have confirmed that the controller may take more time than expected to remove the overload, due to either modeling inaccuracies or other controls/processes acting on the system. This may become critical in situations where the time to clear the overload is fixed, which was the case in almost all our tests. Definitely, the proposed scheme would prove more powerful if the control horizon could be updated in the course of applying the actions. Then, as transmission lines get relieved, more time is left to act, i.e., more control steps become available.

However, failure to alleviate the line overloads in the allotted time can be compensated by reducing, statically or dynamically, the limits assigned to overloaded lines in the optimization problem. This simple method was tested with success on the small system.

When facing a pure voltage (resp. thermal) problem, the undervoltage (resp. thermal alleviation) load shedding scheme was able to complete its task. However, the same did not hold true when dealing with situations where the other problem was either influencing or dominating system evolution. This was to be expected since those situations are beyond the capabilities of individual SPS.

A solution to this problem was to couple the two proposed SPS. Tests performed in the combined thermal-voltage scenarios previously identified on the RTE system have shown that the two SPS acting together succeeded to save the system. Moreover, the amount of load shedding was smaller than when the controllers were left to act alone.

7.2 Directions for future work

The following is a non exhaustive list of possible extensions to the present work.

Cascading event identification

- *modeling refinements*. A more accurate dynamic model is obviously welcome, at the expense, however, of significantly higher computing times. This model would, for instance, allow to check the evolution of frequency and voltages inside islands after a network split. Another improvement would be to better incorporate protections into the system model;
- *probabilistic aspects*. The probability of event sequences could be computed with better accuracy, provided reliable statistical data are available about faults, failures, etc.
- *severity measures*. A welcome outcome of the cascading scenario identification software would be to assess the impact of system failures in terms of unserved energy, restoration times, etc. There are basically two approaches: (i) evaluate the spread of the uncontrolled blackout, or (ii) determine the amount of emergency actions, such as load shedding, needed to contain the blackout. In the second approach, one could monitor the actions taken by the proposed SPS assumed in operation.

Undervoltage load shedding against voltage instability

- *clustering*. Investigation towards "optimal" positioning of monitored buses and clustering of loads may be of interest. One may think of implementing the SPS at a lower level of granularity, such as having one controller per load station;
- *implementation costs*. To minimize investment cost it may be interesting to reduce the number of installed controllers, while keeping reliability at a satisfactory level;
- *protection tuning*. In practice the protection should be tuned over a large set of scenarios. Some concepts of multi-objective optimization could be used to determine the best (C,K) combination;
- *introducing communication between controllers*. As discussed in Chapter 6 one may also think of collecting all voltage measurements at a central point, running the computations in a single processor, and sending back load shedding orders. In this case, additional information exchanges and interactions between controllers may be envisaged without further penalizing the scheme;
- *extension to other controls*. Tap changer blocking is another well-known emergency control that allows to reduce load power without interrupting it. To minimize impact on customers it would be advantageous to also implement tap changer blocking in a distributed manner, with load shedding as a second line of defense for system security;

- *additional input signals* such as generator reactive reserves may be needed in the presence of fast restoring loads. Using signals from a remote generator requires communication. This is maybe where distributed control would meet its limits...
- *short-term voltage instability* caused by induction motors stalling requires a prompt reaction. A distributed load shedding scheme would also prove useful in this respect.

Emergency control of thermal overloads

- *improvement of system model* used in the MPC-based algorithm. It is desirable to upgrade the model from a mere sensitivity representation to a model incorporating the actions of other controllers present in the system, especially if they have a detrimental effect. However, the expected gain in robustness should be carefully assessed with respect to the associated increase in computational effort;
- *receding control horizon*. As already mentioned the proposed scheme would show its effectiveness if the control horizon could be updated in the course of applying the actions.

Last word

Clearly, before implementing the proposed SPS, various important aspects have to be considered, such as validation with detailed time simulation, provision for measurement noise filtering, grossly erroneous measurement rejection, etc.

Appendix A

Fast contingency filtering using linear estimates of phase angle and voltage magnitude changes

A.1 Motivation

Disturbance filtering is an essential step of power system security analysis, needed to discard the numerous disturbances with little impact on the system, which would slow down the analysis. This step is even more needed in real-time applications, when numerous (e.g. N-2) disturbances are involved, or when time simulations are used to assess the system response.

For disturbance analysis purposes, the emphasis is on voltage drops at transmission buses. A simple filtering technique consists of computing the (linear approximation of) voltage changes $\Delta\mathbf{v}$ for each disturbance, and checking either the post-disturbance voltages:

$$V_i^o + \Delta V_i \overset{?}{<} V^{min} \qquad i = 1, \ldots, N$$

or the changes themselves:

$$\Delta V_i \overset{?}{<} -\delta_V \quad \Leftrightarrow \quad |\Delta V_i| \overset{?}{>} \delta_V \qquad i = 1, \ldots, N$$

where V_i^o is the base case voltage at the i-th bus, ΔV_i is the corresponding component of $\Delta\mathbf{v}$ and δ_V is a positive threshold.

Clearly, the first test is more related to the "quality" of post-disturbance voltages. When dealing with voltage stability the second test is more appropriate. Indeed, some voltages may be already low in the base case without a risk of voltage instability, in which case the first test leads to false alarms.

Expectedly, δ_V has to be chosen carefully to reach a compromise between false alarms and non identification of harmful contingencies.

In the development of the event tree the filtering is used in order to classify the cascading scenarios into harmless and potentially harmful. This classification is needed in order to reduce the number of scenarios analyzed with QSS time simulation and to stop the event tree expansion.

A.2 Previous work

A great part of publications on contingency filtering date back to the 80's. At that time the emphasis was on contingency analysis within the context of static security, the objective being to cut down the computational effort of repeated load flow computations without losing accuracy.

In [EW79, ILS79], the DC load flow was used to compute performance indices in order to rank contingencies with respect to their impact on the system. While the DC approximation is often appropriate for identifying branch overloads, more refined methods are needed to deal with voltage magnitudes.

To this purpose, linear approximations of the AC load flow equations were considered in a simple contingency filtering technique which consists of performing a single P-θ followed by a single Q-V iteration of the fast decoupled load flow [ABH82]. In [EMW88], the Q-V iteration was replaced with a fast Q-V iteration, solved only for a subset of voltage sensitive buses, determined with a method inspired of the concentric relaxation [ZWP80]. A direct ranking method for voltage contingency selection was proposed in [CB89], using a second-order performance index which can be computed without determining post-contingency bus voltages.

Experience has shown that contingency ranking is heavily dependent on the performance index used. In particular, it may be prone to masking problems, such as ranking a contingency causing many small limit violations equally with one leading to few large limit violations. To reduce masking problems, it may be required to choose appropriate weighting factors in the index [EMW88].

In the meantime, the computational power has increased dramatically, and dynamic security assessment can now be envisaged in real-time [Tay00, VCK05]. In this context, the objective of contingency filtering has somewhat shifted to reducing the computational effort of repeated time domain simulations.

The proposed method uses linear voltage drop estimates, computed with the so-called CRIC[1] technique initially proposed by Carpentier in [Car86], for filtering purposes. With this method the linearized changes are obtained with high computational efficiency and with acceptable loss in accuracy.

The rationale behind the method presented is as follows:

- in (not all but) many practical cases, a post-contingency load flow allow to identify

[1] CRIC stands for "Calcul des Réseaux Implicitement Couplés" (Computation of Implicitly Coupled Networks)

contingencies with significant impact on long-term voltage stability. Indeed, load flow equations with constant power loads and enforcement of generator reactive power limits correspond to the long-term equilibrium that prevails after load voltages have been restored by LTCs and machine rotor (or stator) currents have been limited. Insofar as voltage instability results from the loss of such an equilibrium, the corresponding load flow equations no longer have a solution and the Newton-Raphson iterations diverge;

- on the other hand, divergence may result from purely numerical results. Furthermore, some dynamic controls helping stability cannot be taken into account in the static load flow calculation. Conversely, instability may result from a dynamic behavior that cannot either be accounted. To compensate for these limitations, when using a load flow computation, *it is appropriate to label potentially harmful those contingencies causing some voltages to drop by more than some value*, in addition to those causing divergence;

- to this purpose, accurate post-contingency voltages need not be computed; estimates obtained from the already mentioned linearized load flow equations may be appropriate to filter out the harmless contingencies. To the authors' knowledge, however, few publications report on the performance of these simple linear methods in the context of voltage stability studies where voltages may experience large drops.

A.3 Brief review of linear methods

Let the traditional power flow equations be written in compact form as:

$$\begin{aligned} \mathbf{p}^o - \mathbf{f}^o(\mathbf{v}^o, \boldsymbol{\theta}^o) &= \mathbf{0} \\ \mathbf{q}^o - \mathbf{g}^o(\mathbf{v}^o, \boldsymbol{\theta}^o) &= \mathbf{0} \end{aligned}$$

where $\mathbf{p}^o$ and $\mathbf{q}^o$ are the active and reactive power injections, $\mathbf{f}^o$ and $\mathbf{g}^o$ are well-known functions, and upperscript ^{o} refers to the base case situation. Let the corresponding post-contingency equations be written as:

$$\mathbf{p} - \mathbf{f}(\mathbf{v}, \boldsymbol{\theta}) = \mathbf{0} \tag{A.1}$$

$$\mathbf{q} - \mathbf{g}(\mathbf{v}, \boldsymbol{\theta}) = \mathbf{0} \tag{A.2}$$

where $\mathbf{p}$ and $\mathbf{q}$ account for generator trippings and $\mathbf{f}$ and $\mathbf{g}$ for branch trippings. We seek to obtain a good estimate $\Delta\boldsymbol{\theta}$ (resp. $\Delta\mathbf{v}$) of the exact change in phase angles $\boldsymbol{\theta} - \boldsymbol{\theta}^o$ (resp. voltage magnitudes $\mathbf{v} - \mathbf{v}^o$).

A simple approach consists of relying on a Taylor series expansion of $\mathbf{f}$ and $\mathbf{g}$ around $(\mathbf{v}^o, \boldsymbol{\theta}^o)$:

$$\mathbf{p} - \mathbf{f}(\mathbf{v}^o, \boldsymbol{\theta}^o) - \mathbf{f}_\theta \, \Delta\boldsymbol{\theta} - \mathbf{f}_v \, \Delta\mathbf{v} = \mathbf{0} \tag{A.3}$$

$$\mathbf{q} - \mathbf{g}(\mathbf{v}^o, \boldsymbol{\theta}^o) - \mathbf{g}_\theta \, \Delta\boldsymbol{\theta} - \mathbf{g}_v \, \Delta\mathbf{v} = \mathbf{0} \tag{A.4}$$

where $\mathbf{f}_\theta$ denotes the Jacobian matrix of $\mathbf{f}$ with respect to $\boldsymbol{\theta}$, and similarly for the other matrices.

Equations (A.3, A.4) are nothing but the first iteration of the Newton-Raphson algorithm initialized from $(\mathbf{v}^o, \boldsymbol{\theta}^o)$. To gain computing time, it has been proposed to estimate $\Delta\mathbf{v}$ and $\Delta\boldsymbol{\theta}$ from the first two half-iterations of the fast decoupled version of this algorithm. Namely, in the first half-iteration, the term $\mathbf{f}_v\ \Delta\mathbf{v}$ is neglected (usual DC approximation). Simplifying and reorganizing (A.3) yields:

$$\mathbf{f}_\theta\ \Delta\boldsymbol{\theta} = \mathbf{p} - \mathbf{f}(\mathbf{v}^o, \boldsymbol{\theta}^o) \tag{A.5}$$

This linear system is solved with respect to $\Delta\boldsymbol{\theta}$ and the phase angles are updated accordingly:

$$\boldsymbol{\theta}^1 = \boldsymbol{\theta}^o + \Delta\boldsymbol{\theta} \tag{A.6}$$

In the second half-iteration, the term $\mathbf{g}_\theta\ \Delta\boldsymbol{\theta}$ is neglected, while the updated phase angles (A.6) are used. Thus, Eq. (A.4) is modified into:

$$\mathbf{g}_v\ \Delta\mathbf{v} = \mathbf{q} - \mathbf{g}(\mathbf{v}^o, \boldsymbol{\theta}^1) \tag{A.7}$$

which is solved to obtain $\Delta\mathbf{v}$.

While experience has shown that it is acceptable to neglect $\mathbf{f}_v\ \Delta\mathbf{v}$ in (A.3), neglecting $\mathbf{g}_\theta\ \Delta\boldsymbol{\theta}$ in (A.4) may be questionable, especially in the stressed system conditions considered in voltage stability studies, or in lower voltage networks where the decoupling assumption does not apply very well (low X/R ratios).

It has been further proposed to use constant $\mathbf{f}_\theta$ and $\mathbf{g}_v$ matrices, computed for $\mathbf{v} = \mathbf{1}$ pu and $\boldsymbol{\theta} = \mathbf{0}$ [ABH82]. This approximation is valid as long as phase angle differences remain small and voltages close to 1 pu, which is even more questionable in voltage stability studies.

A.4 The CRIC method

The CRIC method [Car86] is able to provide estimates of the voltage variations that are more accurate than those based on the linearization of the full load flow equations (A.3, A.4), while retaining the computational efficiency of the fast decoupled method.

As indicated above, reliable estimates of the phase angles are obtained from (A.5) and the CRIC method also relies on this simplification to obtain the updated phase angles (A.6).

While the fast decoupled approach keeps the phase angles constant when evaluating $\Delta\mathbf{v}$, on the contrary, the CRIC method *keeps the active power injections constant at the value obtained after updating the phase angles*, i.e. $\mathbf{f}(\mathbf{v}^o, \boldsymbol{\theta}^1)$. This way of doing matches more closely the original set of equations (A.1, A.2).

Thus, the equations to be solved are:

$$\mathbf{f}(\mathbf{v}^o, \boldsymbol{\theta}^1) - \mathbf{f}(\mathbf{v}, \boldsymbol{\theta}) = \mathbf{0} \tag{A.8}$$

$$\mathbf{q} - \mathbf{g}(\mathbf{v}, \boldsymbol{\theta}) = \mathbf{0} \tag{A.9}$$

Replacing the second term in (A.8) by its Taylor series expansion around $(\mathbf{v}^o, \boldsymbol{\theta}^1)$ yields:

$$\mathbf{f}(\mathbf{v}^o, \boldsymbol{\theta}^1) - \mathbf{f}(\mathbf{v}^o, \boldsymbol{\theta}^1) - \mathbf{f}_\theta \, \Delta\boldsymbol{\theta} - \mathbf{f}_v \, \Delta\mathbf{v} = \mathbf{0}$$

or:

$$\mathbf{f}_\theta \, \Delta\boldsymbol{\theta} + \mathbf{f}_v \, \Delta\mathbf{v} = \mathbf{0} \tag{A.10}$$

Similarly, Eq. (A.9) can be expanded into:

$$\mathbf{q} - \mathbf{g}(\mathbf{v}^o, \boldsymbol{\theta}^1) - \mathbf{g}_\theta \, \Delta\boldsymbol{\theta} - \mathbf{g}_v \, \Delta\mathbf{v} = \mathbf{0}$$

or

$$\mathbf{g}_\theta \, \Delta\boldsymbol{\theta} + \mathbf{g}_v \, \Delta\mathbf{v} = \mathbf{q} - \mathbf{g}(\mathbf{v}^o, \boldsymbol{\theta}^1) \tag{A.11}$$

in which the updated phase angles $\boldsymbol{\theta}^1$ are used to compute the Jacobian matrices and the right-hand side of (A.11).

Solving (A.10) for $\Delta\boldsymbol{\theta}$ and replacing in (A.11) one obtains:

$$\underbrace{\left[\mathbf{g}_v - \mathbf{g}_\theta \, \mathbf{f}_\theta^{-1} \, \mathbf{f}_v\right]}_{\mathbf{J}_{qv}} \Delta\mathbf{v} = \mathbf{q} - \mathbf{g}(\mathbf{v}^o, \boldsymbol{\theta}^1) \tag{A.12}$$

The matrix $\mathbf{J}_{qv}$ is well-known in voltage stability analysis [GMK92]. This matrix, however, is not sparse. To preserve sparsity, one possibility is to solve the unreduced system (A.10, A.11), which is larger but sparse.

Instead, the second idea underlying the CRIC method consists in *computing a good sparse approximation of* $\mathbf{J}_{qv}$. To this purpose, it is assumed that *active power flows in branches are constant rather than active power injections at buses*.

The active power flow in the $i-j$ branch can be written symbolically as:

$$P_{ij} = f(V_i, V_j, \theta_i - \theta_j) \tag{A.13}$$

where $V_i\angle\theta_i$ (resp. $V_j\angle\theta_j$) is the voltage at bus i (resp. j). The phase difference can be obtained from (A.13):

$$\theta_i - \theta_j = \varphi(V_i, V_j, P_{ij})$$

and replaced into the corresponding reactive power flow equation, which takes on the form:

$$Q_{ij} = g(V_i, V_j, \theta_i - \theta_j) = g(V_i, V_j, \varphi(V_i, V_j, P_{ij})) \tag{A.14}$$

P_{ij} being a fixed parameter, (A.14) involves voltage magnitudes only, and can be rewritten formally as:

$$Q_{ij} = \tilde{g}(V_i, V_j, P_{ij}) \tag{A.15}$$

The reactive power injection at bus i is given by:

$$Q_i = Q_{si} + \sum Q_{ij} = Q_{si} + \sum \tilde{g}(V_i, V_j, P_{ij}) \tag{A.16}$$

where Q_{si} accounts for shunt compensation and the sums extend over all branches incident to bus i. Hence, the Jacobian matrix defined by:

$$\left[\tilde{\mathbf{J}}_{qv}\right]_{ij} = \frac{\partial Q_i}{\partial V_i} \qquad i,j = 1,\ldots,n \tag{A.17}$$

has the same sparse structure as the $\mathbf{g}_v$ matrix in (A.7).

To summarize, the method consists of solving (A.5) with respect to $\Delta\boldsymbol{\theta}$, updating $\boldsymbol{\theta}$ according to (A.6), and solving

$$\tilde{\mathbf{J}}_{qv}\ \Delta\mathbf{v} = \mathbf{q} - \mathbf{g}(\mathbf{v}^o, \boldsymbol{\theta}^1) \tag{A.18}$$

with respect to $\Delta\mathbf{v}$.

The generator reactive power limits are checked and if some of them are exceeded, the status of the buses are changed as usual and Eqs. (A.5, A.18) are solved again.

A.5 Accuracy with respect to full load flow

The method has been extensively tested, for filtering purposes in both disturbance analysis and security margin determination, on the real-life system detailed in Chapter 3 and full results were reported in [OVC05].

The accuracy of the proposed linearized method has been checked with respect to a full AC load flow, by comparing the voltage magnitudes computed by both methods on a set of 180 single and double disturbances. The full load flow converges for all of them.

For instance, Fig. A.1 compares the voltage drops provided by both approaches, for a mild and a severe disturbance, respectively. Expectedly, the discrepancies between both approaches increase with the severity of the disturbance. However, the accuracy of the proposed method is quite satisfactory. In any case, it is good enough for filtering purposes in voltage security assessment. It can even be a substitute to full load flow in static security analysis [Car86].

For the most severe disturbance, Fig. A.2 shows the voltage drops sorted by increasing order of magnitude. The error introduced by the linear approximation decreases with the magnitude of the voltage drop itself. In fact, the relative error on the voltage drop is rather constant from one bus to another.

As recalled in Section A.2, severe disturbances may lead to divergence of the Newton-Raphson iterations. This does not occur with the proposed method, which is non iterative. Instead, large voltage drops ΔV_i are expected. As an illustration, Fig. A.3 shows the voltage drops obtained for such a severe disturbance. Several buses exhibit a large voltage drop, i.e. 0.3 pu, thereby clearly identifying this disturbance as potentially dangerous.

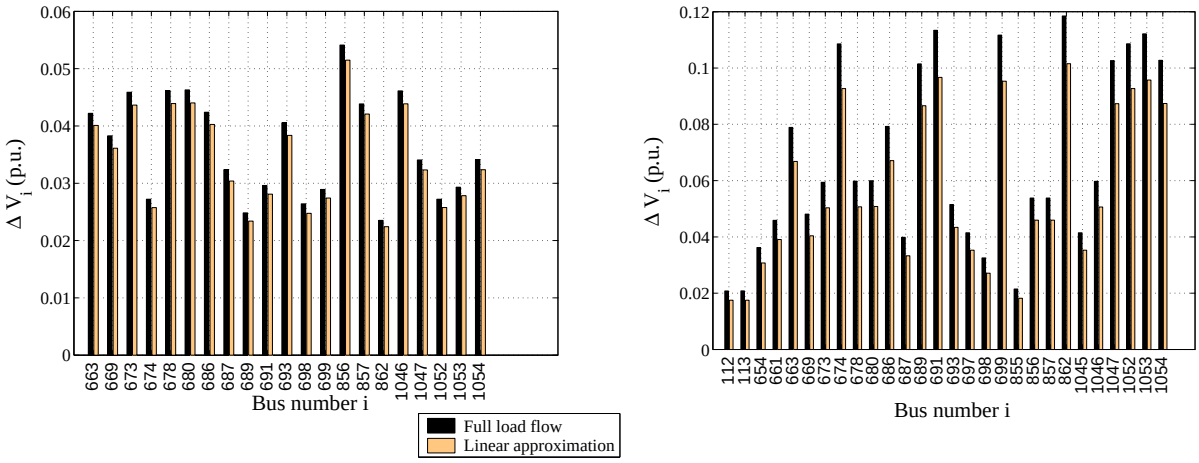

Figure A.1: Largest voltage drops for a mild (left part) and a severe (right part) contingency

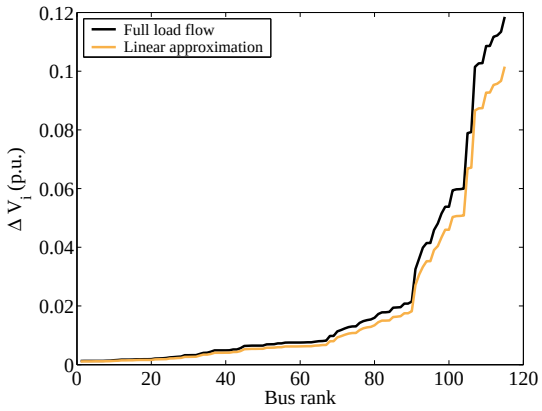

Figure A.2: Sorted voltage drops provided by full load flow and the linear approximation

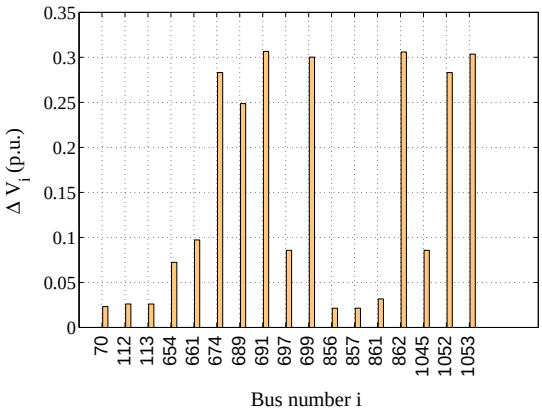

Figure A.3: Linear voltage drop estimates for a severe N-2 contingency

A.6 Voltage drop threshold determination

The threshold δ_V used for filtering purposes has been chosen as follows. QSS simulations have been run to identify the unacceptable contingencies of a large set of 16,000 double dis-

turbances[2]. Then the linear voltage drop estimates have been computed at all buses for all contingencies. δ_V should be as large possible to minimize the number of false alarms, but small enough to have all unacceptable contingencies correctly identified. Based on the above set of results, a value $\delta_V = 0.09$ pu was found to be a good compromise.

The filtering results obtained on the set of 16,000 disturbances are summarized in Table A.1. As can be seen, many harmless disturbances are eliminated. The proposed method leads to 34-11 = 23 false alarms, i.e. slightly less than the full load flow (39-11=28) because the same threshold δ_V has been taken for both methods and the linearly estimated voltage drops are a little smaller, as shown by Fig. A.1. All the dangerous disturbances are correctly included in the "potentially dangerous" set.

Table A.1: Filtering performances

Total Nb. of contingencies	16,000	
Analysis by QSS simulation	11 dangerous	15,989 harmless
Filtering by full load flow	39 potentially dangerous	15,961 harmless
Filtering by proposed method	34 potentially dangerous	15,966 harmless

Same threshold value has been found appropriate to classify the cascading outages into harmless and potentially harmful.

[2]Two single disturbances, randomly chosen, are applied at the same time

Bibliography

[AA82] R.N. Allan and A.N. Adraktas. Terminal effects and protection system failures in composite system reliability evaluation. *IEEE Transactions on Power Apparatus and Systems*, PAS-101, Dec. 1982.

[AAH97] S. Arnborg, G. Andersson, D.J. Hill, and I.A. Hiskens. On undervoltage load shedding in power systems. *Internation Journal of Electrical Power and Energy Systems*, 19:141–149, 1997.

[ABH82] F. Albuyeh, A. Bose, and B. Heath. Reactive power considerations in automatic contingency selection. *IEEE Transactions on Power Apparatus and Systems*, PAS-101:107–112, Jan. 1982.

[ABP90] O. Alsac, J. Bright, M. Prais, and B. Stott. Further developments in lp-based optimal power flow. *IEEE Transactions on Power Systems*, 3:697–711, Aug. 1990.

[ARH03] N. Atic, D. Rerkpreedapong, A. Hasanovic, and A. Feliachi. Nerc compliant decentralized load frequency control design using model predictive control. In *Proc. IEEE Power Engineering Society General Meeting*, volume 2, 2003.

[AS74] O. Alsac and B. Stott. Optimal power flow with steady-state security. *IEEE Transaction on Power Apparatus and Systems*, 93:745–751, 1974.

[AS03] C.A. Aumuller and T.K. Saha. Determination of power system coherent bus groups by novel sensitivity-based method for voltage stability assessment. *IEEE Transactions on Power Systems*, 18:11571164, 2003.

[BB83] W.Z. Black and W.R. Byrd. Real-time ampacity model for overhead lines. *IEEE Transactions on Power Systems*, 102:2289–2293, July 1983.

[BDD99] K.R.W. Bell, A.R. Daniels, and R.W. Dunn. Alleviation of transmission system overloads using fuzzy reasoning. *Journal of Fuzzy Sets and Systems, Elsevier*, 102:41–52, 1999.

[BK97] R. Baldick and E. Kahn. Contract paths, phase-shifters, and efficient electricity trade. *IEEE Transactions on Power Systems*, 12:749–755, May 1997.

[BM81] R. Billinton and T.K.P. Medicherla. Station originated multiple outages in the reliability analysis of a composite generation and transmission system. *IEEE Transactions on Power Apparatus and Systems*, PAS-100, Aug. 1981.

[BM03] M. Begovic and B. Milosevic. Voltage stability protection and control using a wide-area network of phasor measurements. *IEEE Transactions on Power Systems*, 18:121–126, 2003.

[BPA98] R. Balanathan, N.C. Pahalawaththa, U.D. Annakkage, and P.W. Sharp. Undervoltage load shedding to avoid voltage instability. In *IEE Proceedings - Generation, Transmission and Distribution*, volume 145, pages 175–181, March 1998.

[Bro88] H.E. Brown. Alleviating line overload by line switching. *IEEE Computer Application in Power*, 1:30–33, 1988.

[BVN99] M. Begovic, K. Vu, D. Novosel, and M.M. Saha. Use of local measurements to estimate voltage-stability margin. *IEEE Transactions on Power Systems*, 14:1029–1035, Aug. 1999.

[Cal84] M. S. Calovic. Modeling and analysis of under-load tap-changing transformer control systems. *IEEE Transaction on Power Apparatus and Systems*, 103:1909–1915, July 1984.

[Cap04] F. Capitanescu. *Preventive assessment and enhancement of power system voltage stability an integrated approach of thermal and voltage security*. PhD thesis, University of Liège, Belgium, 2004.

[Car86] J.L. Carpentier. Cric, a new active reactive decoupling process in load flows, optimal power flows and system control. In *Proc. of the IFAC Conference on Power Systems and Power Plant Control*, pages 65–70, Beijing, 12-15 Aug. 1986.

[CB89] Y. Chen and A. Bose. Direct ranking for voltage contingency selection. *IEEE Transactions on Power Systems*, 4:1335–1344, Oct. 1989.

[CBC02] S.K. Chan, V. Brandwajn, A.I. Cohen, M. Marwali, R. Gonzales, J. Jia, and A. Hargrave. Phase shifter optimization in security constrained scheduling applications. In *Proc. IEEE Power Engineering Society Winter Meeting*, pages 1278–1283, 2002.

[CBJ02] S.L. Chen, W.Z. Black, and H.W. Loard Jr. High-temperature ampacity model for overhead conductors. *IEEE Transactions on Power Delivery*, 17:1136 – 1141, Oct. 2002.

[CCM96] F. Carbone, G. Castelano, and G. Moreschini. Coordination and control of tap changers under load at different voltage level transformers. In *Proc. Melecon '96 Conference*, Bari (Italy), 1996.

[CGE07] F. Capitanescu, M. Glavic, D. Ernst, and L. Wehenkel. Interior-point based algorithms for the solution of optimal power flow problems. *Electric Power System Research*, 77:508–517, 2007.

[Che04] Q. Chen. *The probability, identification and prevention of rare events in power systems*. PhD thesis, Iowa State University, Ames, Iowa, 2004.

[CM04] Q. Chen and J.D. McCalley. A cluster distribution as a model for estimating high-order event probabilities in power systems. In *Proceedings of the International Conference on Probabilistic Methods Applied to Power Systems*, pages 622 – 628, 12-16 Sept. 2004.

[CM05] Q. Chen and J.D. McCalley. Indentifying high risk n-k contingencies for on-line security assessment. *IEEE Transactions on Power Systems*, 20:823–834, May 2005.

[COL08] F. Capitanescu, B. Otomega, H. Lefebvre, V. Sermanson, and T. Van Cutsem. Prospects of an improved system protection scheme against voltage instability in the rte system. In *Paper submitted to 16th Power Systems Computation Conference (PSCC)*, Glasgow, Scotland, July 14-18, 2008.

[CR03] (editor) C. Rehtanz. *Autonomous Systems and and intelligent agents in power system control and operation*. Springer Verlag, 2003.

[CRB01] C. Canizares, W. Rosehart, A. Berizzi, and C. Bovo. Comparison of voltage security constrained optimal power flow techniques. In *Proc. IEEE Power Engineering Society Summer Meeting*, volume 3, pages 1680–1685, 15-19 July 2001.

[CS79] S.M. Chan and F.C. Schweppe. A generation reallocation and load shedding algorithm. *IEEE Transaction on Power Apparatus and Systems*, 98:26–34, 1979.

[CTD03] J. Chen, J.S. Thorp, and I. Dobson. Cascading dynamics and mitigation assessment in the power system disturbances via hidden failure model. *Journal of Electrical Power and Energy Systems*, 2003.

[CTF01] Final report of CIGRE Task Force 38.02.19. System protection schemes in power networks. Technical report, Nov. 2001. D.H. Karlsson, convener.

[CTF04] IEEE/CIGRE Join Task Force on Stability Terms and Definitions. Definitions and classification of power system stability. *IEEE Transactions on Power Systems*, 19:1387–1401, May 2004.

[CTF07] CIGRE Working Group C4.601. Widea area monitoring and control for transmission capability enhancement. final report. Technical report, January 2007. C. Rehtanz, convener.

[CTF93] Final report of CIGRE Task Force 38.02.10. Modelling of voltage collapse including dynamic phenomena. Technical report, Mar. 1993. C.W. Taylor, editor.

[CTF95] Final report of CIGRE Task Force 38.02.12. Criteria and countermeasures for voltage collapse. Technical report, Apr. 1995. C.W. Taylor, editor.

[CTF98] CIGRE Working Group 38.03.08. Long term dynamics - phase ii. Technical report, Apr. 1998. Final report.

[CVC05] F. Capitanescu and T. Van Cutsem. Unified sensitivity analysis of unstable or low voltages caused by load increases or contingencies. *IEEE Transactions on Power Systems*, 20:321–329, 2005.

[DCN03] I. Dobson, B.A. Carreras, and D.E. Newman. A load-dependent model of probabilistic cascading failure. In *Proceedings of the 36th Annual Hawaii International Conference on System Sciences*, 6-9 Jan. 2003.

[DCN04] I. Dobson, B.A. Carreras, and D.E. Newman. Probabilistic load-dependent cascading failure with limited component interaction. In *Proc. of IEEE International Symposium on Circuits and Systems*, Vancouver, Canada, May 2004.

[DFJ97] J.E. Doran, S. Franklin, N.R. Jennings, and T.J. Norman. On cooperation in multiagent systems. *The Knowledge Engineering Review*, 12:309–314, 1997.

[DH05] A.L. Dimeas and N. Hatziargyriou. Operation of a multiagent system for microgrid control. *IEEE Transactions on Power Systems*, 20:1447–1455, Aug. 2005.

[DKH00] M.J. Damborg, M. Kim, J. Huang, S.S. Venkata, and A.G. Phadke. Adaptive protection as preventive and emergency control. In *Proc. of IEEE Power Engineering Society Summer Meeting*, volume 2, pages 1208–1212, 16-20 July 2000.

[DL03] J.R. Daconti and D.C. Lawry. Increasing power transfer capability of existing transmission lines. *IEEE PES Transmission and Distribution Conference and Exposition*, 3:1004 – 1009, 7-12 Sept. 2003.

[Dob92] I. Dobson. Observations on the geometry of saddle-node bifurcation and voltage collapse in electric power systems. *IEEE Transactions on Circuits and Systems-I*, 39:240–243, 1992.

[Eli03] D.C. Elizondo. *A methodology to assess and rank the effects of hidden failures in protection schemes based on regions of vulnerability and index of severity*. PhD thesis, Virginia Polytechnic and State University, Blacksburg, Virginia, April 16, 2003.

[EMW88] G.C. Ejebe, H.P. Van Meeteren, and B.F. Wollenberg. Fast contingency screening and evaluation for voltage security analysis. *IEEE Transactions on Power Systems*, 3:1582–590, Nov. 1988.

[Ere97] M. Eremia. *Tehnici noi in transportul energiei electrice: Aplicatii ale electronicii de putere*. Editura Tehnica, Bucuresti, 1997.

[ERP01] D.C. Elizondo, J. de la Ree, A.G. Phadke, and S. Horowitz. Hidden failures in protection systems and their impact on wide-area disturbances. In *Proc. of Power Engineering Society Winter Meeting*, 2001.

[EW79] G.C. Ejebe and B.F. Wollenberg. Automatic contingency selection. *IEEE Transactions on Power Apparatus and Systems*, PAS-98:97–109, Jan./Feb. 1979.

[FA02] R. Findeisen and F. Allgower. An introduction to nonlinear model predictive control. In *Proc. of the 21st Benelux Meeting on Systems and Control*, Veldhoven, The Netherlands, Mar. 19-21 2002.

[FAM00] Z. Feng, V. Ajjarapu, and D.J. Maratukulam. A comprehensive approach for preventive and corrective control to mitigate voltage collapse. *IEEE Transactions on Power Systems*, 15:791–797, May 2000.

[GB74] M.S. Grover and R. Billinton. In *A computerized approach to substation and switching station reliability evaluation*, Jan. 27 - Feb. 1, 1974.

[GMK92] B. Gao, G. K. Morison, and P. Kundur. Voltage stability evaluation using modal analysis. *IEEE Transactions on Power Systems*, 7:1529–1542, Nov. 1992.

[GRE04] C. Vournas. Technical summary on the athens and southern greece blackout of july 12, 2004. Technical report, Aug. 2004. Available online: http://www.pserc.org.

[GTZ00] D. Gan, R.J. Thomas, and R.D. Zimmerman. Stability-constrained optimal power flow. *IEEE Transactions on Power Systems*, 15:535–540, May 2000.

[GVC06] M. Glavic and T. Van Cutsem. Some reflections on model predictive control of transmission voltages. In *Proc. 38th North American Power Symposium (NAPS)*, Carbondale (USA), Sept. 2006.

[HD88] J.F. Hall and A.K. Deb. Prediction of overhead transmission line ampacity by stochastic and deterministic models. *IEEE Transactions on Power Delivery*, 3:789–800, Apr. 1988.

[HG06] I.A. Hiskens and B. Gong. Voltage stability enhancement via model predictive control of load. *Intelligent Automation and Soft Computing*, 12:117–124, 2006.

[HLP01] G.T. Heydt, C.C. Liu, A.G. Phadke, and V. Vittal. Solutions for the crisis in electric power supply. *IEEE Computer Applications in Power*, pages 22–30, July 2001.

[HP95] S.H. Horowitz and A.G. Phadke. *Power System Relaying, Second Edition*. John Wiley & Sons, 1995.

[HPT88] S.H. Horowitz, A.G. Phadke, and J.S. Thorp. Adaptive transmission system relaying. *IEEE Transactions on Power Delivery*, 3:1436–1444, Oct. 1988.

[ILK96] B. Ingelsson, P. Lindstrm, D. Karlsson, G. Runvik, and J. Sjdin. Special protection scheme against voltage collapse in the south part of the swedish grid. In *Proc. CIGRE Conference*, pages Paper No. 38–103, 1996.

[ILS79] G. Irisarri, D. Levner, and A.M. Sasson. Automatic contingency selection for online security analasys - real time test. *IEEE Transactions on Power Apparatus and Systems*, PAS-98:1552–1559, Sep./Oct. 1979.

[ITA04] UCTE. Final report of the investigation committee on the 28 september 2003 blackout in italy. Technical report, Apr. 2004. Available online: http://www.ucte.org.

[ITF93] IEEE Task Force on Load Representation for Dynamic Performance. Load representation for dynamic performance analysis. *IEEE Transactions on Power Systems*, 8:472–482, May 1993.

[ITF95] IEEE Task Force on Load Representation for Dynamic Performance. Standard load models for power flow and dynamic performance simulation. *IEEE Transactions on Power Systems*, 10:1302–1313, Aug. 1995.

[IWT97] G.D. Irrisari, X. Wang, J. Tong, and S. Mokhtari. Maximum loadability of power systems using interior point nonlinear optimization methods. *IEEE Transactions on Power Systems*, 12:162–172, 1997.

[JLT02] J. Jung, C.-C. Liu, S.L. Tanimoto, and V. Vittal. Adaptation in load shedding under vulnerable operating conditions. *IEEE Transactions on Power Systems*, 17:1199 – 1205, Nov. 2002.

[KH04] S. Kolluri and T. He. Design and operating experience with fast acting load shedding scheme in the entergy system to prevent voltage collapse. In *Proc. IEEE Power Engineering Society General Meeting*, volume 2, pages 1625 – 1630, 6-10 June 2004.

[Kir07] D. Kirschen. Do investments prevent blackouts? In *Proc. IEEE Power Engineering Society General Meeting*, Tampa, Florida USA, 24-28 June 2007.

[KN02] D.S. Kirschen and D.P. Nedic. Consideration of hidden failures in security analysis. In *Proceedings of the 14th Power Systems Computation Conference*, Sevilla, 24-28 June 2002.

[Kun94] P. Kundur. *Power System Stability and Control*. EPRI Power system Engineering Series. McGraw Hill, 1994.

[LBC04] D. Lefebvre, S. Bernard, and T. Van Cutsem. Undervoltage load shedding scheme for the hydro-quebec system. In *Proc. IEEE Power Engineering Society General Meeting*, volume 2, pages 1619 – 1624, 6-10 June 2004.

[LG01] Editor-in-Chief L.L. Grigsby. *The Electric Power Engineering Handbook*. A CRC Handbook Published in Cooperation with IEEE Press, CRC Press LLC, 2001.

[LK03] M. Larsson and D. Karlsson. Coordinated system protection scheme against voltage collapse using heuristic search and predictive control. *IEEE Transactions on Power Systems*, 18:1001–1006, 2003.

[LMC03] D. Lefebvre, C. Moors, and T. Van Cutsem. Design of an undervoltage load shedding scheme for the hydro-qubec system. In *Proc. IEEE PES General Meeting*, Toronto (Canada), July 13-17, 2003.

[LR04] S.S. Ladhani and W. Rosehart. Under voltage load shedding for voltage stability overview of concepts and principles. In *Proc. IEEE Power Engineering Society General Meeting*, volume 2, pages 1597 – 1602, 6-10 June 2004.

[LSL89] P. Lagonotte, J.C. Sabonnadiere, J.Y. Leost, and J.P. Paul. Structural analysis of the electrical system: application to secondary voltage control in france. *IEEE Transactions on Power Systems*, 4:479485, May 1989.

[LSR93] T. Lie, R.A. Schlueter, P.A. Rusche, and R. Rhoades. Method of identifying weak transmission network stability boundaries. *IEEE Transactions on Power Systems*, 8:293301, 1993.

[Mac02] J.M. Maciejowski. *Predictive control with constraints*. Prentice Hall, Harlow (England), 2002.

[Mae95] P. Maess. Artificial life meets entertainment: Life like autonomous agents. *Communications of the Association for Computing Machinery*, 38:108–114, 1995.

[MBS79] T.K.P. Medicherla, R. Billinton, and M.S. Sachdev. Generation rescheduling and load shedding to alleviate line overloads-analysis. *IEEE Transactions on Power Apparatus and Systems*, PAS-98:1876–1884, Nov./Dec. 1979.

[MC99] C. Moors and T. Van Cutsem. Determination of optimal load shedding against voltage instability. In *Proc. 13th PSCC Conference*, pages 993–1000, Trondheim (Norway), 1999.

[MC04] B. Marinescu and J.M. Coulondre. A coordinated phase shifting control and remuneration method for a zonal congestion management scheme. In *Proc. IEEE Power Engineering Society, Power System Conference and Exposition, PSCE-2004*, pages 72–77, 2004.

[MCT05] B. Marinescu, J.M. Coulondre, P. Tsamasphyrou, and J.Y. Bourmaud. Improving tso's coordination for cross-border redispatch: A discussion of possible approaches in the european context. In *CIGRE/IEEE PES International Symposium*, pages 378–385, Oct. 2005.

[MDJ93] N.W. Miller, R. D'Aquila, K.M. Jimma, M.T. Sheehan, and G.L. Comegys. Voltage stability of the puget sound system under abnormally cold weather conditions. *IEEE Transactions on Power Systems*, 8:1133–1142, Aug. 1993.

[MEC04] J. Mechenbier, A. Ellis, R. Curtner, and S. Ranade. Design of an under voltage load shedding scheme. In *Proc. IEEE Power Engineering Society General Meeting*, volume 2, pages 1611 – 1618, 6-10 June 2004.

[MKB97] J.A. Momoh, R.J. Koessler, M.S. Bond, B. Stott, D. Sun, A. Papalexopoulos, and P. Ristanovic. Challenges to optimal power flow. *IEEE Transactions on Power Systems*, 12:444–455, 1997.

[Moo02] C. Moors. *On the design of load shedding schemes against voltage instability in electric power systems*. PhD thesis, University of Liège, Belgium, 2002.

[MRR00] D.Q. Mayne, J.B. Rawlings, C.V. Rao, and P.O.M. Scokaert. Constrained model predictive control: Stability and optimality. *Automatica*, 36:789–814, 2000.

[MZB01] J.A. Momoh, J.Z. Zhu, G.D. Boswell, and S. Hoffman. Power system security enhancement by opf with phase shifter. *IEEE Transactions on Power Systems*, 16:287–293, 2001.

[Ned03] D. Nedic. *Simulation of large system disturbances*. PhD thesis, University of Manchester Institute for Science and Technology, Manchester, United Kingdom, Dec. 2003.

[NERC] North American Electric Reliability Council. Disturbances analysis working group database. [online]. Technical report.

[NK94] D. Novosel and R.L. King. Using artificial neural networks for load shedding to alleviate overloaded lines. *IEEE Transactions on Power Delivery*, 9:425–433, 1994.

[OCG03] A. Oudalov, R. Cherkaoui, A.J. Germond, and M. Emery. Coordinated power flow control by multiple facts devices. In *Proc. of the IEEE PowerTech conference*, Bologna (Italy), June 2003.

[OSC03] B. Otomega, V. Sermanson, and T. Van Cutsem. Reverse-logic corrective control of load tap changers. In *Proc. of the IEEE PowerTech conference*, Bologna (Italy), June 2003.

[OVC05] B. Otomega and T. Van Cutsem. Fast contingency filtering based on linear voltage drop estimates. In *Proc. of the IEEE PowerTech conference*, St. Petersburg (Russia), 2005.

[PD00] L. Pereira and D. DeBerry. Double contingency transmission outages in a generation and reactive power deficient area. *IEEE Transactions on Power Systems*, 15, Feb. 2000.

[Pha01] A.G. Phadke. Hidden failures in protection systems, security and reliability in a changing environment. In *Proc. of Bulk Power Systems Dynamics and Control*, Onomichi, Japan, Aug. 2001.

[PLT87] J.-P. Paul, J.-Y. Leost, and J.-M. Tesseron. Survey of the secondary voltage control in france: Present realization and investigations. *IEEE Transactions on Power Systems*, 2:505–511, 1987.

[PT96] A.G. Phadke and J.S. Thorp. Expose hidden failures to prevent cascading outages [in power systems]. *IEEE Computer Applications in Power*, 9, July 1996.

[QB97] S.J. Qin and T.A. Badgwell. An overwiev of industrial model predictive control technology. *Chemical Process Control*, 93:232–256, 1997.

[RB02] C. Rehtanz and J. Bertsch. Wide area measurement and protection system for emergency voltage stability control. In *Proc. IEEE Power Engineering Society Winter Meeting*, volume 2, pages 842–847, 2002.

[RCQ03] W.D. Rosehart, C.A. Canizares, and V.H. Quintana. Effect of detailed power system models in traditional and voltage-stability-constrained optimal power-flow problems. *IEEE Transactions on Power Systems*, 18:27–35, Feb. 2003.

[Reh01] C. Rehtanz. Wide area protection and online stability assessment based on phasor measurement units. In *IREP - Bulk Power Systems Dynamics and Control V*, Onomichi, Japan, 26-31 Aug. 2001.

[RN95] S. Russel and P. Norvig. *Artificial intelligence - A modern approach*. Prentice Hall, 1995.

[SAB84] D.I. Sun, B. Ashley, B. Brewer, A. Hughes, and W.F. Tinney. Optimal power flow by newton approach. *IEEE Transaction on Power Apparatus and Systems*, 103:2864–2880, Oct. 1984.

[SAM87] B. Stott, O. Alsac, and A.J. Monticelli. Security analysis and optimization. In *Proceedings of the IEEE*, volume 75, pages 1623–1644, Dec. 1987.

[SDE76] Ieee standard dictionary of electrical and electronic terms. Technical report. IEEE Standard 100-1972, ANSI C42.100-1976.

[SG90] G. Schnyder and H. Glavitsch. Security enhancement using an optimal switching power flow. *IEEE Transactions on Power Systems*, 5:674–681, 1990.

[SHC91] R.A. Schlueter, I. Hu, M.W. Chang, J.C. Lo, and A. Costi. Methods for determining proximity to voltage collapse. *IEEE Transactions on Power Systems*, 6:285292, 1991.

[SLK03] H. Song, B. Lee, S.H. Kwon, and V. Ajjarapu. Reactive reserve-based contingency constrained optimal power flow (rccopf) for enhancement of voltage stability margins. *IEEE Transactions on Power Systems*, 18:1538–1546, Nov. 2003.

[SMC98] V. Sermanson, C. Moisse, T. Van Cutsem, and Y. Jacquemart. Voltage security assessment of systems with multiple instability modes. In *Proc. 4th Intern. Workshop on Bulk power systems dynamics and control (Re-structuring)*, pages 185–195, Santorin (Greece), Aug. 1998.

[SPC] Working Group C6 IEEE PES System Protection Subcommittee. Wide area protection and emergency control. Technical report.

[SV00] P. Stone and M. Veloso. Multi-agent systems: a survey from a machine learning perspective. *Autonomous Robots*, 8:345–383, 2000.

[SV05] W. Shao and V. Vittal. Corrective switching algorithm for relieving overloads and voltage violations. *IEEE Transactions on Power Systems*, 20:1877–1885, 2005.

[SV06] W. Shao and V. Vittal. Lp-based opf for corrective facts control to relieve overloads and voltage violations. *IEEE Transactions on Power Systems*, 21:1832–1839, 2006.

[SWE03] Svenska Kraftnat. The black-out in southern sweden and eastern denmark, 23 september, 2003, preliminary report. Technical report, Oct. 2003. Available online: http://www.svk.se.

[Tay92] C.W. Taylor. Concepts of undervoltage load shedding for voltage stability. 7:480–488, 1992.

[Tay94] C.W. Taylor. *Power system voltage stability*. McGraw-Hill, 1994.

[Tay00] C.W. Taylor. The future in on-line security assessment and wide-area stability control. In *Proc. of Power Engineering Society Winter Meeting*, volume 1, pages 78–83, Jan. 2000.

[TCM01] J.C. Tan, P.A. Crossley, P.G. McLaren, P.F. Gale, I. Hall, and J. Farrell. Application of a wide area back-up protection expert system to prevent cascading outages. In *Proc. of IEEE Power Engineering Society Summer Meeting*, volume 2, pages 903–908, July 2001.

[THP96] S. Tamronglak, S.H. Horowitz, A.G. Phadke, and J.S. Thorp. Anatomy of power system blackouts: preventive relaying strategies. *IEEE Transaction on Power Delivery*, 11, Apr. 1996.

[TJH05] S. Talukdar, D. Jia, P. Hines, and B.H. Krogh. Distributed model predictive control for the mitigation of cascading failures. In *Proc. 44th Conf. on Decision and Control and European Control Conference, CDC-ECC 2005*, Dec. 2005.

[TQ98] G.L. Torres and V.H. Quintana. An interior-point method for nonlinear optimal power flow using rectangular coordinates. *IEEE Transactions on Power Systems*, 13:1211–1218, 1998.

[TSM05] B.K. Talukdar, A.K. Sinha, S. Mukhopadhyay, and A. Bose. A computationally simple method for cost-efficient generation rescheduling and load shedding for congestion management. *International Journal of Electric Power and Energy Systems*, 27:379–388, 2005.

[TSO74] A. Thanikachalam, V.T. Sulzberger, P. Van Olinda, and J.N. Wrubel. On-line operation of phase shifters using energy control center computers. In *Proc. IEEE Power Engineering Society Winter Meeting*, New York, Jan. 27 - Feb. 1, 1974.

[UCT06] UCTE. Final report on system disturbance on 4 november 2006. Technical report, 2007. Available online: http://www.ucte.org.

[UK03] National Grid Transco. Investigation report into the loss of supply incident affecting parts of south london at 18:20 on thursday, 28 august 2003. Technical report, Sept. 2003. Available online: http://www2.tech.purdue.edu.

[USC04] U.S.-Canada Power System Outage Task Force. Final report on the august 14, 2003 blackout in the united states and canada: Causes and recomandations. Technical report, Apr. 2004. Available online: http://www.nerc.com.

[VC00] T. Van Cutsem. Voltage instability: phenomena, countermeasures, and analysis methods. In *Proc. of the IEEE*, volume 88, pages 208–227, Feb. 2000.

[VCG06] T. Van Cutsem, M.-E. Grenier, and D. Lefebvre. Combined detailed and quasi steady-state time simulations for large-disturbance analysis. *Electrical Power and Energy Systems*, 28:634–642, 2006.

[VCK05] T. Van Cutsem, J. Kabouris, G. Christoforidis, and C.D. Vournas. Application of real-time voltage security assessment to the hellenic interconnected system. In *IEE Proc. on Generation, Transmission and Distribution*, volume 152, pages 123–131, Jan. 2005.

[VCM97] T. Van Cutsem and R. Mailhot. Validation of a fast voltage stability analysis method on the hydro-quebec system. *IEEE Transactions on Power Systems*, 12:282–292, Feb. 1997.

[VCT95] T. Van Cutsem. An approach to corrective control of voltage instability using simulation and sensitivity. *IEEE Transactions on Power Systems*, 10:616–622, 1995.

[VCV07] T. Van Cutsem and C. D. Vournas. Emergency voltage stability controls: an overview. 24-28 June 2007.

[VCV98] T. Van Cutsem and C. D. Vournas. *Voltage Stability of Electric Power Systems*. Kluwer Academic Publishers, 1998.

[VM01] C.D. Vournas and G.A. Manos. Emergency tap-blocking to prevent voltage collapse. In *Proc. IEEE PowerTech conference*, Porto (Portugal), 10-13 Sept. 2001.

[VS05] M.K. Verma and S.C. Srivastava. Approach to determine voltage control areas considering impact of contingencies. *IEE Proc.-Gener. Transm. Distrib.*, 152:342350, May 2005.

[VVR86] F. Vakili, M.R. Viles, J.L. Reding, and N.G. Sherry. Dynamic thermal line loading monitor. *IEEE Transactions on Power Systems*, pages 62–66, 1986.

[WEC99] WECC. Undervoltage load shedding guidelines. Technical report, 1999.

[Weh99] L. Wehenkel. Emergency control and its strategies (invited paper). In *Proc. of the 13th PSCC Conference*, pages 35–48, Trondheim (Norway), 1999.

[WFM82] T.Y. Wong, J.A. Findlay, and A.N. McMurtrie. An on-line method for transmission ampacity evaluation. *IEEE Transactions on Power Apparatus and Systems*, 101:309–315, February 1982.

[WSK98] H. Wei, H. Sasaki, J. Kubokawa, and R. Yokoyama. An interior point nonlinear programming for optimal power flow problems with a novel data structure. *IEEE Transactions on Power Systems*, 13:870–877, Aug. 1998.

[WWT04] J.Y. Wen, Q.H. Wu, D.R. Turner, C.J. Cheng, and J. Fitch. Optimal coordinated voltage control for power system voltage stability. *IEEE Transactions on Power Systems*, 19:1115–1122, 2004.

[YKS03] Y. Yuan, J. Kubokawa, and H. Sasaki. A solution of optimal power flow with multicontingency transient stability constraints. *IEEE Transactions on Power Systems*, 18:1094–1102, Aug. 2003.

[ZA03] M. Zima and G. Andersson. Stability assessment and emergency control method using trajectory sensitivities. In *Proc. IEEE PowerTech conference*, Bologna (Italy), June 2003.

[ZA06] M. Zima and G. Andersson. *Model predictive control of electric power systems under emergency conditions, In* Real-time stability in power systems: Techniques for early detection of the risk of blackouts. Springer, 2006.

[ZLK05] M. Zima, M. Larsson, P. Korba, C. Rehtanz, and G. Andersson. Design aspects for wide-area monitoring and control system. *Proceedings of the IEEE*, 93:980–996, May 2005.

[ZWP80] J. Zaborszky, K.W. Whang, and K. Prasad. Fast contingency evaluation using concentric relaxation. *IEEE Transactions on Power Apparatus and Systems*, PAS-99, Jan./Feb. 1980.